ΠΑΝΕΠΙΣΤΗΜΙΟ ΚΡΗΤΗΣ
ΤΜΗΜΑ ΙΑΤΡΙΚΗΣ
ΤΟΜΕΑΣ ΒΑΣΙΚΩΝ ΕΠΙΣΤΗΜΩΝ

Μεταπτυχιακό Πρόγραμμα Σπουδών

"Κυτταρική και Γενετική Αιτιολογία, Διαγνωστική και Θεραπευτική των Ασθενειών του Ανθρώπου"

Μεταπτυχιακό Δίπλωμα Ειδίκευσης

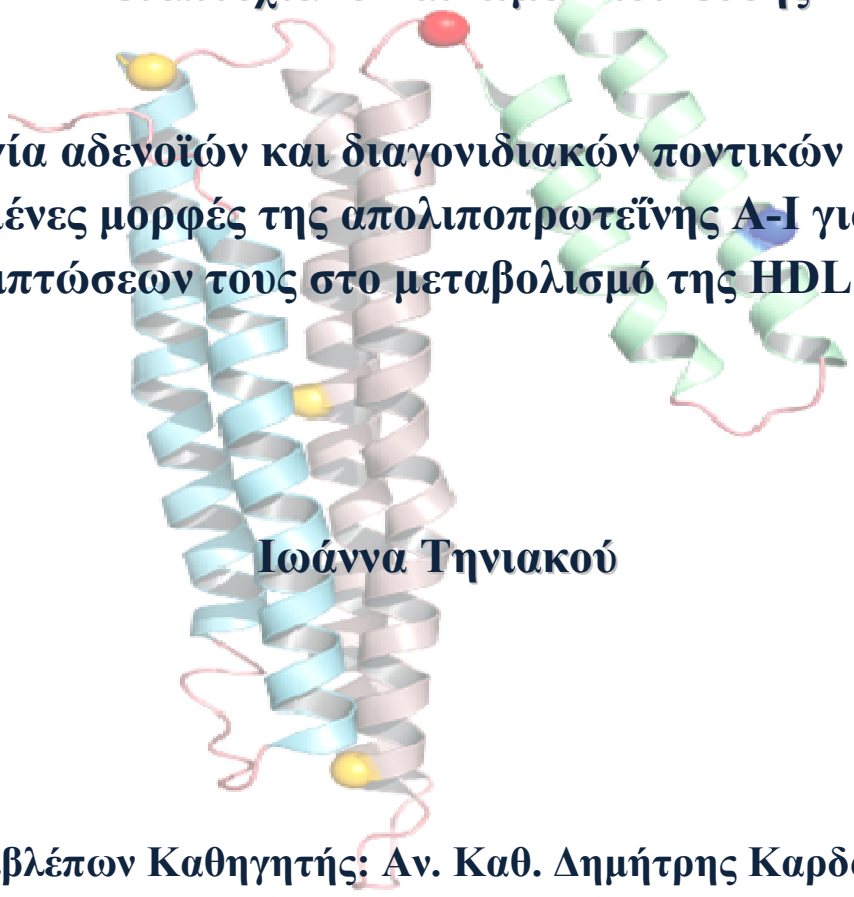

«Δημιουργία αδενοϊών και διαγονιδιακών ποντικών που φέρουν μεταλλαγμένες μορφές της απολιποπρωτεΐνης A-I για τη μελέτη των επιπτώσεων τους στο μεταβολισμό της HDL *in vivo*»

Ιωάννα Τηνιακού

Επιβλέπων Καθηγητής: Αν. Καθ. Δημήτρης Καρδάσης

Ηράκλειο, Οκτώβριος 2009

UNIVERSITY OF CRETE
FACULTY OF MEDICINE
DIVISION OF BASIC SCIENCES

Graduate Program

"Cellular and Genetic Etiology, Diagnosis and Treatment of Human Disease"

Master Thesis

"Generation of recombinant adenoviruses and transgenic mice bearing mutant apolipoprotein A-I forms for *in vivo* studies"

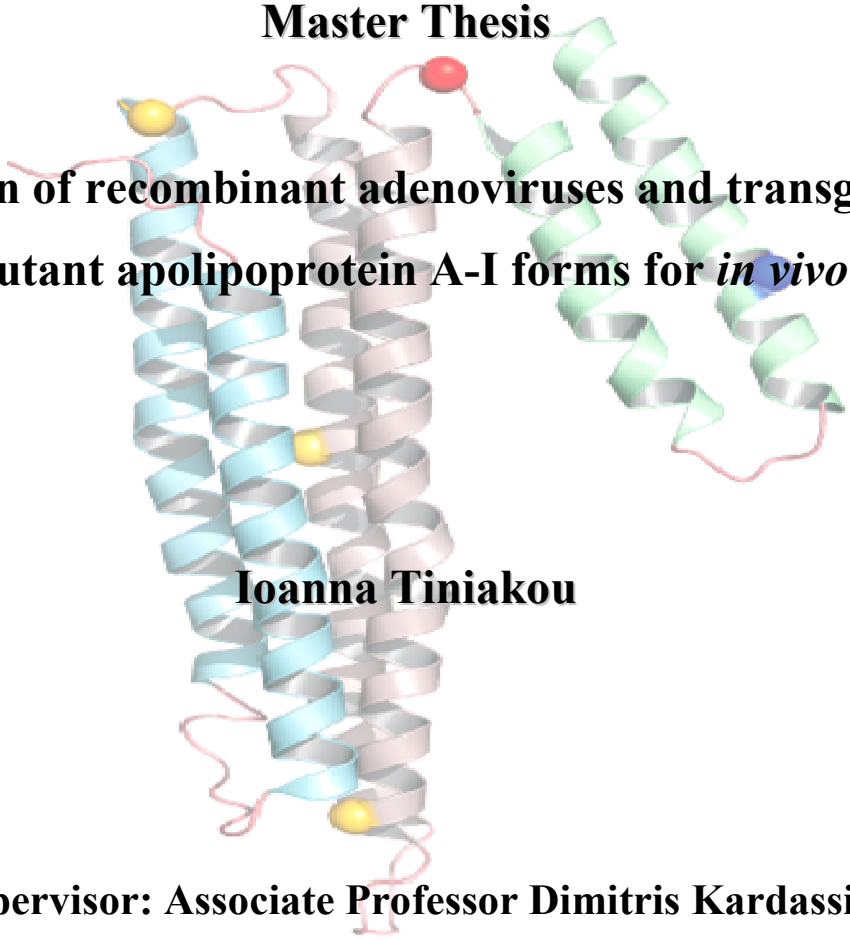

Ioanna Tiniakou

Supervisor: Associate Professor Dimitris Kardassis

Heraklion, October 2009

The journey of a thousand miles
must begin with a single step.

Abstract

An inverse relationship between the levels of high density lipoprotein (HDL)-cholesterol and the risk of developing cardiovascular disease has been well established. As the major protein component of HDL, apolipoprotein A-I (apoA-I) possesses a critical role in biogenesis, structure and function of this lipoprotein. The atheroprotective properties of apoA-I are mediated through its key-interactions with other factors participating in HDL metabolism.

Recent studies have demonstrated that myeloperoxidase (MPO)-dependent oxidation of apoA-I can convert the cardioprotective HDL into dysfunctional forms through targeting of specific methionine and tyrosine residues of apoA-I, such as Met148 and Tyr192. In order to investigate the mechanisms resulting in MPO-mediated impediment of normal apoA-I function, the Met148Ala and Tyr192Ala mutations in the apoA-I gene were generated using the overlapping PCR method. The apoA-I(Met148Ala) and apoA-I(Tyr192Ala) sequences were subsequently cloned into the appropriate shuttle vector and the respective recombinant adenoviruses were generated using the AdEasy method. The properties of each of the Ad-GFP-apoA-I mutants will be studied both *in vitro* and *in vivo* through adenovirus-mediated gene transfer in apoA-I knockout mice. Finally, co-infection of the mice with adenoviruses expressing either of the two mutants and human MPO will also be performed to assess the *in vivo* effect of MPO on plasma lipids, size and shape of HDL.

The present study also addressed another aspect of the role of apoA-I in HDL biogenesis and function; the effect of two naturally occurring apoA-I mutations, apoA-I(Leu141Arg)$_{Pisa}$ and apoA-I(Leu159Arg)$_{Finland}$, on HDL metabolism. Heterozygous subjects for either mutation exhibit very low plasma HDL-cholesterol levels attributed to apoA-I's reduced capacity of LCAT activation. Previous studies in our laboratory using adenovirus-mediated gene transfer in apoA-I deficient mice have demonstrated that both mutations fail to form discoidal or spherical HDL particles and that treatment with LCAT can restore the aberrant HDL phenotype present in these cases. In order to further study the properties of these structural mutations in apoA-I *in vivo*, transgenic mice carrying these naturally occurring variants of human apoA-I, apoA-I(Leu141Arg)$_{Pisa}$ and apoA-I(Leu159Arg)$_{Finland}$, were generated. In this context, wild-type hapoA-I, hapoA-I(Leu141Arg) and hapoA-I(Leu159Arg) were subcloned into the pBluescript-TTR1 vector, downstream of the TTR1 promoter which was used

to drive the liver-specific expression of the transgenes. Following preparation of the TTR1-apoA-I injection fragments and transgenesis procedures, the founders for each line were identified by genotyping using both PCR and Southern Blot. Next, one founder of each line will be selected according to the expression levels of each transgene in a way that all three founders will exhibit similar protein levels of human apoA-I. The selected founders will be subsequently crossed with apoA-I -/- mice in order to transfer the transgenic lines in an apoA-I deficient background. Finally, these mice will be used for studying the effect of these mutations on the interactions between apoA-I and other factors involved in key-steps of HDL metabolism. Moreover, the contribution of these mutants in the molecular mechanisms affecting HDL biogenesis and lipoprotein homeostasis in the plasma will also be evaluated. Overall, the generation of hapoA-I(Leu141Arg)$_{Pisa}$ and hapoA-I(Leu159Arg)$_{Finland}$ transgenic mice will provide long-term animal models that will facilitate in-depth investigation of their abnormal phenotype and could possibly uncover the etiology of genetically determined low levels of HDL, offering a new perspective in diagnosis, prognosis or even therapy.

Περίληψη

Επιδημιολογικές και κλινικές μελέτες έχουν καταδείξει μια αντιστρόφως ανάλογη συσχέτιση μεταξύ των επίπεδων της HDL χοληστερόλης και του κινδύνου εμφάνισης στεφανιαίας νόσου στον άνθρωπο. Κύριο πρωτεϊνικό συστατικό των λιποπρωτεϊνών υψηλής πυκνότητας (HDL) αποτελεί η απολιποπρωτεΐνη A-I, η οποία και κατέχει σημαντικό ρόλο στη βιογένεση, τη δομή, καθώς και τη λειτουργία της HDL. Η απολιποπρωτεΐνη A-I δρα προστατευτικά ως προς την εμφάνιση καρδιαγγειακών νοσημάτων μέσω των αλληλεπιδράσεων της με άλλες πρωτεΐνες που συμμετέχουν ενεργά στο μεταβολισμό της HDL.

Πρόσφατες έρευνες υποστηρίζουν πως η φυσιολογικά αθηροπροστατευτική HDL μπορεί να μετατραπεί σε αθηρογόνο ως αποτέλεσμα των οξειδωτικών τροποποιήσεων που υφίσταται η απολιποπρωτεΐνη A-I από το ένζυμο μυελοπεροξειδάση. Οι τροποποιήσεις αυτές αφορούν σε συγκεκριμένα αμινοξικά κατάλοιπα της πρωτεΐνης μεταξύ των οποίων συγκαταλέγονται τα κατάλοιπα μεθειονίνης και τυροσίνης στις θέσεις 148 και 192, αντίστοιχα. Για τη μελέτη των μηχανισμών δράσης της μυελοπεροξειδάσης που διαταράσσουν τη φυσιολογική λειτουργία της HDL, δημιουργήθηκαν ανασυνδυασμένοι αδενοϊοί που εκφράζουν τις μεταλλαγμένες μορφές apoA-I(Met148Ala) και apoA-I(Tyr192Ala). Για το σκοπό αυτό, αρχικά δημιουργήθηκαν στο γονίδιο της απολιποπρωτεΐνης A-I με τη μέθοδο του overlapping PCR οι παραπάνω μεταλλάξεις, Met148Ala και Tyr192Ala. Στη συνέχεια, οι apoA-I(Met148Ala) και apoA-I(Tyr192Ala) αλληλουχίες που προέκυψαν, κλωνοποιήθηκαν σε κατάλληλο παλινδρομικό φορέα και οι αντίστοιχοι ανασυνδυασμένοι αδενοϊοί παράχθηκαν με τη μέθοδο AdEasy. Μελλοντικά, πρόκειται να μελετηθούν οι ιδιότητες αυτών των αδενοϊών τόσο *in vitro* όσο και *in vivo* με μεταφορά γονιδίων μέσω αδενοϊών σε επίμυες με έλλειψη apoA-I (apoAI-/-). Επιπλέον, θα πραγματοποιηθεί ταυτόχρονη μόλυνση επίμυων με αδενοϊούς που εκφράζουν οποιαδήποτε από τα δύο μεταλλάγματα της αποA-I μαζί με αδενοϊό που εκφράζει τη μυελοπεροξειδάση, με σκοπό να αξιολογηθεί *in vivo* η επίδραση του ενζύμου αυτού στα επίπεδα των λιπιδίων του πλάσματος, το σχήμα και το μέγεθος της HDL.

Το δεύτερο μέρος της παρούσας μελέτης αφορά στη μελέτη της επίδρασης δύο φυσικά απαντώμενων μεταλλάξεων της απολιποπρωτεΐνης A-I, των apoA-I(Leu141Arg)$_{Pisa}$ και apoA-I(Leu159Arg)$_{Finland}$ στο μεταβολισμό της HDL.

Ετεροζυγώτες για οποιαδήποτε από τις δύο παραπάνω μεταλλάξεις παρουσιάζουν πολύ χαμηλά επίπεδα HDL χοληστερόλης στο πλάσμα λόγω της μειωμένης ικανότητας ενεργοποίησης της LCAT. Προηγούμενες μελέτες με πειράματα μεταφοράς γονιδίων μέσω αδενοϊών σε επίμυες με έλλειψη αποA-I φανερώνουν ότι και οι δύο μεταλλάξεις αδυνατούν να σχηματίσουν είτε δισκοειδή είτε σφαιρικά HDL σωματίδια, και ότι χορήγηση του ενζύμου LCAT μπορεί να διορθώσει τον παθολογικό φαινότυπο της HDL που παρατηρείται. Για την περαιτέρω μελέτη των ιδιοτήτων των συγκεκριμένων δομικών αλλαγών της απολιποπρωτεΐνης A-I *in vivo*, δημιούργηθηκαν διαγονιδιακοί επίμυες που φέρουν τις παραπάνω μεταλλάξεις. Για το σκοπό αυτό, η αγρίου τύπου ανθρώπινη απολιποπρωτεΐνη A-I, καθώς και οι apo(Leu141Arg) και apoA-I(Leu159Arg) κλωνοποιήθηκαν σε κατάλληλο φορέα κλωνοποίησης σε κατιούσα θέση σε σχέση με τον TTR1 υποκινητή, ο οποίος χρησιμοποιήθηκε για την ιστοειδική έκφραση του εκάστοτε διαγονιδίου στο ήπαρ. Στη συνέχεια ακολούθησε απομόνωση των TTR1-apoA-I τμημάτων από τις κατασκευές, τα οποία και χρησιμοποιήθηκαν για την πραγματοποίηση των ενέσεων κατά τη διαδικασία δημιουργίας των διαγονιδιακών ζώων. Η γονοτύπηση των ζώων πραγματοποιήθηκε με τις μεθόδους της PCR και της ανοσοτύπωσης κατά Southern. Μελλοντικά, ένας ιδρυτής από κάθε διαγονιδιακή σειρά πρόκειται να επιλεγεί έτσι ώστε τα πρωτεϊνικά επίπεδα έκφρασης των τριών διαγονιδίων να είναι παρόμοια. Έπειτα τα ζώα αυτά θα διασταυρωθούν με επίμυες με έλλειψη apoA-I για τη δημιουργία διαγονιδιακών επίμυων που θα εκφράζουν μόνο την αντίστοιχη, είτε αγρίου τύπου είτε μεταλλαγμένη, ανθρώπινη απολιποπρωτεΐνη A-I. Στα ζώα που θα προκύψουν θα θα μελετηθεί η επίδραση της κάθε μετάλλαξης στην ικανότητα αλληλεπίδρασης της απολιποπρωτεΐνης A-I με άλλους παράγοντες του HDL μονοπατιού, καθώς και στην ομοιόσταση των λιποπρωτεϊνών στο πλάσμα. Η δημιουργία των apoA-I(Leu141Arg)$_{\text{Pisa}}$ και apoA-I(Leu159Arg)$_{\text{Finland}}$ διαγονιδιακών επίμυων καθιστά δυνατή τη μακροπρόθεσμη και εις βάθος μελέτη του παθολογικού φαινότυπου των συγκεκριμένων μεταλλάξεων. Τέλος, μπορεί να συνεισφέρει σημαντικά στη διαλεύκανση της αιτιολογίας των γενετικής προέλευσης χαμηλών επιπέδων HDL στο πλάσμα, προσφέροντας με αυτόν τον τρόπο νέα προοπτική στη διάγνωση, την πρόγνωση και τη θεραπεία.

TABLE OF CONTENTS

1. INTRODUCTION

1.1 THE BIOLOGICAL ROLE OF LIPOPROTEINS

Cholesterol is an essential component of mammalian cell membranes that is required to establish proper membrane permeability and regulate membrane fluidity. Overall, it participates in various biological functions ranging from membrane trafficking to signal transduction. Abnormal plasma cholesterol levels have been associated with the pathogenesis of several diseases [1-4]. Therefore, the regulation of cholesterol levels is of critical importance.

Transport and distribution of cholesterol and other lipids through the bloodstream is achieved by their packaging in water-soluble complexes called lipoproteins. The plasma lipoproteins are either spherical or discoidal particles. The spherical particles are composed of a non-polar core (cholesteryl esters and triglycerides) and a hydrophilic surface layer (phospholipids, free cholesterol and apoproteins). The discoidal particles consist of mostly polar lipids and proteins in a bilayer conformation. The composition and ratio of protein to lipids determines the size and density of the lipoproteins (Table 1.1). Based on their density, plasma lipoproteins have been grouped into the following five major classes: chylomicrons (CM), very low density lipoproteins (VLDL), intermediate-density lipoproteins (IDL), low-density lipoproteins (LDL), and high-density lipoproteins (HDL) (Figure 1.1) [5].

Table 1.1 Physical properties and lipid composition of major human plasma lipoproteins (modified from [6]).

Particles	Source	Density (g/mL)	Protein (%)	TG (%)	PL (%)	free CH (%)	CE (%)
Chylomicrons	Intestine	<0.94	1-2	80-95	3-6	1-3	2-4
VLDL	Liver	0.94 -1.006	6-10	45-65	15-20	4-8	16-22
IDL	VLDL	1.006-1.019	10-12	25-30	25-27	8-10	32-35
LDL	VLDL	1.019-1.063	18-22	4-8	18-24	6-8	45-50
HDL	Liver, intestine	1.063-1.210	45-55	2-7	26-32	3-5	15-20
Lp(a)	Liver	1.040-1.090	~32	~1	~22	~8	~37

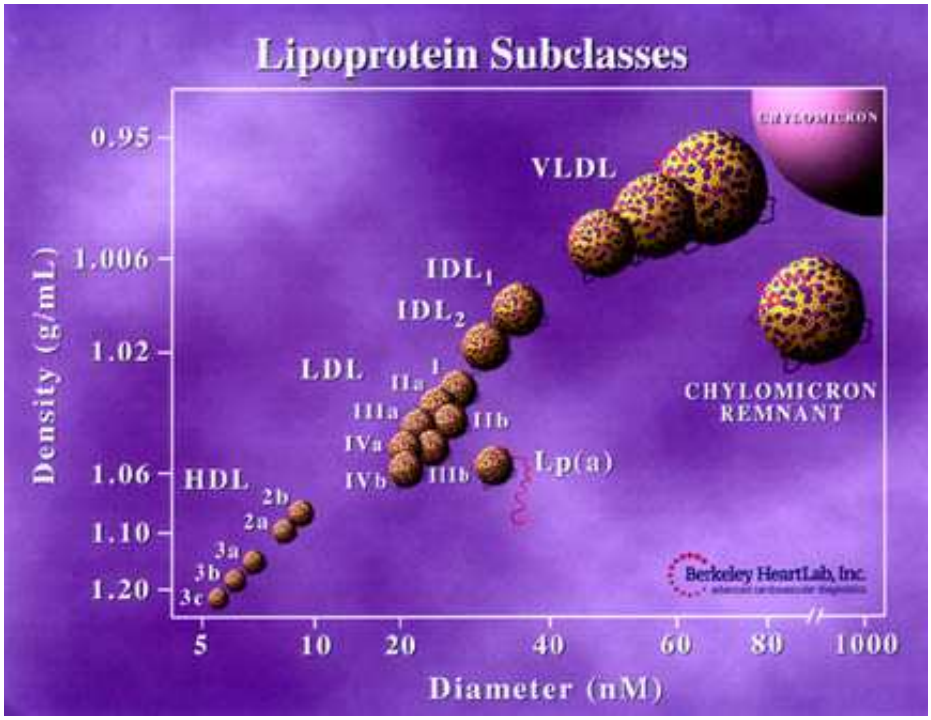

Figure 1.1 An illustration of the different plasma lipoprotein subclasses separated according to their density (g/mL) and size (nm) ((Berkley HeartLab, Inc.).

Lipoprotein synthesis and catabolism occur through three distinct, yet interconnected pathways: the chylomicron pathway, the VLDL/IDL/LDL pathway and the HDL pathway [7-10] (Figure 1.2). The intestine absorbs dietary fat and packages it into chylomicrons, which are transported to peripheral tissues through the bloodstream. In muscle and adipose tissues, the enzyme lipoprotein lipase (LPL) breaks down chylomicrons, and fatty acids enter these tissues. The chylomicron remnants are subsequently taken up by the liver. The liver loads lipids onto apoB and secretes VLDLs, which also undergo lipolysis by LPL to form LDLs. LDLs are then taken up by the liver through binding to the LDL receptor (LDLR), as well as through other pathways. By contrast, HDLs are generated by the intestine and the liver through the secretion of lipid-free apoA-I. ApoA-I then acquires phospholipid and cholesterol via its interactions with the ATP-binding cassette A1 (ABCA1) lipid transporter and other processes. ApoA-I is gradually lipidated and forms discoidal particles that are subsequently converted to spherical particles by the action of lecithin: cholesterol acyl transferase (LCAT). Spherical HDL particles interact functionally with the scavenger receptor class B type I (SR-BI) for the catabolism of esterified cholesterol. Cholesteryl esters are also transferred from HDL to VLDL/LDL

particles for eventual catabolism by the LDLR. Finally, the hydrolysis of phospholipids and residual triglycerides is mediated by various lipases (lipoprotein, hepatic and endothelial lipase), while the transfer of phospholipids from VLDL/LDL to HDL is achieved by the action of phospholipid transfer protein (PLTP).

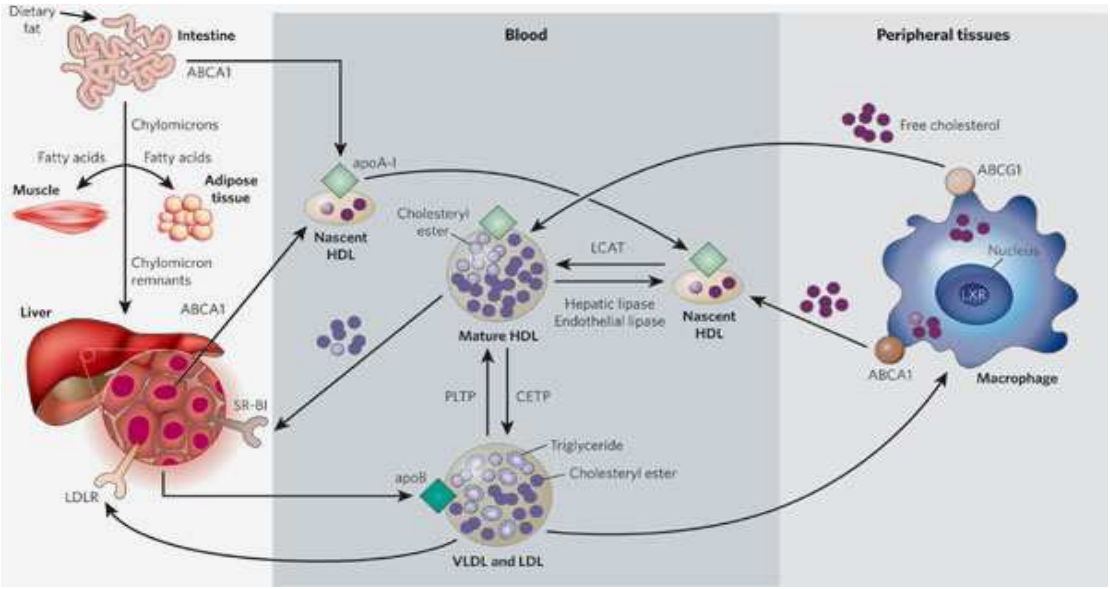

Figure 1.2 An overview of the lipoprotein metabolism (see text for details) [11].

1.2 HDL SUBPOPULATIONS

As mentioned above, the HDL fraction in human plasma is heterogeneous in terms of shape, size, density, composition, and surface charge [12]. According to the current methodology, HDL particles can be classified by density (ultracentrifugation), gradient gel electrophoresis, apolipoprotein composition (immunoaffinity chromatography), nuclear magnetic resonance and two-dimensional gel electrophoresis.

When isolated on the basis of density by ultracentrifugation, human HDL separate into two major subfractions designated HDL_2 (1.063-1.125 g/ml) and HDL_3 (1.125-1.21 g/ml). Non-denaturing polyacrylamide gradient gel electrophoresis separates HDL by particle size into at least five distinct subpopulations HDL_{2b} (10.6 nm), HDL_{2a} (9.2 nm), HDL_{3a} (8.4 nm), HDL_{3b} (8.0 nm), HDL_{3c} (7.6 nm). Based on their apolipoprotein composition HDL can be divided into two main

subpopulations. One subpopulation comprises HDL that contain apoA-I but no apoA-II (A-I HDL or LpA-I), while another comprises particles that contain both apoA-I and apoA-II (A-I/A-II HDL or LpA-I/LpA-II). In most human subjects, apoA-I is distributed approximately equally between A-I HDL and A-I/A-II HDL, while almost all of the apoA-II is in A-I/A-II HDL. Most of the LpA-I/A-II are found in the small HDL_3 density range, while LpA-I are prominent components of both HDL_2 and HDL_3. Results of some human population studies and some transgenic animal studies have raised the possibility that A-I HDL may be superior to A-I/A-II HDL in their ability to protect against atherosclerosis [13,14], while other studies have suggested that the protection conferred by A-I HDL and by A-I/A-II HDL is comparable [15].

HDL classification by both size and surface charge is achieved by non-denaturing two-dimensional gel electrophoresis followed by immunoblotting with apoA-I antibody [16]. In the horizontal dimension, HDL is separated by charge into three subpopulations on the basis of electrophoretic mobilities relative to albumin. The derived subpopulations are designated as preβ-HDL (mobility slower than albumin), α-HDL (mobility similar to albumin) and preα-HDL (mobility faster than albumin). These HDL particles are then further separated in the vertical dimension according to size, to give rise into a total of twelve subpopulations: preβ-1a, preβ-1b, preβ-2a, preβ-2b, preβ-2c, α1, α2, α3, α4, preα-1, preα-2 and preα-3 (Figure 1.3). The α-migrating particles are spherical lipoproteins and account for the major proportion of HDL in plasma. They include the HDL_2 and HDL_3 subfractions, as well as A-I HDL and A-I/A-II HDL subpopulations. Preβ-HDL are either lipid-poor apoA-I or discoidal particles consisting of two or three molecules of apoA-I complexed with phospholipids and possibly a small amount of unesterified cholesterol. Although it has been reported that populations of larger HDL are more protective than those of smaller HDL [17], other studies have also suggested that minor subpopulations of discoidal, preβ-migrating HDL are superior to spherical, α-migrating HDL in their ability to inhibit atherosclerosis because such particles are the preferred acceptors of cholesterol released from cells by the ABCA1 transporter. However, the discovery that ABCG1 transporter promotes cholesterol efflux from cells to large HDL particles supports the epidemiological finding that larger HDL particles are also protective. Other studies have documented that both preβ-1 and α-2 HDL particles serve as acceptors of free cholesterol by the ABCA-I pathway, while the large α-1 and α-2 particles interact with SR-BI to promote cholesterol efflux from liver cells [18]. In

fact, it has been estimated that preβ-1 HDL accounts for 40 % of cholesterol effluxed from cultured cells into the plasma and thus may also contribute to the reverse transport of cholesterol from the periphery to the liver [19].

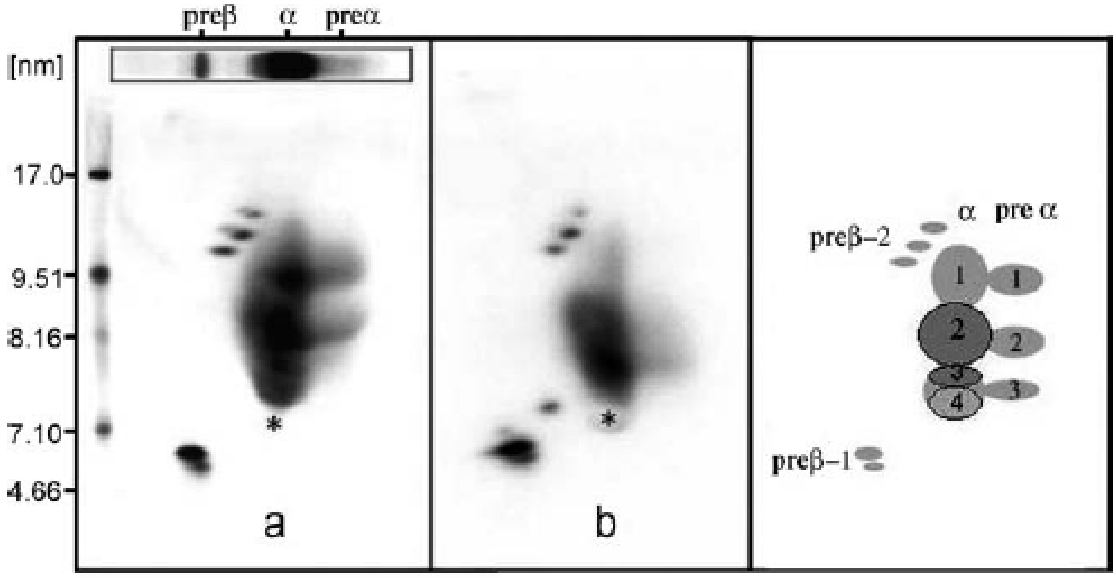

Figure 1.3 Two-dimensional gel patterns of apoA-I-containing HDL particles as detected in whole plasma as shown in **(a)** a normal subject, and **(b)** a patient with premature coronary artery disease with rearrangements in certain HDL subspecies. The asterisk depicts the location of human plasma albumin. **(c)** Locations of the apoA-I containing HDL particles [20].

2-D non-denaturing gel electrophoresis has been used to study the role of HDL and its subspecies in the development of coronary heart disease (CHD). Although no significant differences in LDL-cholesterol, triglyceride, and apoA-I levels were detected in CHD patients compared with control levels, CHD subjects exhibited deficiencies in the α1, preα-1, preα-2, and preα-3 subspecies, whereas the concentrations of the α3 and preβ-1 particles are significantly higher [21,22]. Decreased α and preα-1 levels and increased α3 levels have been recognized as better predictors of new cardiovascular events than HDL-cholesterol [23]. However, the overall evidence linking protection against CHD to specific HDL subpopulations in humans is conflicting, therefore whether the cardioprotective effects of HDL are influenced by their apolipoprotein composition, size, density, or electrophoretic mobility remains unknown.

1.3 THE APOLIPOPROTEIN A-I

HDL biogenesis and catabolism occurs through a complex pathway called reverse cholesterol transport (RCT) [24] (Figure 1.2). RCT includes the return of cholesterol effluxed from peripheral cells via the plasma to the liver for reutilization or excretion in the form of free cholesterol or bile acids. This process is of fundamental importance for maintenance of whole body cholesterol homeostasis [25]. As the main protein found in HDL particles and the obligatory cofactor of the enzyme LCAT [26], human apolipoprotein A-I (apoA-I) is inevitably a major participant in the regulation of reverse cholesterol transport [7,27]. Since this pathway is considered to be protective against atherosclerosis [28], deficiencies of apoA-I are associated with abnormalities in lipoprotein metabolism that result in low plasma HDL levels and may contribute to atherogenesis [29].

The human apoA-I gene

The human apoA-I gene has a molecular size of 1870 bp and consists of 4 exons and 3 introns [30,31]. Regional mapping has localized the human apoA-I gene on the long arm of chromosome 11q23-q24 [32,33]. This particular chromosomal region additionally codes for two more apolipoprotein genes; apoC-III and apoA-IV [34,35]. All three genes exist in close physical linkage and are arranged in a ~17 kb DNA region in tandem (Figure 1.4a).

Transcriptional regulation of human apoA-I gene

In apolipoproteins, regulation of gene expression is known to primarily occur at the level of transcription [36]. The proximal human apoA-I promoter comprises of three cis-acting elements, designated D, C, and B [37,38] (Figure 1.4a). Regulatory elements D (-220 to -190) and B (-128 to -77) contain HREs that serve as sites of action for various nuclear receptors including hepatic nuclear factor-4 (HNF-4), retinoid X receptor α (RXRα), apoA-I regulatory protein-1 (ARP-1), v-Erb-related receptor 3 (EAR-3) [39-41], homodimers of the above nuclear receptors, as well as heterodimers of RXRα with RARα or T3Rβ, ARP-1 and PPAR [42-44] (Figure 1.4b). The liver X receptor (LXR) has recently been recognized as a significant negative regulator of apoA-I transcription and HDL synthesis, since displacement of HNF4

from site B of the apoA-I promoter in the presence of a LXR agonist resulted in inhibition of apoA-I synthesis by human hepatocytes [45]. In addition, liver receptor homolog-1 (LRH-1) and farnesoid X receptor (FXR) can bind next to the regulatory element B of the apoA-I promoter. LRH-1 activates whereas FXR inhibits apoA-I expression. Downregulation of the apoA-I gene transcription by FXR can occur either by direct binding to the apoA-I promoter or indirectly, by inducing small heterodimers partner (SHP), which in turn represses the activity of LRH-1 [46]. Furthermore, the TNFα-responsive element D has been implicated in suppression of the apoA-I promoter activity through a mechanism that requires the MEK/ERK and JNK signaling pathways [47]. Element C (-175 to -148) binds the CAAT/Enhancer Binding Protein (C/EBP), Nuclear Factor Y (NFY) and HNF-3β [37,48,49].

Although the proximal apoA-I promoter can function independently, its effect is very weak. However, linkage of the apoA-I promoter to the apoCIII enhancer increases the strength of this promoter by several fold [50]. The apoCIII enhancer contains three binding sites of the ubiquitous transcription factor Specificity Protein 1 (SP1) on elements F, H, and I and two HREs on elements G and I_4 that bind orphan and different combinations of ligand-dependent nuclear receptors (Figure 1.4b).

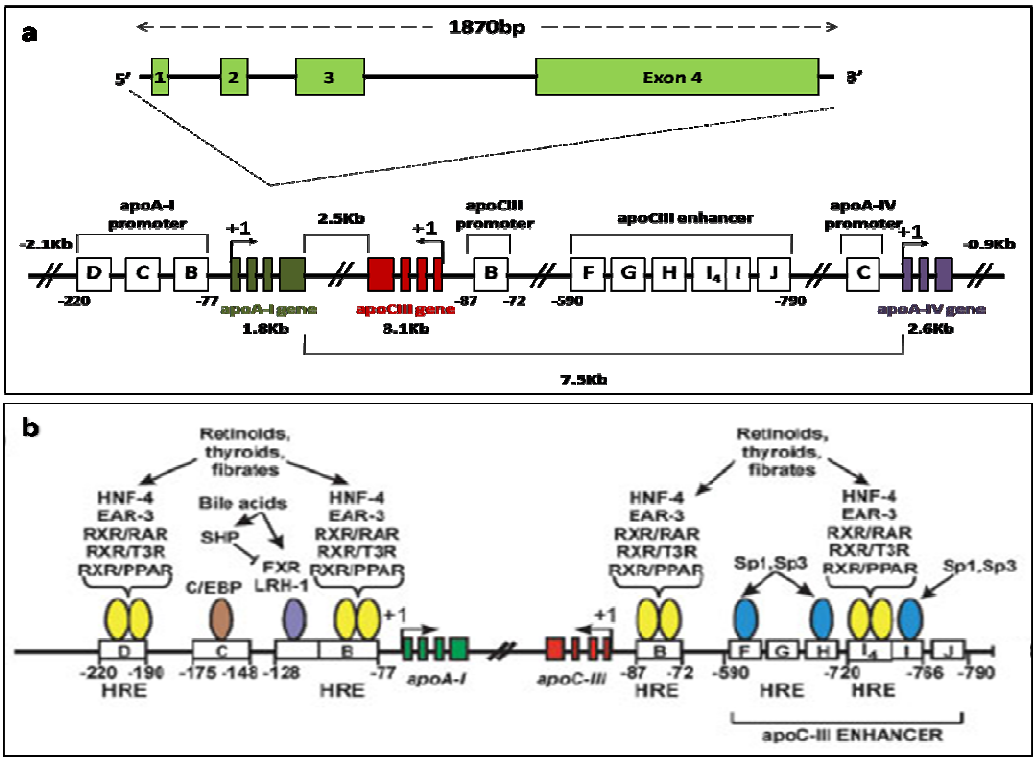

Figure 1.4 (a) Schematic representation of the human apoA-I/apoC-III/apoA-IV gene cluster and **(b)** the regulatory elements and transcription factors that control its expression [20].

The contribution of each site in the expression of the apoA-I gene has been evaluated with a series of *in vitro* and *in vivo* experiments [36]. In vitro mutagenesis of the apoA-I promoter/apoCIII enhancer cluster has revealed that mutations in the HREs of elements B or D diminish their activity [42]. Furthermore, deletion of the regulatory elements J, I, and H causes a dramatic reduction of enhancer activity [50]. Studies on transgenic mice carrying mutations of individual HREs suggest that HREs of either the proximal apoA-I promoter or the apoCIII enhancer can independently promote low levels of hepatic and intestinal expression of the apoA-I gene *in vivo* [51,52]. Moreover, the I_4 HRE of the apoCIII enhancer is required for intestinal expression and also contributes to the hepatic expression of the apoA-I gene [51]. Based on the way the apoA-I gene transcription is affected when different regulatory elements of the cluster are inactivated, a model has been proposed to describe the combined action of the regulatory elements of the cluster (Figure 1.5). According to this mechanism, complete activation of transcription is achieved by the synergistic interactions of the proximal apoA-I promoter and the apoCIII enhancer.

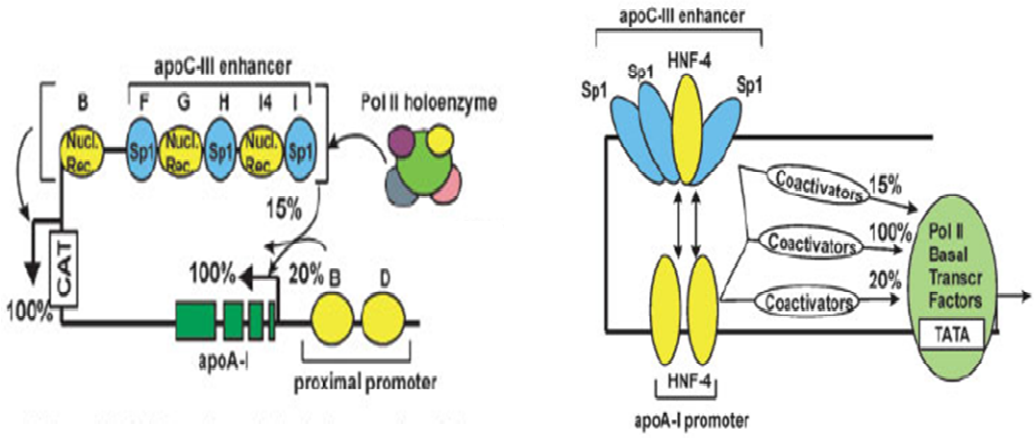

Figure 1.5 Model of transcriptional synergism in the apoA-I gene. The contribution of each of the apoA-I promoter and the apoC-III enhancer alone to the transcription of apoA-I is 20% and 15%, respectively. Normal (100%) hepatic and intestinal expression of the apoA-I gene requires synergistic activation of the two regulatory elements which may be attributed to protein-protein interactions of the promoter and enhancer complexes via coactivators with the proteins of the basal transcription complex [20].

Human apolipoprotein A-I and HDL

In humans, the apoA-I gene is abundantly expressed in liver and intestine and to a much lesser extent in other tissues [53]. The intestinally synthesized apoA-I is initially associated with chylomicrons. However, after entering the circulation it is rapidly transferred to HDL particles [54]. Hepatic apoA-I enters the circulation associated with nascent HDL particles having little or no core of cholesteryl ester. ApoA-I is synthesized and secreted as precursor protein isoforms which subsequently undergo proteolytic processing in order to attain the major isoform observed in the plasma [55]. The coding region of the mature apoA-I mRNA specifies a primary translation product that consists of 267 amino acids (Figure 1.6). This preproprotein includes the 243-residue-long plasma form of apoA-I and a 24-amino-acid N-terminal extension (prepropeptide) [56]. During translocation of prepro-apoA-I, the first 18 amino acids of the prepropeptide are intracellularly cleaved off by the signal peptidase and the remaining pro-apoA-I is secreted into plasma or lymph [56]. The maturation of apoA-I involves the extracellular removal of the 6-amino-acid-long prosegment (RHFWQQ) by a recently identified metallo-enzyme, the C-terminal procollagen endoproteinase/bone morphogenetic protein-1 (BMP-1) [57]. The mature apoA-I is a 243-residue single polypeptide with a calculated mass of 28079.

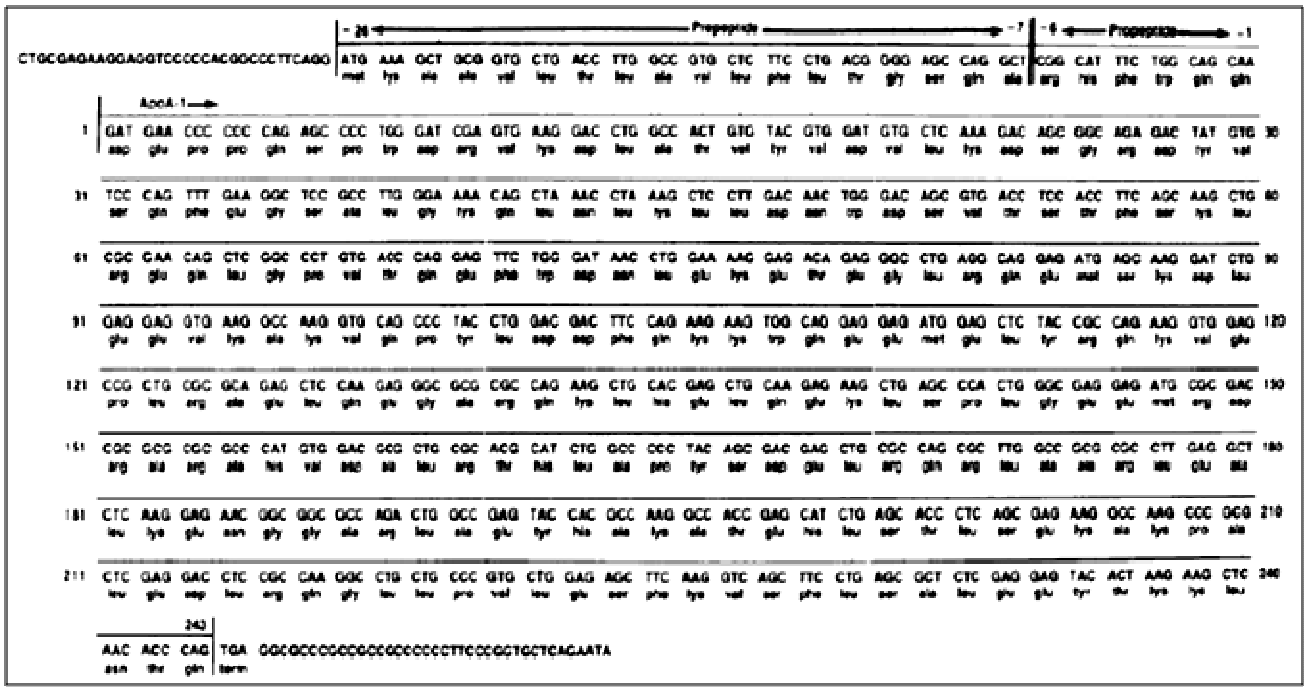

Figure 1.6 The complete nucleotide and inferred 267-amino-acid sequence of human preproapoA-I mRNA as determined from analysis of cloned apoA-I cDNA [58].

The role of apoA-I in HDL metabolism

HDL exists in human plasma in two main forms, one containing apoA-I with apoA-II (AI/AII-HDL) and another containing apoA-I only (AI-HDL). ApoA-I comprises approximately 70% of the HDL protein mass. ApoA-II covers another 15–20% while according to a recent proteomics study the remainder includes a variety of amphipathic proteins (apoCs, apoE, apoD, apoM, apoA-IV, paraoxonase and many others) [59]. Being the major protein component of HDL, apoA-I plays a key role in the biogenesis and functions of HDL.

HDL synthesis and catabolism occurs through a complex pathway as shown in Figure 1.7 [7,27]. In the first steps of this pathway, lipid-free apoA-I is secreted by the liver and directly interacts with the ABCA1 lipid transporter in order to acquire cellular phospholipid and cholesterol, this way forming the nascent or lipid-poor HDL [60,61]. Binding of apoA-I to ABCA1 also prevents internalization and proteolytic degradation of the transporter [62], as well as protects apoA-I from being rapidly degraded in the kidneys. In the peripheral tissues, nascent HDLs promote the efflux of cholesterol from tissues, including macrophages, through the actions of ABCA1. Lipid-bound apoA-I then activates the enzyme LCAT which esterifies the HDL free cholesterol (FC). As esterification proceeds, rapid cholesteryl ester (CE) accumulation

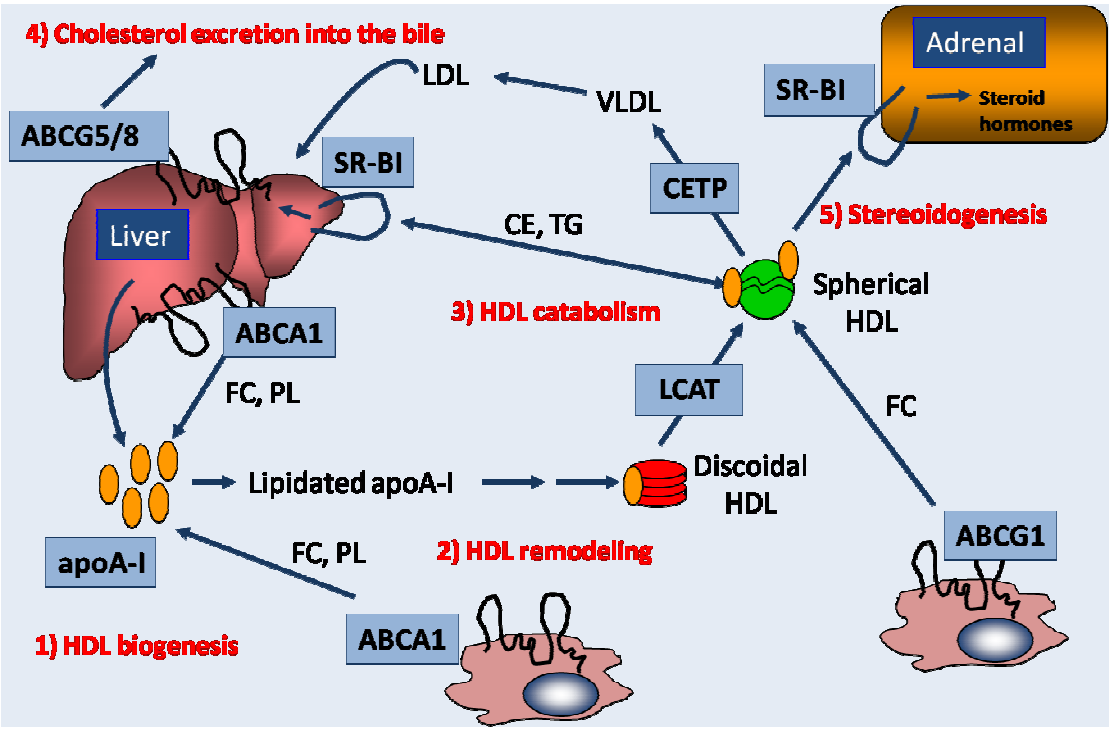

Figure 1.7 The HDL pathway (see text for details).

and phospholipid (PL) transfer correlates with the gradual conversion of the lipid-poor discoidal HDL into CE-rich spherical HDL particles. The mature HDL particles may promote cellular cholesterol efflux through the actions of the ABCG1 transporters [63-65]. This interaction does not require direct binding of the acceptor to ABCG1. Following synthesis, cholesterol from plasma HDL is transferred both to steroidogenic tissues for synthesis of steroid hormones and through the liver to the bile for excretion. HDL-cholesterol can be returned to the liver both directly, through uptake by the receptor SR-BI [66-68], and indirectly, by transfer to VLDL/LDL through CETP and subsequent catabolism by the LDL receptor. Finally, the lipid content of HDL is altered by the action of various lipases (lipoprotein, hepatic and endothelial lipase), while the transfer of phospholipids from VLDL/LDL to HDL is mediated by PLTP.

The ability of apoA-I to exert three distinct functions by interacting with ABCA1, LCAT and SR-BI presumes conformational plasticity of the protein. Therefore, the physical state and domain structure of apoA-I significantly contribute to this protein's functionality.

The structure of apoA-I in HDL

Primary and secondary structure

In human apoA-I, exon 3 encodes for the N-terminal residues 1-43 while exon 4 codes for a primary structure of eight 22- and two 11-amino acid tandem repeats that span the remaining region of apoA-I (residues 44-243). With respect to the secondary structure of the protein, each of these repeats is organized in an amphipathic α-helix with the majority of the helices separated by proline residues [69,70] (Figure 1.8a). The N- (residues 1-43, 44–65) and C-terminal (residues 220–241) α-helices exhibit the greatest lipid affinity [71] and therefore contribute significantly to the lipid-binding properties [72,73] and other functions of apoA-I.

Tertiary structure

Regardless of the state, lipid-free or lipidated, in which apoA-I exists, it appears that the driving force of protein folding lies in the effort to minimize the aqueous exposure of the non-polar helical surfaces. Studies based on physical-biochemical measurements are consistent with a two-domain tertiary structure that comprises of an

N-terminal anti-parallel helix bundle domain and a distinct less organized C-terminal domain [74-76]. The stability of the N-terminal helix bundle along with the hydrophobicity and α-helix content of the C-terminal domain are to a significant extent responsible for determining the overall functionality of apoA-I [77].

Lipid-free apoA-I

Only a small percentage of human plasma apoA-I exists in a lipid-free state. Structural studies so far have reached a certain level of information on lipid-free apoA-I and suggested a number of comparable structures [76,78]. However, in all cases completely delipidated apoA-I was studied in aqueous solution. Recently, full-length lipid-free apoA-I was crystallized by Ajees *et al* in the presence of chromium tris-acetylacetonate and the protein's structure was described at 2.4 Å resolution [74]. The crystal structure of full-length lipid-free apoA-I indicated that the N-terminal two-thirds of the molecule are organized in a four-helix bundle while the C-terminal 50 amino acids form an independent two helix bundle (Figure 1.8b).

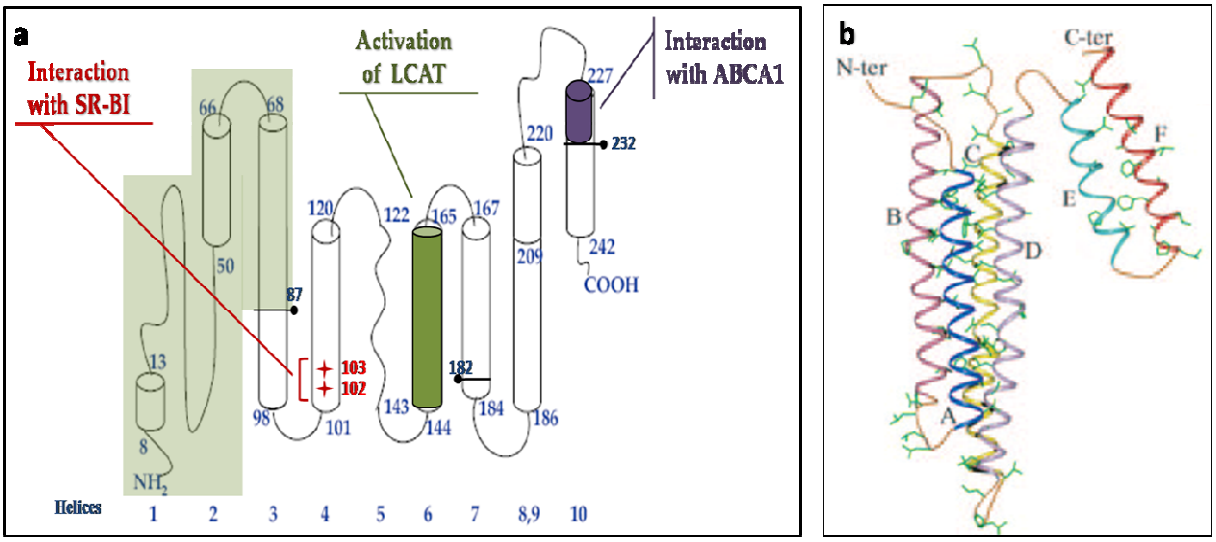

Figure 1.8 (a) The secondary structure and the properties of human apoA-I (adapted from [7]). Cylinders represent amphipathic α–helices and grey shading indicates the N- and C-terminus of the protein. Purple and green colors indicate regions that affect interactions of apoA-I with ABCA1 and LCAT, respectively. Red asterisks indicate amino acids that are involved in interactions of apoA-I with SR-BI. **(b)** Stereoview of the crystal structure of human apoA-I [74]. The six helices in the structure are depicted in blue (A), pink (B), yellow (C), lavender (D), cyan (E), and red (F). Loops are colored gold. Hydrophobic residues are shown as green sticks.

Lipid-bound apoA-I: discoidal and spherical HDL

Over the past three decades a large number of different technical approaches, from chemical crosslinking to mass spectrometry, have been employed in an attempt to solve the lipid-bound conformation of apoA-I [79]. Based on the crystal structure and other structural studies, detailed belt and hairpin models have been proposed to describe the binding of apoA-I in discoidal and spherical HDL particles [80,81].

Although originally destined to describe the lipid-free structure of apoA-I, Borhani's crystal structure [82] introduced the idea of a belt-like orientation in lipoproteins. Since then, studies have clearly supported the belt model for apoA-I [83,84]. According to the currently prevailing model for discoidal HDL, designated as the "double belt" model, the best characterized particles consist of two ring-shaped apoA-I molecules which are wrapped around the circumference of a small discoidal patch of bilayer containing 160 lipid molecules and are organized in an anti-parallel orientation [85-87] (Figure 1.9). The conversion of discoidal HDL into its spherical form postulates the readjustment of the apoA-I structure on the helical surface. Unfortunately, the information on the conformation of apoA-I in spherical particles is limited. It has been argued that the fundamental interactions of apoA-I helices with the phospholipid acyl chains should not alter significantly in spherical HDL [88,89]. However, other studies have demonstrated noteworthy conformational differences in apoA-I on spheres versus discs [90]. An interesting study by Curtiss *et al* [91] has opened up the possibility that depending on the lipid cargo of a given particle the conformation of apoA-I may change.

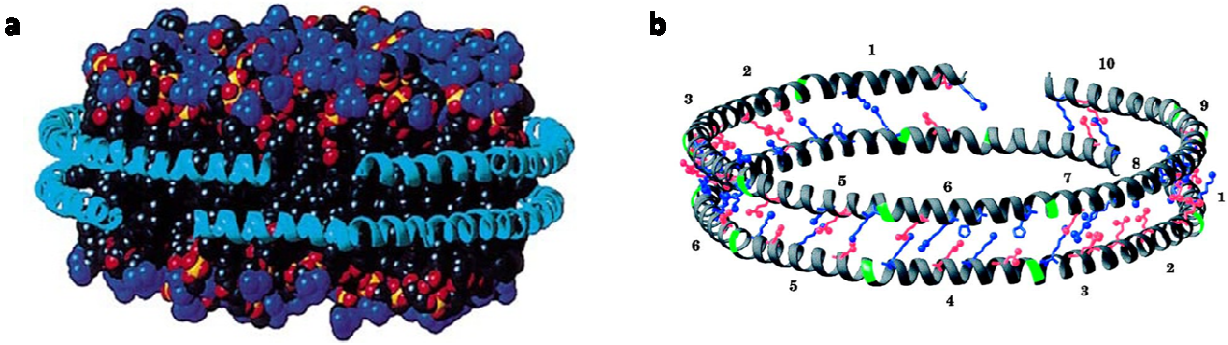

Figure 1.9 (a) The "double belt" model of discoidal HDL [85]. Two apoA-I molecules, displayed as light blue helical ribbons, are docked around 85Å diameter patch of phospholipid bilayer. **(b)** Structure and interhelical salt bridges of the double belt model [85]. The apoA-I backbone is shown as a helical ribbon diagram in which prolines are colored green. The charged residues that form the proposed interhelical salt bridges are depicted in extended conformation. The amphipathic α-helices (1–10) are labeled.

Structure – function relationship in apoA-I

It has been made clear so far that the functionality of apoA-I is modulated by its physical state, thus allowing the binding of various amounts of lipids as well as the formation of HDL particles that differ both in size and shape. A recent study has provided great insight into the multiple lipid-bound conformations that the N-terminal helix bundle of apoA-I can adopt on a lipoprotein particle, depending on space availability and composition of the surface [92]. Current understanding on the contribution of the structural domains of apoA-I in its functions is outlined below.

Interaction with ABCA1

As aforementioned, HDL assembly is initiated by the ABCA1-mediated transfer of cellular phospholipids and cholesterol to the extracellular lipid-free apoA-I. The initial lipidation of apoA-I through the action of ABCA1 mainly takes place in the liver, whereas ABCA1 interactions with apoA-I in the peripheral tissues merely appear to enrich the initial particle with cholesterol and to increase its stability [93,94]. As far as the mechanism of action is concerned, ABCA1-mediated lipid efflux has been shown to involve the internalization of ABCA1/apoA-I complexes into endosomes, the interaction with intracellular lipid pools and, finally, the resecretion of the lipidated apoA-I [95]. In other words, it appears that ABCA1 possesses a dual function, as a receptor for apoA-I and as a lipid transporter.

Structure-function analysis of apoA-I interactions with ABCA1 as presented by both *in vivo* and *in vitro* studies has led to certain conclusions. The C-terminal segment (220-231) of apoA-I is required for the ABCA1-dependent formation of α-HDL (Figure 1.8a), since deletion of this region results in defective lipid efflux, poor interaction with ABCA1, and failure to form any other type of HDL particles except for preβ-HDL [60,96]. Consistent with this lies the observation that although the central helices of apoA-I have the capacity to cross-link to ABCA1, promote lipid efflux, and form discoidal HDL particles, these properties are diminished in the absence of the C-terminal segment of apoA-I [60,75]. In general, a concept that emerges from the existing data is that formation of a productive ABCA1/apoA-I complex requires not only interactions between ABCA1 and apoA-I but efficient ABCA1-mediated lipidation of apoA-I as well [97].

Interaction with LCAT

Initial lipidation of apoA-I is followed by the remodeling of HDL particles, a process that involves the esterification of cholesterol by the enzyme LCAT. Although LCAT is capable of direct binding to lipids, optimum reaction requires activation by apoA-I. This reaction includes LCAT binding to the activator, hydrolysis of the fatty acid at the *sn*-2 position of a phospholipid and finally transesterification of cholesterol and concomitant release of cholesteryl esters [98]. Lipid composition of HDL has been shown to affect the ability of apoA-I to activate LCAT-mediated esterification of cholesterol [99].

Studies on the exact region of apoA-I responsible for the interaction with LCAT have pointed towards the central helices of the protein [100]. It is now well established that region 143–164 is the LCAT activator domain of apoA-I (Figure 1.8a) [101]. Moreover, adenovirus-mediated gene transfer studies of specific apoA-I mutants in apoA-I-deficient mice suggest that the hydrophobic residues of the C-terminus of apoA-I may also critically participate in the *in vivo* activation of LCAT [102]. On the other hand, the role of the N-terminus of apoA-I in LCAT activation appears to be restricted [103].

Interaction with SR-BI

SR-BI is a membrane glycoprotein mainly expressed in the liver and the steroidogenic glands that can bind a variety of ligands, including lipid-bound apoA-I [67]. Direct binding of SR-BI to apoA-I triggers selective uptake of both cholesteryl ester and other lipids from HDL, as well as bidirectional movement of unesterified cholesterol [104,105].

The physiological importance of SR-BI interactions with lipid-bound apoA-I has emerged by numerous studies using SR-BI transgenic and SR-BI-deficient mouse models [106]. It appears that the SR-BI/apoA-I interaction controls the structure, composition, and concentration of plasma HDL [106,107]. Attempts to elucidate the mechanism that drives the SR-BI-mediated lipid transport have yet implicated certain residues on helices 4 and 6 of apoA-I (Figure 1.8a) [108]. However, it has been implied that efficient SR-BI-mediated cholesterol efflux may not only require direct binding of the lipoprotein to the receptor, but also the formation of a ‘‘productive complex’’. However, the information available on the apoA-I interaction with SR-BI remains limited.

1.4 THE ROLE OF APOA-I IN ATHEROPROTECTION

Clinical and epidemiological studies have shown that HDL acts in an atheroprotective manner. In fact, HDL-cholesterol levels are inversely associated with coronary heart disease and other forms of vascular disease, thus it is considered a powerful inverse predictor of cardiovascular risk [109].

The anti-atherogenic functions of HDL are largely attributed to its ability to promote the efflux of cholesterol from peripheral tissues to the liver through the interactions of apoA-I with several proteins (ABCA1, LCAT, SR-BI), a process that may minimize the accumulation of foam cells in the artery wall. However, apart from its role in RCT, HDL exhibits several other well-documented functions that are likely to contribute to the atheroprotective action of this lipoprotein. HDL and apoA-I have been reported to possess anti-oxidant and anti-inflammatory properties [110,111] and can alter prostacyclin levels and platelet function this way exerting their anti-thrombotic effects [112]. Furthermore, HDL can activate endothelial nitric oxide synthase (eNOS) and modulate nitric oxide release through a process that requires the interaction of apoA-I with SR-BI [113,114]. Some of these actions are at least in part attributed to HDL-associated enzymes, such as paraoxonase (PON1), glutathione selenoperoxidase (GSPx) and platelet-activating factor acetylhydrolase (PAF-AH).

Despite the favorable effects on oxidation, inflammation, thrombosis and endothelial function, HDL can become dysfunctional and pro-atherogenic under certain circumstances. In fact, all of these atheroprotective functions are lost in the dysfunctional plasma HDL of subjects with systemic inflammation, coronary heart disease, diabetes, and chronic renal disease. Given the physical heterogeneity of HDL, lately, it has been postulated that particle “quality” is more defining in terms of atheroprotection than the “quantity”. In other words, the concentration of the total HDL fraction alone does not delineate the atheroprotective capacity of this lipoprotein, since it appears that the composition of HDL is of equal importance.

So far, the evidence linking protection against CVD to specific HDL subpopulations is conflicting. Discordance in these data may be partly attributed to the complex relationships between the different HDL subfractions [115]. Although, initially, large HDL particles were considered to be more protective than smaller HDL [17], more recent reports show that small HDL particles, either discoidal or mature spherical, are preferred over larger HDLs as initial acceptors of cellular cholesterol

[116]. Apart from the impact on RCT, small HDLs possibly acquire oxidized lipids more efficiently than larger particles and are primarily responsible for HDL anti-inflammatory properties due to their greater capacity to inhibit adhesion molecule expression in the endothelium [115]. Since there is no consensus on the value of HDL subspecies in CHD risk assessment, Asztalos *et* al have examined the association of specific HDL subpopulations with CHD prevalence. According to this study, α1 and preα-3 levels had an inverse association, whereas α3 and preα-1 particle levels had a positive association with CHD [117]. Among these particles, α3 contains both apoA-I and apoA-II; the rest contain apoA-I but not apoA-II. The authors concluded that measurement of HDL subpopulations provides useful information about CHD risk beyond that obtained from traditional CHD risk factors, especially in subjects with normal LDL-C and triglyceride levels.

Anti-inflammatory and anti-oxidant properties of apoA-I

Inflammation has been implicated in the genesis, progression, and instability of atherosclerotic plaques [118]. The macrophages accumulating in atherosclerotic plaques are derived mainly from blood monocytes that adhere to endothelial cells before migrating into the subendothelial space. Within the artery wall, the monocytes differentiate into macrophages that express a range of scavenger receptors, some of which have the ability to bind and internalize modified LDLs. The foam cells that result are considered to be the hallmark cells of atherosclerosis (Figure 1.10). An early step in this inflammatory process is monocyte adhesion to endothelial cells, which have been injured or stimulated in some other way to express adhesion molecules. Activated endothelial cells express vascular cell adhesion molecule-1 (VCAM-1), intercellular adhesion molecule-1 (ICAM-1) and E-selectin [119]. Expression of these adhesion molecules in endothelial cells is upregulated in response to cellular reactive oxygen species induced by oxidized LDL or TNFα [120]. Once they bind to the adhesion proteins on the surface of endothelial cells, monocytes are recruited into the subendothelial space by chemokines such as monocyte chemotactic protein-1 (MCP-1).

The anti-inflammatory properties of HDL include its ability to decrease the expression of adhesion molecules on endothelial cells and inhibit monocyte adhesion

to the endothelium. Specifically, HDL inhibits VCAM-1, ICAM-1, E-selectin, interleukin-1 and endotoxin expression through a process that involves the participation of apoA-I [121,122]. The same result is achieved by the HDL-mediated inhibition of reactive oxygen species generation [123]. Moreover, HDL can prevent MCP-1 expression and thus monocyte migration to endothelium [124], as well as the PAF-induced adhesion of leukocytes to the activated endothelium [125]. Finally, since oxidized phospholipids stimulate arterial inflammation, the anti-oxidant actions of HDL significantly confer to its anti-inflammatory properties.

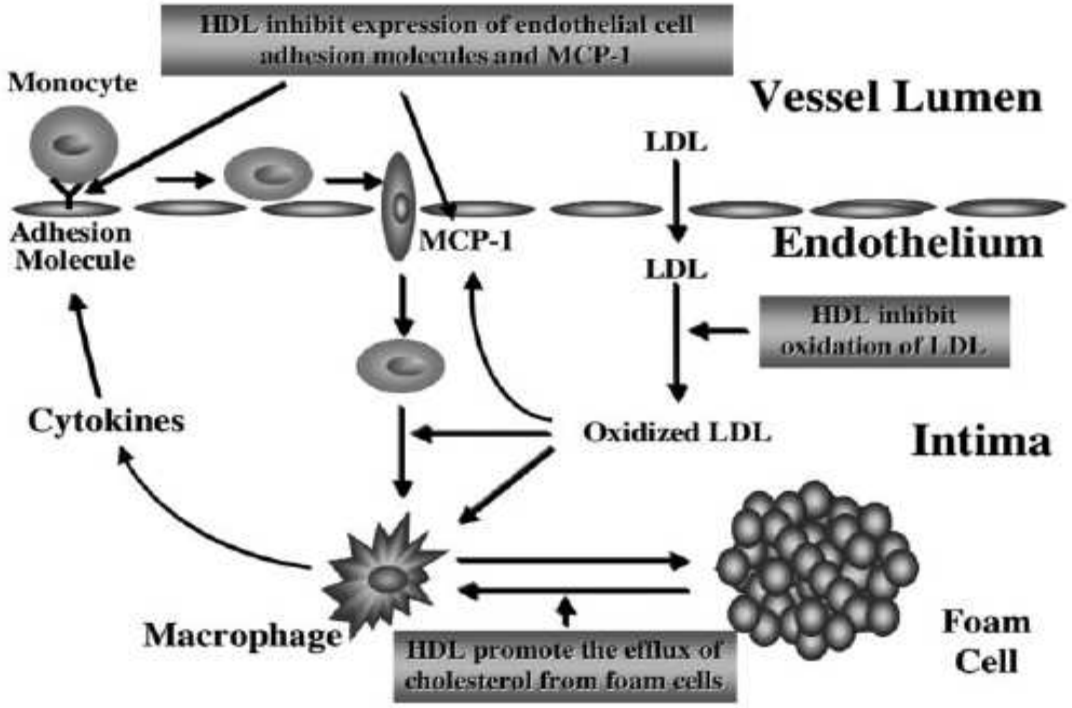

Figure 1.10 Anti-oxidant and anti-inflammatory properties of HDL contribute to the anti-atherogenic potential of these lipoproteins. Atherosclerosis is an inflammatory disorder initiated by an accumulation and subsequent oxidation of LDL in the arterial intima. The oxidized LDLs stimulate endothelial cells to express MCP-1 that, in turn, attracts monocytes into the subendothelial space. The monocytes differentiate into macrophages that take-up the oxidized LDL in a process that converts them into foam cells. Macrophages also express a range of cytokines, some of which stimulate endothelial cells to express adhesion proteins. This leads to binding of blood monocytes to the endothelium. HDL has the potential to impact at several points in this process through inhibition of the pro-atherogenic oxidative modification of LDL and the expression of endothelial cell adhesion proteins and MCP-1, thus reducing the infiltration of monocytes into the artery wall [110].

LDL oxidation is commonly considered to contribute to the initiation and progression of atherosclerosis [126]. As a consequence of LDL entering the subendothelial space and binding to the complex matrix beneath the endothelium, the trapped LDL receive additional lipid hydroperoxides produced by the lipoxygenase and myeloperoxidase pathways operating in cells within the artery wall. When the level of oxidized lipids in the trapped LDL exceeds a critical threshold, the LDL phospholipids that contain arachidonic acid in the *sn*-2 position become oxidized and pro-inflammatory. HDL protects both the lipid and protein moieties of LDL from oxidation via several mechanisms.

The main protein in HDL, apoA-I, is capable of acquiring and removing LDL lipid hydroperoxides and other lipid peroxidation products, which oxidize LDL phospholipids, and transports them to the kidney [127,128]. LCAT and PAF-AH, two HDL-associated enzymes, can also remove oxidized phospholipids from LDL [129].Thus, one of the main anti-oxidant/anti-inflammatory functions of HDL is mediated by a transport mechanism that binds and carries away oxidant molecules. HDLs are also carriers of enzymes, such as paraoxonase-1 (PON1) and glutathione phospholipid peroxidase that destroy the lipid hydroperoxides that oxidize LDL phospholipids [124,130]. PON1 along with PAF-AH are responsible for the degradation of oxidized LDL phospholipids, thus inhibiting their pro-inflammatory action [131]. Moreover, PON1 significantly reduces the ability of oxidized LDL to trigger monocyte–endothelial cell interactions [132] and contributes to the attenuation of atherosclerosis development by stimulating HDL binding and HDL-mediated macrophage cholesterol efflux via the ABCA1 transporter [133]. Finally, HDL can prevent 12-lipoxygenase-mediated synthesis of lipid hydroperoxides [127] as well as inhibit the penetration of LDL into the vessel wall [134], thus preventing atherosclerosis progression.

In conclusion, HDL possesses several favorable properties independently of RCT, which may contribute to its anti-atherogenic effects. These properties are exerted not only by apolipoproteins but also by lipid components and enzymes associated with HDL. However, in the presence of inflammation, as is the case in atherosclerosis, HDL can become dysfunctional or even pro-inflammatory [135]. HDL modification includes alterations in the concentration or function of HDL components, which is accompanied by impairment of RCT and HDL antioxidant capacity.

Oxidation of apoA-I by myeloperoxidase

Atherosclerosis is characterized by the accumulation of lipoprotein-derived lipids and inflammatory cells in the affected arterial wall, resulting in a state of heightened oxidative stress that is manifested by the appearance of oxidized lipoproteins. While oxidized LDL (oxLDL) induces atherosclerosis, HDL promotes atheroprotection by reversing the stimulatory effect of oxLDL on monocyte infiltration. Despite the undeniable atheroprotective properties of HDL, it is now acknowledged that high HDL levels do not necessarily imply atheroprotection, suggesting that the quality of HDL may be just as crucial as its quantity. Lately, the oxidation of apoA-I bound to HDL by myeloperoxidase (MPO) has been identified as an important pathway for generating dysfunctional HDL particles.

Myeloperoxidase is a heme protein that is highly expressed by macrophages in human atherosclerotic lesions [136]. This enzyme mediates the production of hypochlorous acid (HOCl), which converts tyrosine to 3-chlorotyrosine. A series of findings strongly indicate that MPO contributes to HDL oxidation, this way producing dysfunctional forms of the lipoprotein. Specific MPO-mediated nitrosylation and chlorination of Tyr-192 of apoA-I has been observed in HDL isolated from atherosclerotic tissues [137]. The chlorination of Tyr-192 selectively impairs the ability of apoA-I to promote ABCA1-dependent cholesterol efflux [137-139]. Although the exact mechanism remains under investigation, it has been proposed that the lysine residue (Lys226) of the YxxK motif (Y = tyrosine, K = lysine, x = unreactive amino acid) in which Tyr192 lies (Figure 1.11a), is responsible for the site-specific chlorination of tyrosine residues by MPO [140]. Furthermore, the resistance of Tyr115, which also resides in a YxxK motif, to chlorination has been associated with the presence of a nearby methionine residue (Met112) in an MxxY motif (Figure 1.11a) [140]. The fact that the alkyl thiol of methionine reacts with HOCl more readily than the side chain of any other common amino acid [141], including tyrosine, further supports the hypothesis that adjacent methionine residues inhibit tyrosine chlorination, either by scavenging chlorinating intermediates or by disrupting the secondary structure of the protein [142].

Based on the data available and the crystal structure of lipid-free apoA-I, two different models have been proposed to describe the oxidative inactivation of apoA-I by myeloperoxidase (Figure 1.11b). According to the first one, the oxidation of

Met112 and chlorination of Tyr 192 or modification of Lys226 might cause disruption of the central and C-terminal bundle domain of lipid-free apoA-I, respectively. This could alter the distribution of surface charge which would prevent apoA-I interaction with ABCA1. The second model is based on the observation that residues Tyr192, Met86, Met148, and Lys226 reside in or near loops that likely serve as hinges when the protein remodels in order to associate with lipid. It is, therefore, suggested that oxidative modification of these residues alters the remodeling pathway and generates abnormal apoA-I structures that fail to interact with ABCA1 [143].

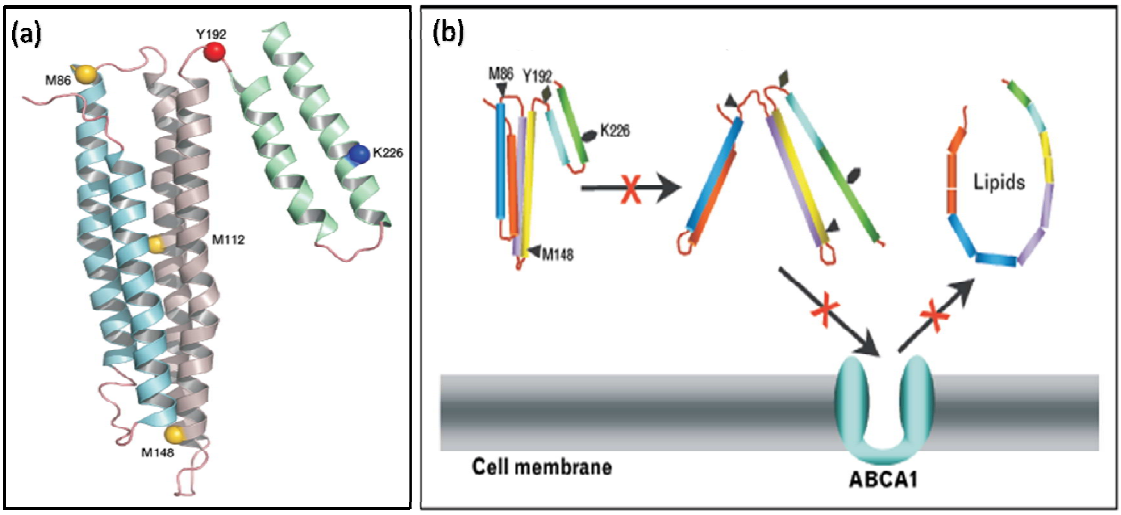

Figure 1.11 (a) Amino acids implicated in the oxidative inactivation of ABCA1 activity of apoA-I are located in critical regions of the apolipoprotein [143]. **(b)** A model for altered remodeling of apoA-I after oxidation by myeloperoxidase [143].

Finally, a recent study demonstrates that MPO-mediated oxidation of Met148 can lead to apoA-I's inability to activate LCAT *in vitro* [144]. In more detail, oxidation of Met148 to methionine sulfoxide associated quantitatively with the loss of LCAT activity, while reversing oxidation with methionine sulfoxide reductase restored the ability of HDL to activate LCAT. These results are also theoretically supported by the localization of this specific methionine residue near the center of the LCAT activation domain of apoA-I. In fact, the authors propose that oxidation of Met148 disrupts the central loop and the conformation of helix 6 in a way that leads to the relocation of these residues from the protein's hydrophobic face to its hydrophilic face. This process disturbs the LCAT activation site and diminishes apoA-I's ability to activate this enzyme.

In conclusion, the oxidative regulation of reverse cholesterol transport implicates the MPO-mediated modification of specific methionine and tyrosine residues in apoA-I which results in the inability of the oxidized protein to activate ABCA1 and LCAT, two key-steps in cholesterol efflux from macrophages. Thus, oxidation of apoA-I by MPO probably plays a critical role in promoting foam cell formation and atherogenesis. In the future, it would be worth to determine whether oxidation of apoA-I interferes with ABCG1- and SR-BI-mediated cholesterol efflux, two pathways which are also implicated in macrophage cholesterol homeostasis.

1.5 NATURALLY OCCURING MUTATIONS OF APOA-I

Various naturally occurring mutations of apoA-I have been described in humans (Figure 1.12), most of which are caused by single amino acid substitutions. From a total of 46 reported natural mutations in apoA-I to date, roughly half of them (25) are associated with low plasma HDL levels while the rest are known to cause no alterations in HDL [145]. Mutations associated with low concentrations of HDL are divided into two main groups; those which exhibit reduced capacity to activate LCAT and those associated with amyloidosis. The mutations that result in poor activation of LCAT, span the 107-235 region of apoA-I but are mainly clustered on and in the vicinity of helix 6. The rest of the mutations, which are found in amyloid deposits, are predominantly located at the N-terminus of the protein [145,146]. The natural apoA-I mutants that were examined in the present study are described below.

ApoA-I(Leu141Arg)$_{Pisa}$

In apoA-I(L141R)$_{Pisa}$ the thymidine to guanosine conversion in the apoA-I gene leads to the substitution of the hydrophobic leucine by the positively charged arginine at residue 141 of the encoded protein, which according to its secondary structure is located on helix 5 (Figure 1.8a). It has been shown that this single-amino acid substitution does not significantly alter the number of α-helical residues in the lipid-free protein. However, this mutation destabilizes the protein, suggesting that Leu141 may be involved in a small number of tertiary interactions, such as leucine zipper-like structures that may be affected by the mutation. The destabilizing effect of the L141R mutation may also result from new electrostatic interactions created by Arg141 in the

mutant protein, which may affect both the tertiary conformation and the stability of apoA-I [147].

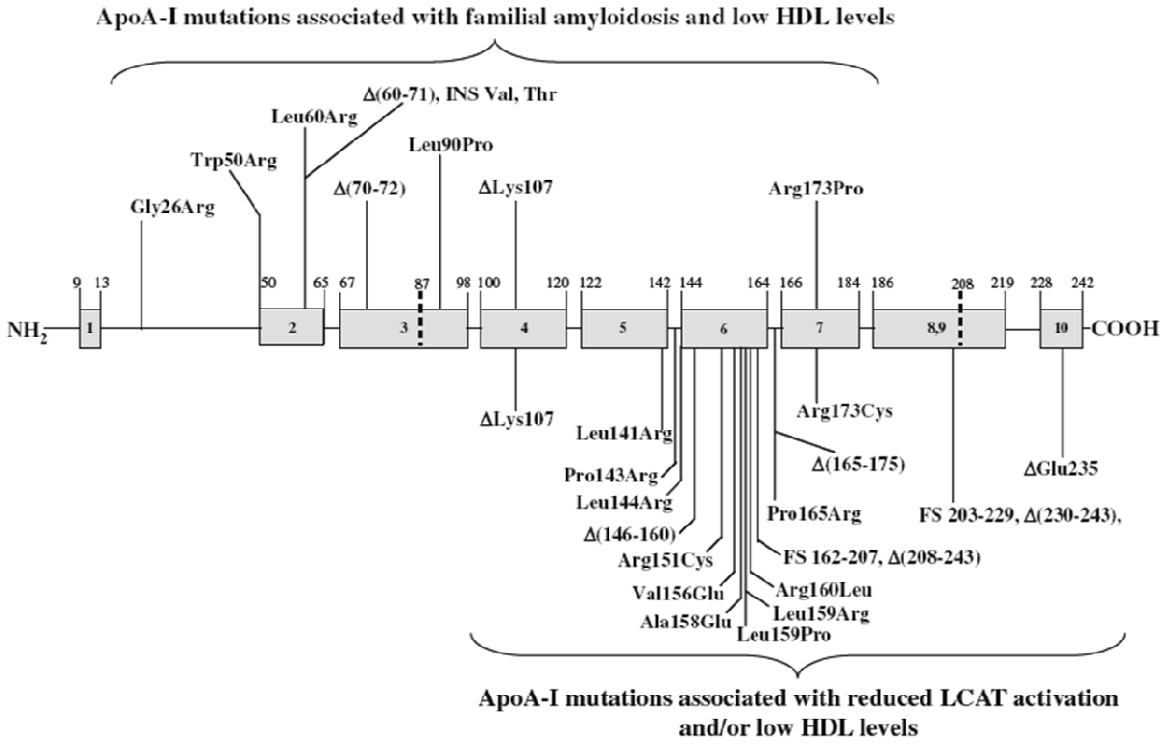

Figure 1.12 Naturally occurring apoA-I mutations that produce pathological phenotypes. The shaded boxes represent the α-helices of the molecule as determined by its sequence [7].

Compound heterozygotes (hemizygotes) for a null allele and the Leu141Arg missense mutation in the apoA-I gene are presented with complete HDL deficiency, relatively increased concentration of proapoA-I in their plasma relative to mature apoA-I and elevated LDL cholesterol concentration [148]. The increased plasma concentration of the precursor of apoA-I indirectly indicates that apoA-I(L141R)$_{Pisa}$ undergoes enhanced catabolism and thereby contributes to HDL deficiency. Since hemizygotes for apoA-I(L141R)$_{Pisa}$ develop massive corneal opacities, arterial hypertension and premature coronary heart disease (CHD), it is understandable that this structural variant of apoA-I may well confer a risk for premature atherosclerosis. On the other hand, heterozygotes for either the null allele or the apoA-I(L141R)$_{Pisa}$ variant develop hypoalphalipoproteinemia with half-normal levels of HDL compared to unaffected subjects [148].

Subsequent studies in four hemizygotes for this mutation have revealed that the ability of their plasmas to esterify cholesterol in either endogenous or exogenous lipoproteins as well as promote cholesterol efflux was significantly reduced [149]. Analysis of the distribution of HDL subclasses in plasmas of hemizygotes has demonstrated the presence of preβ1-HDL and low concentrations of α-migrating particles corresponding to α4-HDL. Interestingly, preβ-HDL particles consisted of both the wild type and the mutated isoform of apoA-I at approximately equal amounts, while the mutated isoform was absent in larger α-migrating HDL particles [149]. In other words, apoA-I(L141R)$_{Pisa}$ was found to interfere with the formation of lipid-rich α-HDL but not with that of lipid-poor preβ-HDL. However, latest data have shown that the functional defect caused by this apoA-I variant can be corrected by treatment with LCAT [150]. According to this study, simultaneous treatment of mice with adenoviruses expressing the apoA-I(L141R)$_{Pisa}$ variant and human LCAT normalized the plasma apoA-I, HDL cholesterol levels, and the CE/TC ratio. It has also restored normal preβ- and α-HDL subpopulations and generated spherical HDL.

ApoA-I(Leu159Arg)$_{Finland}$

The thymidine to guanosine point mutation substituting arginine for leucine at residue 159 (helix 6) of the mature apoA-I protein (Figure 1.8a) gives rise to apoA-I(L159R)$_{Finland}$. Serum lipid and lipoprotein analysis of heterozygous patients has indicated a significant reduction in serum HDL-cholesterol (80%) as well as apoA-I (75%) concentrations compared to the unaffected subjects. However, despite the noticeably low levels of HDL-cholesterol, heterozygotes for apoA-I(L159R)$_{Finland}$ do not develop CAD. In addition, serum apoA-II concentration was also reduced to about 50% of normal, while serum triglyceride concentrations were elevated [151]. Pedigree analysis has revealed an autosomal-dominant inheritance pattern of this phenotype.

Miettinen *et al* have studied the effect of the apoA-I(L159R)$_{Finland}$ mutation on lipoprotein profile, apoA-I kinetics, LCAT activation, and cholesterol efflux in nine carriers of this apoA-I variant [152]. Apart from diminished serum HDL-cholesterol level, these patients exhibited several other lipoprotein abnormalities. Non-denaturing gradient gel electrophoresis of HDL showed disappearance of particles at the 9.0- to 12-nm size range (HDL_2-type) and the presence of small 7.8- to 8.9-nm (mostly HDL_3-type) particles only. Experiments with reconstituted proteoliposomes showed

that the LCAT activation by mutant apoA-I was severely compromised. In fact, the capacity of apoA-I(L159R)$_{Finland}$ protein to activate LCAT was reduced to 40% of that of the wild-type apoA-I. Interestingly, *in vitro* experiments using [^{3}H]cholesterol-loaded human fibroblasts and the apoA-I(L159R)$_{Finland}$ isoform combined with phospholipid revealed no impact of the mutant protein neither on phospholipid binding or nor on cholesterol efflux [152]. Moreover, studies on apoA-I kinetics supported the accelerated catabolism of the mutant protein which could account for the dramatic reduction of serum HDL-cholesterol and apoA-I levels. These results have been later confirmed by combined *in vivo*, *ex vivo*, and *in vitro* approaches [153]. In more detail, adenovirus-mediated expression of apoA-I(L159R)$_{Finland}$ in both wild-type mice and in apoA-I-deficient mice expressing native human apoA-I, decreased apoA-I and high density lipoprotein cholesterol concentrations. In this case, apoA-I(L159R)$_{Finland}$ was degraded in the plasma, and the extent of proteolysis correlated with the most significant reductions in murine apoA-I concentrations. Secretion of apoA-I was also decreased from primary apoA-I-deficient hepatocytes when human apoA-I was co-expressed with apoA-I(L159R)$_{Finland}$ following infection with recombinant adenoviruses, a condition that mimics secretion in heterozygotes. Based on the above data by McManus *et al,* the increased proteolytic degradation along with the impaired secretion of the mutant protein is recognized as the mechanism responsible for the hypoalphalipoproteinemia in heterozygous carriers of the naturally occurring apoA-I(L159R)$_{Finland}$ variant [153].

In conclusion, although the apoA-I(L159R)$_{Finland}$ point mutation does not alter the properties of apoA-I involved in promotion of cholesterol efflux, it interferes with the formation of lipid-rich α-HDL due to the inefficient esterification of the cholesterol in preβ-HDL particles by the endogenous LCAT. Similar to apoA-I(L141R)$_{Pisa}$, treatment with LCAT can rescue the abnormal phenotype produced by apoA-I(L159R)$_{Finland}$ [150].

1.6 THERAPEUTIC TARGETING OF APOA-I

Pharmacologic intervention for the treatment of atherosclerosis originally focused on lowering serum LDL-cholesterol concentrations as a therapeutic target. Since then, numerous studies highlighting the powerful anti-atherogenic effects of HDL have turned efforts to reduce cardiovascular morbidity and mortality, towards the elevation of apoA-I and HDL-cholesterol levels. In order to achieve this, several therapeutic strategies have been developed.

In this context, the beneficial effects of parenteral infusion of full-length apoA-I on atherosclerosis have been examined. In more detail, subjects with heterozygous familial hypercholesterolemia were infused with recombinant proapoA-I, which resulted in stimulation of fecal steroid excretion, suggesting promotion of RCT [154]. In addition, recombinant $apoAI_{Milano}$ has also been used for treatment of atherosclerosis. This apoA-I variant has displayed remarkable atheroprotective activities and has introduced the possibility of directly reducing the burden of atherosclerosis in experimental models [155]. In fact, in a small clinical trial, infusion of recombinant apoA-I_{Milano} complexed with phospholipids caused regression of atherosclerotic lesions in coronary patients [156]. An alternative strategy that involves the selective delipidation of HDL *ex vivo* resulting in lipid-poor apoA-I is currently under development [157]. Among the anti-atherogenic strategies targeting apoA-I lies the generation of several apoA-I mimetic peptides. These are small amphipathic peptides of 18-22 amino acids, based on the apoA-I sequence in a way that they maintain the fundamental properties of apoA-I, such as the ability to promote cholesterol efflux and to activate LCAT. So far, a considerable number of apoA-I mimetic peptides has been examined for their therapeutic potential. Administration of the prototypical peptide L-5F has reduced the progression of atherosclerosis in mice [158]. Another peptide with an almost identical sequence to L-5F, called D-4F, has been shown to reduce atherosclerosis without raising plasma levels of HDL-cholesterol [159]. This orally administered peptide can also promote macrophage RCT in mice and has been suggested to enhance the anti-inflammatory functions of HDL [160]. Finally, ETC-642, a single helical 22-amino-acid-long amphipathic peptide complexed with phospholipids, demonstrates enhanced LCAT-activating ability and has now reached Phase II stage of clinical development.

Emerging strategies to raise the levels of apoA-I, and hence of HDL-cholesterol, include increasing the production or inhibiting the catabolism of this protein. According to current understanding on the transcriptional regulation of the apoA-I gene (Figure 1.4b), elevating de novo production of apoA-I could at least theoretically be achieved by the use of PPARα agonists, such as fibrates. Furthermore, the orphan nuclear receptor LRH-1 has been shown to directly bind to the apoA-I promoter and upregulate apoA-I transcription, this way offering a potential therapeutic strategy. On the other hand, farnesoid X receptor (FXR) negatively regulates apoA-I transcription, therefore, suggesting that FXR antagonism could present another approach to upregulation of apoA-I expression. As far as inhibiting the catabolism of apoA-I is concerned, lipolytic enzymes of the HDL pathway have gained the main focus (Figure 1.7). Hepatic lipase (HL) hydrolyzes both HDL triglycerides and phospholipids and leads to increased filtration and catabolism of the remaining apoA-I. Consequently, pharmacological inhibition of HL is expected to impede apoA-I catabolism and increase plasma levels of the protein. Nevertheless, the involvement of HL in the lipolysis of atherogenic apoB-containing particles raises significant concerns. Endothelial lipase (EL) is also active in hydrolyzing HDL phospholipids and results in renal catabolism of apoA-I. Several findings support the idea that pharmacological inhibition of EL would most probably increase apoA-I and HDL-cholesterol levels [161,162]. Therefore, EL is considered a rather promising target for drug development.

In the context of raising HDL levels as the current focus on CHD treatment, the rationale of CETP inhibition has also been extensively examined. Given that CETP transfers cholesteryl esters (CE) from HDL to apoB-containing lipoproteins in exchange for triglycerides, inhibition of this molecule's function results in an increase of the cholesterol ester content in HDL. On the basis of this principle, several CETP inhibitors, such as JTT-705 and torcetrapib, as well as an anti-CETP vaccine (CETi-1) have been developed. To date, four large-scale clinical trials evaluating the efficacy of torcetrapib on cardiovascular morbidity and mortality have been completed [163-168]. However, the results of these studies disproved all expectations. Although treatment with this CETP inhibitor associated with a considerable increase in HDL cholesterol and a decrease in LDL cholesterol, no significant decrease in the progression of coronary atherosclerosis was observed. In fact, patients on torcetrapib exhibited a substantial increase in major cardiovascular events. Furthermore,

administration of torcetrapib associated with elevated systolic blood pressure, augmented levels of aldosterone and electrolytes disturbances. Apart from these off-target effects, the inability of very high blood HDL cholesterol levels to protect, the induction of dysfunctional HDL and the direct atherogenic effect of CETP inhibition have all been considered as possible causes for the unfavorable clinical outcome of torcetrapib treatment. Despite the overall disappointment, the failure of the CETP inhibitor torcetrapib has opened up a new perspective in the field of HDL targeting in a way that HDL-cholesterol concentration is no longer considered to reflect the atheroprotective properties of the HDL particles. Consequently, the HDL-focused therapeutic approaches should not limit in raising plasma HDL-cholesterol levels rather than raising the anti-atherosclerotic components of HDL.

On the whole, since search for therapies to reduce cardiovascular morbidity and mortality have turned to raising HDL-cholesterol levels and/or improving HDL function, apoA-I has emerged as a promising therapeutic potential. This fact has lead to several therapeutic approaches many of which directly or indirectly target apoA-I in multiple ways.

Specific Aims, Work Plan and Goals

Taking all the above into consideration, it becomes clear that elucidating the pathways that render apoA-I, and consequently HDL, dysfunctional will provide valuable insights in the atherogenic process and probably offer a solid therapeutic approach. In order to understand the etiology of genetically determined low levels of HDL as well as investigate the mechanisms leading to the ineffective actions of this lipoprotein, the present master thesis aimed at generating the appropriate biological tools for the future exploration of these research fields.

For this purpose, the project comprised of two specific aims: a) the generation of recombinant adenoviruses carrying the apoA-I(Met148Ala) and apoA-I(Tyr192Ala) mutations, and b) the generation of wild-type hapoA-I, hapoA-I(Leu141Arg) and hapoA-I(Leu159Arg) transgenic mice.

The work plan of the above specific aims included the following steps:

(I) Generation of recombinant adenoviruses expressing apoA-I(Met148Ala) and apoA-I(Tyr192Ala)

- Generation of the Met148Ala and Tyr192Ala mutations in the apoA-I gene.
- Cloning of the apoA-I(Met148Ala) and apoA-I(Tyr192Ala) into the pAdTrack-CMV shuttle vector.
- Generation of recombinant adenoviral vectors using the AdEasy method.
- Titration of adenoviruses using the Fluorescence Forming Assay.

(II) Generation of wild-type hapoA-I, hapoA-I(Leu141Arg) and hapoA-(Leu159Arg) transgenic mice

- Subcloning of the wild-type apoA-I, apoA-I(Leu141Arg) and apoA-I(Leu159Arg) into the pBluescript-TTR1 vector.
- Preparation of the TTR1-apoA-I injection fragments.
- Genotyping of the founders by Southern blot and PCR.

As far as the first part of the project is concerned, the ultimate goal is to investigate the MPO-mediated mechanisms for generating dysfunctional HDL. Although normal HDL is anti-inflammatory, recent studies have demonstrated that MPO-dependent oxidation of apoA-I blocks HDL's ability to remove excess cholesterol from cells through the ABCA1 pathway, thus bringing HDL into a pro-inflammatory state. Furthermore, myeloperoxidase has been found to target specific tyrosine and methionine residues of apoA-I, including Met148 and Tyr192. In order to investigate the mechanisms resulting in MPO-mediated impediment of normal apoA-I function, the apoA-I(M148A) and apoA-I(Y192A) adenoviruses were generated. The properties of each of the Ad-GFP-apoA-I mutants will be studied both *in vitro* and *in vivo* through adenovirus-mediated gene transfer in apoA-I knockout mice. Apart from Ad-GFP- apoA-I(M148A) and Ad-GFP- apoA-I(Y192A), Ad-GFP-MPO will also be generated and co-infection of the mice with adenoviruses expressing either of the two mutants and human myeloperoxidase will offer valuable information on the *in vivo* effect of myeloperoxidase on plasma lipids, distribution, size and shape of HDL. Overall, since MPO-oxidation represents a mechanism for converting cardioprotective HDL into a dysfunctional form, this research will provide valuable insights in biogenesis of atherogenic HDL.

With regard to the second part of the project, the generation of transgenic mice carrying the naturally occurring variants of human apoA-I, apoA-I(Leu141Arg)$_{Pisa}$ and apoA-I(Leu159Arg)$_{Finland}$, will provide long-term animal models that will facilitate their *in vivo* study. Both mutants belong to the apolipoprotein A-I variants whose reduced capacity of LCAT activation accounts for the low HDL levels observed in carriers of either mutation. Previous studies in our laboratory using adenovirus-mediated gene transfer in mice have demonstrated that treatment with LCAT can restore the aberrant HDL phenotype present in these cases. Generating transgenic mice carrying either of the two apoA-I mutants will allow in-depth investigation of their abnormal phenotype and possibly offer a new perspective in diagnosis, prognosis or even therapy. Studying the properties of these structural mutations in apoA-I *in vivo* can significantly contribute to the understanding of the molecular mechanisms affecting HDL biogenesis and lipoprotein homeostasis in the plasma. Finally, investigation of the effect of these mutations on the interactions between apoA-I and proteins involved in key-steps of HDL metabolism, could uncover the etiology of genetically determined low levels of HDL.

2. MATERIALS AND METHODS

2.1 MATERIALS

Cell Culture Media and Reagents

Dulbecco's modified Eagle medium (DMEM high glucose), the heat inactivated Horse Serum, the antibiotics penicillin/streptomycin, as well as Lipofectamine 2000 were all purchased from Invitrogen/Life Technologies. The Fetal Bovine Serum (FBS) was purchased from BioChrom Labs.

Restriction Endonucleases and Modifying Enzymes

The restriction enzymes were purchased from New England Biolabs and Minotech, IMBB. The T4 DNA ligase was purchased from New England Biolabs, while the Shrimp Alkaline Phosphatase (SAP) and the Large Fragment of DNA Polymerase I (Klenow Fragment) was purchased from Roche and GIBCO/BRL, respectively.

PCR Reagents

The dNTPs, the GoTaq Flexi DNA Polymerase along with the 5x Green GoTaq Flexi Buffer and the $MgCl_2$ solution were purchased from Promega.

Oligonucleotides

All DNA oligonucleotides used in this study were synthesized in the laboratory of Michrochemistry in IMBB, FORTH.

Antibodies

The goat anti-human apolipoprotein A-I polyclonal antibody and the mouse anti-actin monoclonal antibody were purchased from Chemicon International Inc. The anti-mouse-HRP antibody, as well as the anti-goat-HRP antibody was purchased from Sigma-Aldrich.

2.2 METHODS

Agarose Gel Electrophoresis

The used agarose gels were set up in 1x TAE (50x TAE: 121 g Tris, 18,6 g EDTA, 28,55 mL acetic acid glacial) containing 0.5 % - 1.5 % agarose, depending on the estimated size of the expected DNA fragments. The solution was boiled in a microwave oven and cooled down to approximately 50 °C. 4 μL of ethidium bromide solution (10 mg/ml) were added per 100 mL of agarose solution. λDNA digested with BstEII was used as a DNA ladder. The samples were then mixed with 6x gel loading dye (0,25% bromophenol blue, 0,25% xylene cyanol FF, 30% glycerol) and run in tanks under the appropriate electrical field (50-120 V). The bands were visualized using the TFX-35M UV transilluminator (GIBCO/BRL).

Extraction of DNA Fragments from Agarose Gels

To extract DNA from an agarose gel, the Wizard® SV Gel and PCR Clean-Up System by Promega was used following the manufacturer's protocol after cutting the desired band from the gel with a scalpel blade. The concentration of the gel-purified DNA fragment was determined by either gel quantitation or spectrophotometry.

Restriction Enzyme Digestion of DNA

The plasmids and PCR products were digested with the appropriate restriction enzymes. The digestions were performed in the proper reaction conditions as recommended by the manufacturer (New England Biolabs or Minotech, IMBB). Generally, small amounts of DNA (≤1 μg of DNA) were incubated at 37 °C for 1 h, while in large-scale digests 5-15 μg of DNA were incubated at 37 °C for 3-5 hrs.

Dephosphorylation of DNA

The Shrimp Alkaline Phosphatase (SAP) was used for the dephosphorylation of digested DNA fragments. The reaction assay was performed by adding 1 μL of SAP in the digestion, followed by incubation at 37^{o}C for 1 h and heat inactivation of the enzyme at 65^{o}C for 20min. The reaction mixture was then purified with Wizard® SV Gel and PCR Clean-Up System by Promega. The concentration of the purified DNA fragment was determined by gel quantitation.

Treatment of Digested DNA Fragments with Klenow Fragment

The Large Fragment of DNA Polymerase I (Klenow Fragment) was used to fill in 5′-protruding ends of digested DNA fragments. The reaction was set up according to the manufacturer's recommendations and the mixture was incubated at room temperature for 15 minutes. The reaction was terminated by addition of 0,5M EDTA pH 8.0 at a final concentration of 10 mM and heat inactivation of the enzyme at 75^{o}C for 20min. The reaction mixture was then purified with Wizard® SV Gel and PCR Clean-Up System by Promega. The concentration of the purified DNA fragment was determined by gel quantitation.

Ligation Reaction

For ligations of digested DNA fragments, the T4 DNA Ligase purchased from New England Biolabs was used and the reactions were performed in a final volume of 20 μL. The molar ratio of insert to vector was 3:1 to 5:1 molecules by using 50-100 ng of the vector DNA. The final mixture was incubated at 4 ^{o}C overnight, and the terminated ligation reaction was subsequently used for transformation of 100 μL chemically competent DH10β cells.

Transformation of Chemically Competent DH10β Cells

- ✓ Approximately 100 μL of frozen competent cells is thawed on ice.
- ✓ The appropriate amount of DNA, depending on the specific reaction setup, is added to the cells. In the case of a ligation reaction, the entire amount is used for the transformation.
- ✓ Incubate on ice for 30 min.
- ✓ Perform heat shock at 42 °C for 45 sec in a heat block.
- ✓ Cells are immediately quick-chilled on ice.
- ✓ Add 900 μL LB.
- ✓ Incubate cells at 37°C for 1 h.
- ✓ If the cells were transformed with DNA derived from a ligation reaction:
  - Centrifuge at 2000 rpm for 5min, RT.
  - Decant ~850 μL of the LB and resuspend pellet in the remaining LB.
  - Spread the entire amount of resuspended bacteria on the appropriate selective plate and incubate at 37°C overnight.

✓ If the cells were transformed with plasmid DNA for amplification:
- Spread 100 µL of bacteria on the appropriate selective plate.
- Incubate at 37°C overnight.

Cultivation of Bacteria

Escherichia coli cells were grown in and on LB medium (10g NaCl, 5g yeast extract, 10g tryptone, ddH_2O up to 1L and autoclave). Depending on the resistance cassette on the transformed plasmids, appropriate antibiotics were used to a final concentration of 100µg/mL for ampicillin, 50µg/mL for kanamycin and 25µg/mL for chloramphenicol. The bacterial cells in shaking cultures had a ratio of one volume growth medium to five volumes air. *E.coli* cultures were incubated at 37 °C overnight.

Plasmid Mini-Preparation by Alkaline Lysis of Bacterial Cells

The preparation of small amounts of plasmids was performed as described below:

✓ 2 mL of the appropriate selective LB medium is inoculated with a single bacterial colony and incubated at 37 ^{o}C overnight by vigorous shaking.
✓ ~1,5 mL of the culture is transferred into a 1,5 mL eppendorf tube.
✓ Spin down culture at 13000 rpm for 1 min.
✓ Discard supernatant and resuspend pellet in 150 µL P1 Buffer (QIAGEN) with 100 µg/mL RNase A by pipetting.
✓ Add 150 µL P2 Buffer (QIAGEN) and mix by vigorous shaking.
✓ Incubate at room temperature for maximum 5 minutes.
✓ Add 150 µL P3 Buffer (QIAGEN) and mix by vigorous shaking.
✓ Incubate on ice for 10 min.
✓ Centrifuge at 13000 rpm for 15 minutes.
✓ Transfer supernatant in a new 1,5 mL eppendorf tube.
✓ Add 2/3 volumes (300 µL) isopropanol. Mix by inversion.
✓ Centrifuge at 13000 rpm for 15 minutes.
✓ Discard supernatant and add 500 µL 75% ethanol.
✓ Centrifuge at 13000 rpm for 5 minutes.
✓ Discard supernatant and allow pellet to air-dry.
✓ Resuspend pellet in 30-35 µL water.

Plasmid Midi- and Maxi-Preparation

The large-scale preparations of plasmids were performed using QIAGEN-tip100 and tip-500 according to the QIAGEN Plasmid Midi and Maxi kit protocols, respectively. The concentration of the purified DNA was determined by spectrophotometry.

Ethanol Precipitation of DNA

- ✓ Add 2 ½ volumes of ethanol absolute and 1/10 volumes of CH_3COONa 3M.
- ✓ Incubate at -80^{o}C for 20 minutes or at -20^{o}C overnight.
- ✓ Centrifuge at 13000 rpm for 15 minutes.
- ✓ Discard supernatant and add 500 μL cold 75% ethanol.
- ✓ Centrifuge at 13000 rpm for 5 minutes.
- ✓ Discard supernatant and air-dry DNA pellet.
- ✓ Resuspend pellet in H_2O.

Quantitation of Nucleic Acids by Spectrophotometry

To determine the concentration of nucleic acids the Jenway 6405 UV/VIS Spectrophotometer was used. 1 mL of ddH_2O was added in the cuvette and used to calibrate the instrument. The samples were diluted 1:200 in ddH_2O (5 μL DNA or RNA sample + 995 μL ddH_2O) and the readings were taken at wavelengths of 260 nm and 280 nm. The reading at 260 nm allows calculation of the concentration of nucleic acid in the sample. Pure preparations of DNA and RNA have OD_{260}/OD_{280} values of 1.8 to 2.0. The concentration of each sample is calculated as indicated below:

OD_{260} * 50 ng/μL * dilution factor, for double-stranded DNA
OD_{260} * 35 ng/μL * dilution factor, for single-stranded DNA
OD_{260} * 40 ng/μL * dilution factor, for RNA

DNA Sequencing

All sequencing reactions were performed by the laboratory of L. Spanos in IMBB, FORTH.

Site-Directed Mutagenesis by Overlap Extension Using PCR

Single base substitutions in the ApoA-I gene were generated by overlapping PCR. In this technique of site-directed mutagenesis, complementary oligodeoxyribonucleotide primers are used in PCR to generate two DNA fragments having overlapping ends. These fragments are combined in a subsequent 'fusion' reaction and the resulting product is amplified further by PCR. The pCDNA3.1-apoAIg(ΔBglII) (Koukos *et al*, 2007) plasmid was used as template for the generation of Met148Ala and Tyr192Ala mutations in the apoA-I gene. For the amplification, a set of 5'- and 3'-flanking primers designated apoAIg F and apoAIg R was used. The first primer was designed to carry the XbaI (5'-TCTAGA-3') and BglII (5'-AGATCT-3') recognition sites, and the second primer carried the EcoRV (5'-GATATC-3') recognition site. The primers and the PCR conditions used to create apoA-I(M148A) and apoA-I(Y192A) are shown in the tables below.

Oligonucleotide sequence of primers used in PCR amplifications	
apoAIg F	5' - GCTCTAGATCTGACATAAATAGGCCCTGC - 3'
apoAIg R	5' - GCGGATATCCAGGCCTTGTTTGAGCC - 3'
apoAI(M148A) F	5' - CCACTGGGCGAGGAG**GCG**CGCGACCGCGCGCG - 3'
apoAI(M148A) R	5' - CGCGCGCGGTCGCGCGCCTCCTCGCCCAGTGG - 3'
apoAI(Y192A) F	5' - GCCAGACTGGCCGAG**GCC**CACGCCAAGGCCAC - 3'
apoAI(Y192A) R	5' - GTGGCCTTGGCGTGGGCCTCGGCCAGTCTGGC - 3'

apoA-I (M148A) fragments		
94°C	3min	
94°C	1min	**30 cycles**
62°C	1min	
72°C	2min	
72°C	5min	

apoA-I (Y192A) 1-1710bp		
94°C	3min	
94°C	1min	**33 cycles**
70°C	1.5min	
72°C	2min	
72°C	5min	

apoA-I (Y192A) 1680-2210bp		
94°C	3min	
94°C	1min	**30 cycles**
62°C	1min	
72°C	2.5min	
72°C	5min	

Overlapping PCR		
94°C	3min	
94°C	1min	**30 cycles**
64°C	1min	
72°C	2.5min	
72°C	5min	

.

Subculture of Cell Lines

In the present study four different cell lines were used; HepG2 (human hepatocellular liver carcinoma cells), 911 (human embryonic retinoblasts), HEK293T (human embryonic kidney 293T cells) and HaCaT (human keratinocytes). All cell cultures were grown in T75 flasks and maintained at 37°C in a 5% CO_2 incubator. Each cell line was subcultured as soon as a confluent monolayer had been formed in the flask according to the procedure described below:

- ✓ Discard supernatant fluid from a confluent monolayer of a T75 cell culture flask.
- ✓ Wash with 2 mL trypsin pre-warmed at 37^{o}C.
- ✓ Add 2 mL trypsin to the T75 flask and incubate at 37^{o}C for maximum 5 minutes.
- ✓ Add 2 mL of complete growth medium (DMEM, 10% FBS, 1% P/S) to the flask and gently detach the cells from the surface by use of a 5 mL serologic pipette.
- ✓ Transfer the cells in a 15 mL falcon tube and pipette up and down using a blue tip adjusted to a 10 mL serologic pipette in order to break cell clumps.
- ✓ Add 6 mL growth medium.
- ✓ Distribute the appropriate amount (1 mL HepG2, 0,5 mL HEK293T, 1 mL 911, 1 mL HaCaT) of the diluted cell suspension to a new T75 cell culture flask.
- ✓ Incubate at 37°C in a 5% CO_2 incubator for 4-7 days depending on the cell line.
- ✓ The growth medium in the flask is replaced with fresh one every 48h.

Transient Transfection Assay with the $CaPO_4$ method

Overexpression of proteins by transient transfection assays was performed in order to assess the levels of protein expression. For this purpose, p60 and p100 cell culture plates were used. One day before the transfection experiment, the appropriate number of cells (see table below) was plated in the dish and incubated in complete growth medium at 37°C overnight. After 24 hrs the cells have reached the desired density of 60-80% confluency.

Cell culture dish	**Number of cells**		**Final volume of growth medium (mL)**	**DNA (μg)**	**2M $CaCl_2$ (μL)**	**H_2O (μL)**	**2x HBS (μL)**
	HepG2	**HEK293T**					
p60	10^6	500.000	3	15	15,5	up to 125	125
p100	2 x 10^6	10^6	5	30	31	up to 250	250

- ✓ In a 1,5 mL eppendorf tube add the proper amount of DNA, 2M $CaCl_2$ and H_2O. Salmon Sperm DNA Solution (GIBCO/BRL) is used either in samples to be used as controls or to equilibrate the DNA amount in all samples.
- ✓ Add the DNA/ $CaCl_2$ mix to a 2 mL eppendorf tube containing an equal amount of 2x HBS (274 mM NaCl, 10 mM KCl, 1,5 mM $Na_2HPO_4 \cdot H_2O$, 12 mM Dextrose, 42 mM Hepes, pH 7±0,1) dropwise while vortexing.
- ✓ Incubate the final mixture for 15 minutes at room temperature.
- ✓ Mix sample and add the DNA/ HBS mix, dropwise, to the cells.
- ✓ Rock plate back and forth to mix and incubate cells at 37°C in the incubator.
- ✓ 7-17 hrs post-transfection replace the growth medium with fresh one.
- ✓ Incubate for another 24 hrs.
- ✓ Harvest cells and/or collect supernatant.

Cell Lysis Using the Co-IP Lysis Buffer

Cell extracts were collected using the following Co-IP lysis buffer protocol:

- ✓ Remove growth medium from cultured cells.
- ✓ Rinse cells carefully with 2 mL/ 3 mL 1x PBS for each p60 / p100, respectively.
- ✓ Add 1 mL chilled 1x PBS per dish.
- ✓ Scrape attached cells from the dish and transfer cells to a pre-chilled 1,5 mL eppendorf tube.
- ✓ Pellet cells by centrifugion at 5000 rpm for 5 minutes, 4^oC.
- ✓ Discard supernatant.
- ✓ Resuspend pellet in 150 μL Co-IP lysis buffer (20 mM Tris-Cl pH 7,5, 150 mM NaCl, 10% glycerol, 1% Triton X-100) with protease inhibitors PMSF (100 mM stock solution) and Benzamydine (0,5 M stock solution) added prior to use to final concentration 10 μL/mL and 1 μL/mL, respectively.
- ✓ Rotate samples for 30 minutes at 4^oC.
- ✓ Pellet debris by centrifugation at 13000 rpm for 5 minutes, 4^oC.
- ✓ Transfer supernatant in a new 1,5 mL eppendorf tube.
- ✓ Store cell extracts at -80^oC.

Determination of Protein Concentration

The protein concentration in the collected cell extracts was determined using the Bio-Rad *DC* Protein Assay according to the manufacturer's instructions. The reaction of this colorimetric assay is similar to the Lowry protein assay method.

Sodium Dodecyl Sulfate Polyacrylamide Gel Electrophoresis

SDS-PAGE used to fractionate proteins by size. All protein samples were mixed 3:1 with 4 x Sample buffer (5 mL Tris-Cl 1M pH 6.8, 1,6 mL β-mercaptoethanol, 4 mL glycerol, 1,6 g SDS, 8 mg bromophenol blue, ddH_2O up to 20 mL), denatured at 100 °C for 5-10 minutes and loaded on the gel. The BenchMark Prestained Protein Ladder (Invitrogen) was used as a size marker. In the present study 12.5 % acrylamide gels were used to detect and characterize ApoA-I expression. The quantities used for the preparation of the gels are the following:

Separating Gel	**12.5%**	**Stacking Gel**	
ddH_2O	3.2 mL	ddH_2O	3.6 mL
30% acrylamide	4.2 mL	30% acrylamide	900 µL
Separating buffer	2.5 mL	Separating buffer	1.5 mL
10% APS	160 µL	10% APS	60 µL
TEMED	8 µL	TEMED	6 µL
Final Volume	10 mL	Final Volume	6 mL

10x TGS	
Tris	30.3 g
Glycine	144.2 g
SDS	10 g
Final Volume	1 L

Separating Buffer	
Tris	18.165 g (1.5 M)
SDS	0.4 g (0.4% w/v)
pH adjusted with HCl	8.8
Final Volume	100 mL

Stacking Buffer	
Tris	6.05 g (0.5 M)
SDS	0.4 g (0.4% w/v)
pH adjusted with HCl	6.8
Final Volume	100 mL

Electrophoresis was performed in a Bio-Rad Mini-Protean II Vertical Electrophoresis apparatus in 1 x TGS buffer. The running conditions were 50 V until the samples had entered the stacking gel and then 150 V.

Western Blot

Following electrophoresis the proteins were transferred from the gel to a nitrocellulose membrane, where they were detected using antibodies specific to the target protein. The transfer was performed in the Bio-Rad Mini-Protean II by electroblotting in 1 L transfer buffer (100 mL 10x TGS, 200 mL methanol and 700 mL ddH_2O) at 400 mA for 1,5 h. After blotting, the membrane was processed as described below:

- ✓ Wash membrane with TBS-T 0,05 % (1x TBS + 0,05 % Tween 20) for 5 minutes at room temperature shaking slowly.
- ✓ Block membrane with 5 % w/v milk for 1 h at room temperature shaking slowly.
- ✓ Wash membrane with TBS-T 0,05 % for 5 minutes at room temperature shaking.
- ✓ Incubate membrane in the primary antibody according to the table below:

Primary antibody	Dilution	Diluted in	Incubation conditions
goat α – apoAI	1:2000	5 % w/v milk in TBS-T 0,05 %	37°C, 1 h
mouse α – actin	1:5000	TBS-T 0,05 %, 0,02 % NaN_3	4°C, overnight

- ✓ Wash membrane three times with TBS-T 0,05 % for 10 minutes at room temperature shaking.
- ✓ Incubate membrane in the secondary antibody according to the table below:

Secondary antibody	Dilution	Diluted in	Incubation conditions
α – goat IgG HRP	1:4000	5 % w/v milk in TBS-T 0,05 %	RT, 1 h
α – mouse IgG HRP	1:10000	5 % w/v milk in TBS-T 0,05 %	RT, 1 h

- ✓ Wash membrane three times with TBS-T 0,05 % for 10 minutes at room temperature shaking slowly.
- ✓ Wash membrane with 1x TBS for 5 minutes at room temperature shaking slowly.
- ✓ Prepare 1 mL ECL reagent (SuperSignal West Pico Chemiluminescent Substrate, Pierce) per blot, and place on membrane 5 minutes.
- ✓ Drain membrane, wrap in Saran Wrap and place properly in cassette.
- ✓ Expose to film in dark room.

10x TBS	
NaCl	180 g
Tris	121.14 g
pH adjusted with HCl	7.3
Final Volume	2 L

Generation of Recombinant Adenoviral Vectors

The adenoviral recombinants Ad-hapoAI(M148A) and Ad-hapoAI(Y192A) were generated according to the following procedure:

Generation of recombinant adenoviral plasmids by homologous recombination in E. coli

- ✓ Clone the gene of interest into the pAdTrack-CMV shuttle vector.
- ✓ Confirm the presence and orientation of the transgene by restriction analysis.
- ✓ Confirm transgene expression in the shuttle vector by transient transfection assay.
- ✓ Linearize the shuttle vector with *Pme*I restriction enzyme.
- ✓ Gel extraction of the linearized DNA and purification with the Wizard SV Gel and PCR Clean-Up System.
- ✓ Introduce the purified linear DNA into E.coli BJ5183-AD1 cells that carry the pAdEasy-1 adenoviral backbone plasmid by transformation.
- ✓ Plate the entire amount of transformed bacterial cells on an LB/kanamycin plate and grow overnight at 37°C.
- ✓ Pick ~10 of the smallest colonies and perform minipreps using the alkaline lysis method.
- ✓ Perform *Pac*I restriction digestion on candidate clones. Correct recombinants usually yield a large fragment (+30 kb) and a smaller fragment of 3.0 or 4.5 kb, depending on the sites of the homologous recombination. Both types of clones are correct and equally efficient in generating adenoviruses.
- ✓ One of the correct clones is retransformed into competent DH10β cells that are not prone to recombination for large-scale amplification.
- ✓ Pick a single colony and perform maxi-prep using QIAGEN Plasmid Purification kit.

Production of adenovirus in mammalian cells

- ✓ Perform *Pac*I restriction digestion on an appropriate amount (~15 μg) of the recombinant DNA.
- ✓ Precipitate the digested plasmid with ethanol and resuspend in 50 μL ddH_20.
- ✓ ~4,5 μg of *Pac*I-digested DNA are used for transfection of 911 packaging cells with Lipofectamine 2000 as described below:
  - Plate 1,5-2 x 10^6 911 cells in a p100 cell culture plate 24h prior to transfection
  - Prepare 2 separate 1,5 mL eppendorf tubes:
    A: Dilute 20 μL DNA in 230 μL Opti-MEM I medium. Mix gently.
    B: Mix 15 μL of Lipofectamine 2000 reagent in 235 μL Opti-MEM I medium.
  - Incubate for 5 minutes at room temperature.
  - Combine the diluted DNA with diluted Lipofectamine reagent. Mix gently.
  - Incubate the DNA/Lipofectamine reagent mix for 20 min at room temperature.
  - Replace the growth medium in the p100 cell culture plate with DMEM enriched with 2% Heat Inactivated Horse Serum (HIHS) only.
  - Add the DNA/Lipofectamine transfection mix dropwise to the p100 cell culture plate and mix gently by rocking the plate back and forth.
  - Incubate cells at 37°C in a 5% CO2 humidified incubator overnight.
  - Remove the growth medium containing DNA/Lipofectamine mix and add 7 ml fresh DMEM enriched with 2% HIHS, 1% P/S.

- ✓ 48 hrs later confirm transfection efficiency and virus production by monitoring GFP expression, visible with fluorescence microscopy.
- ✓ Maintain transfected cells in the 37°C, 5% CO_2 incubator for 10 to 14 days, until lysis occurs.

Amplification of adenovirus

- ✓ Collect the viral lysate from the p100 cell culture dish and use it to infect a confluent T175 flask of 911 cells in DMEM with 2% HIHS, 1% P/S.
- ✓ 2-3 days later the cells lyse and 2-3mL of viral lysate is used to infect each of 4-5 confluent T175 flasks of 911 cells in DMEM with 2% HIHS, 1% P/S.
- ✓ The cells are harvested 2-3 days post-infection before lysis occurs.
- ✓ Centrifuge cells at 1000 rpm for 10 minutes, 4^oC
- ✓ Decant medium and resuspend pellet in 1mL DMEM, 2% HIHS, 1% P/S.

- ✓ Freeze cells at -80^{o}C and thaw in a 37°C water bath to release virus from cells. Vortex vigorously. Repeat freeze/thaw cycle twice more.
- ✓ Centrifuge at 3500 rpm for 10 minutes, 4^{o}C to pellet the cell debris.
- ✓ The viral lysate is distributed in 1,5mL cryovials and stored at -80^{o}C.

Titration of adenovirus

The Fluorescence Forming Assay (FFA) was performed in order to determine the infectious titer of virus stock. The infectivity titer of adenoviruses is expressed as fluorescence-forming units (FFU) per milliliter.

- ✓ Coat 3 x p35 cell culture plates with grid with 1mL collagen (25 μg/mL).
- ✓ Incubate for 30 minutes at room temperature in the hood.
- ✓ Remove collagen and allow plates to dry.
- ✓ Plate 1-1,5 x 10^6 911 cells in DMEM, 10% FBS, 1% P/S in each p35 cell culture plate and incubate cells at 37°C in a 5% CO_2 humidified incubator overnight.
- ✓ Prepare successive dilutions (from 10^2 to 10^7) of the virus in complete growth medium to a final volume of 1,3 mL.
- ✓ Remove growth medium and add 1 mL from each of the virus dilutions 10^5, 10^6, 10^7 in each of the 3 x p35 plates.
- ✓ Rock plates back and forth to achieve an even distribution of the virus and incubate at 37^{o}C for 2 hrs.
- ✓ Wash each p35 plate once with 1mL of complete growth medium.
- ✓ Add 1 mL of fresh medium and incubate at 37^{o}C for 48 hrs.
- ✓ Remove medium from the plates and wash once with 1 mL 1x PBS.
- ✓ Allow plates to dry in the hood for 15 minutes.
- ✓ Add 1 mL 3% paraformaldehyde (PFA) in each plate for cell fixation.
- ✓ Incubate plates in the hood for 5 minutes.
- ✓ Wash each p35 plate once with 1 mL 1x PBS.
- ✓ Add 1 mL 1x PBS in each plate.
- ✓ Count green cells under a fluorescence microscope.

Titer determination

Example: The total area of the plate is 8 cm^2. If an average of 8 green cells per grid area (0,04 cm^2) is counted in the plate where the 10^6 dilution was added, the titer of the virus is 8 x 200 x 10^6 = 1,6 x 10^9 FFU/mL (*total area*: 0,04 cm^2 x 200 = 8 cm^2).

Preparation of Injection Fragments for the Generation of Human Apolipoprotein A-I Transgenic Mice

Following the construction of plasmids that carry mutated forms of human ApoA-I fused with the transthyretin promoter, the QIAGEN EndoFree Plasmid Maxi Kit was used according to the manufacturer's instructions for the purification of endotoxin-free plasmid DNA. The purified DNA was quantified by spectrophotometry and digested with BamHI/SalI. The 6 kb DNA fragment that would be used for the generation of the transgenic mice was subsequently processed as described below:

Extraction and purification of DNA fragments from low melting point agarose gel

Prepare gel containing 1% low melting point SeaPlaque GTG Agarose, BMA. Load the whole amount of the large-scale digest and 6 μL of the 1 kb DNA Ladder, NEB. Run gel at 75 V for 3-4 hrs. Excise the gel segment containing the DNA fragment using a scalpel blade. In order to extract the DNA from the gel, the agarose was digested with β-Agarase I (New England Biolabs), and the DNA was purified according to the following protocol:

Agarose digestion

- ✓ Weigh the gel slice and equilibrate agarose by adding 1/10 of the final volume 10x β-Agarase I buffer.
- ✓ Incubate samples at 65^{o}C until the agarose is completely melted.
- ✓ Cool to 42^{o}C and incubate the molten agarose with 1 unit of β-Agarase I for each 100 μL of molten agarose for at least 1 h.

DNA purification

- ✓ Chill on ice for 15 minutes.
- ✓ Centrifuge at 13000 rpm for 15 minutes.
- ✓ Remove the DNA-containing supernatant.
- ✓ Add 2 volumes of isopropanol. Mix thoroughly and chill on ice.
- ✓ Centrifuge at 13000 rpm for 15 minutes, 4^{o}C.
- ✓ Discard the supernatant and add 200 μL cold 70% isopropanol.
- ✓ Centrifuge at 13000 rpm for 10 minutes.
- ✓ Discard supernatant and air-dry pellet.
- ✓ Resuspend pellet in 50 μL injection buffer (7,5 mM Tris, 0,1 mM EDTA).

The injection fragments were further purified using the GENECLEAN® Turbo Kit (Q·BIOgene) according to the manufacturer's instructions. The concentration of the DNA fragments was determined both by gel quantitation and by following the Quant-iT™ dsDNA BR Assay Kit protocol for use with the Qubit™ fluorometer. Finally, the purified injection fragments were diluted in EmbryoMAX injection buffer to a final concentration 3 ng/μL.

Serum Collection from Mouse Blood

Blood samples (100-200 μL) from mice were collected in 1,5 mL eppendorf tubes by tail bleeding. Following centrifugation at 5000 rpm for 10 minutes, the serum was transferred in 0,2 mL eppendorf tubes and stored at -80^{o}C. Western Blot was performed in all serum samples for detection of human ApoA-I expression.

Preparation of Genomic DNA from Mouse Tail

- ✓ Remove mouse from cage. Label the mouse's ear.
- ✓ Cut 0,5-1 cm of mouse tail and put it in a 1,5 mL eppendorf tube.
- ✓ Add 500 μL tail buffer and 5 μL proteinase K (stock solution: 10 mg/mL).
- ✓ Incubate at 55^{o}C overnight.
- ✓ Add 1 μL RNase A (stock: 10 mg/mL) and incubate at 37^{o}C for 45 minutes to 1 h.
- ✓ Add 500 μL phenol/chloroform/isoamyl alcohol (25:24:1) and vortex.
- ✓ Centrifuge at 13000 rpm for 15 minutes.
- ✓ Transfer supernatant in a fresh 1,5 mL eppendorf tube.
- ✓ Add 500 μL phenol/chloroform/isoamyl alcohol (25:24:1) and vortex.
- ✓ Centrifuge at 13000 rpm for 15 minutes.
- ✓ Transfer supernatant in a fresh 1,5 mL eppendorf tube.
- ✓ Add 500 μL chloroform and vortex.
- ✓ Centrifuge at 13000 rpm for 10 minutes.
- ✓ Transfer supernatant in a fresh 1,5 mL eppendorf tube.
- ✓ Add 250 μL isopropanol and mix. Notice DNA cloud.
- ✓ Spool DNA on the closed tip of a pasteur pipette and allow to air-dry.
- ✓ Wash DNA into 70% ethanol.
- ✓ Wash DNA into 100% ethanol.
- ✓ Allow DNA to air-dry.
- ✓ Break the tip of the pasteur pipette into a fresh 1,5 mL eppendorf tube.

- ✓ Dissolve DNA in 30 µL TE buffer (10 mM Tris-Cl pH 8.0, 1mM EDTA).
- ✓ Incubate at 37°C for 1 h shaking.
- ✓ Store at 4°C.

Tail Buffer	
1 M Tris pH 8.0	50 mL (50 mM)
0,5 M EDTA	200 mL (100 mM)
5 M NaCl	20 mL (100 mM)
10 % SDS	100 mL (1 %)
Final Volume	1 L

Genotyping of Transgenic Mice Using PCR

The mice were tested for the presence of the transgene by PCR. The genomic DNA extracted from mouse tail was used as template in the PCR reaction. For the amplification, a set of primers designated huApoA-I F and huAapoA-I R was used. The PCR reaction was set up according to the Phusion® Hot Start High-Fidelity DNA Polymerase manual (Finnzymes). The primers and the PCR conditions used for mouse genotyping are shown in the tables below.

Oligonucleotide sequence of primers used in genotyping	
huApoA-I F	5' - AGTTTGAAGGCTCC GCCTTGGGAAA - 3'
huApoA-I R	5' - CACTTCTTCTGGAAGTCGTCCAGGTA - 3'

PCR conditions		
98°C	30 sec	
98°C	10 sec	**35 cycles**
72,4°C	10 sec	
72°C	20 sec	
72°C	5 min	

Genotyping of Transgenic Mice Using Southern Blot

The Southern Blotting technique was used to confirm the successful insertion of the transgene in the mouse genome. 10 µg of each genomic DNA preparation were digested with EcoRI overnight and the resulting fragments were separated by electrophoresis through 0,8% agarose gel set up in 1x TAE. 1 kb DNA ladder purchased from New England Biolabs was used as a size marker. The samples were mixed with 6x gel loading dye and run in tanks for 3-4 hrs under the appropriate electrical field (120 V). The DNA was then denatured *in situ* and transferred from the gel to Amersham Hybond™-N+ positively charged nylon membrane. The DNA attached to the membrane was hybridized to an appropriate radiolabeled probe, and autoradiography was carried out to detect the transgene.

Southern transfer to nylon membrane

- ✓ After electrophoresis, place the agarose gel in a plastic tray and rinse in ddH_2O.
- ✓ Shake gel in denaturing buffer (1,5M NaCl, 0,5 mL NaOH) for 30 min at room temperature. Rinse gel in ddH_2O.
- ✓ Shake gel in neutralizing buffer (1,5M NaCl, 0,5M Tris-Cl pH 7.2, 1mM EDTA pH 8.0) for 15 min at room temperature. Rinse gel in ddH_2O.
- ✓ Repeat the last step.
- ✓ Set up capillary blot as described below.

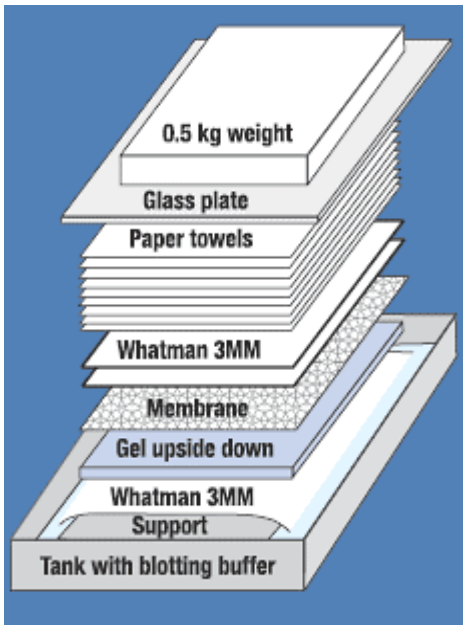

- Fill tray with blotting buffer (20x SSC: 3M NaCl, 0,3M Na_3citrate).Place a platform inside the tray and cover it with 3 sheets of Whatman™ 3 MM filter paper, saturated with blotting buffer.
- Place the gel upside down on the wick and avoid trapping air bubbles beneath it.
- Cut a sheet of Hybond™-N+ nylon membrane to match the size of the gel and place it on the top. Avoid trapping air bubbles beneath the membrane.
- Place 3 sheets of Whatman™ 3 MM filter paper wetted with blotting buffer on top of the Hybond™-N+ nylon membrane.
- Place a stack of absorbent paper towels on top of the 3 MM paper.
- Place a glass plate on the top of the paper towels and put a 0.5 kg weight on the top.

- ✓ Perform upward capillary transfer of DNA at room temperature for 4-16 hrs.

- ✓ After blotting, carefully dismantle apparatus. Confirm transfer of DNA by visualizing the gel under UV-light.
- ✓ Remove membrane and allow it to air-dry at room temperature for 15 minutes.
- ✓ Fix membrane either by UV-crosslinking or by oven baking (80^{o}C for 2 hrs).

Prehybridization

- ✓ Place the membrane into the hybridization box and add the appropriate amount of pre-hybridization solution (5x SSPE, 5x Denhardt's solution, 0,5% w/v SDS).
  - ❖ **20x SSPE pH 7.4**: 3M NaCl, 0,2M NaH_2PO_4, 0,2M EDTA
- ✓ Denature an appropriate amount of sonicated salmon sperm DNA solution by heating to 100°C for 5 min. Chill on ice and add to the pre-hybridization solution to a final concentration of 20 μg/ mL.
- ✓ Carry out the pre-hybridization in a hyb-oven rotating at 65^{o}C for 1 hour.

Radioactive labeling of probe

The ApoA-I probe that was used for detection of the transgene, was radiolabeled following the instructions of the Nick Translation System manual (Invitrogen). The radiolabeled probe was then purified through G-50 Sephadex Columns (Quick Spin Columns, Roche).

Hybridization

- ✓ Denature labeled probe by heating to 100°C for 5 min. Chill on ice immediately and add the probe to the pre-hybridization solution.
- ✓ Carry out hybridization in a hyb-oven rotating at 65^{o}C overnight.

Wash and detection

- ✓ Wash membrane in 2x SSPE + 0,1% w/v SDS at room temperature for 10 minutes.
- ✓ Repeat wash.
- ✓ Wash membrane in 1x SSPE + 0,1% w/v SDS at 65^{o}C for 15 minutes.
- ✓ Wash membrane in 0,1x SSPE + 0,1% w/v SDS at 65^{o}C for 5-10 minutes.
- ✓ Remove membrane and allow it to air-dry.
- ✓ Wrap membrane in SaranWrap and place it face up in the hybridization cassette.
- ✓ Expose to a phosphoimager (~3 hrs) or a film with an intensifying screen (-80^{o}C overnight).

3. RESULTS - DISCUSSION

PART I: Generation of Recombinant Adenoviruses Expressing ApoA-I(Met148Ala) and ApoA-I(Tyr192Ala)

❖ *Generation of the Met148Ala and Tyr192Ala mutations in the apoA-I gene using the overlapping PCR method.*

Single base substitutions in the human apoA-I gene were generated by site-directed mutagenesis using the overlapping PCR method (Figure 3.2). The pCDNA3.1-apoAIg(ΔBglII) plasmid was used as template in the initial PCR reactions (Figure 3.1). The conditions of each PCR reaction, as well as the sequences of the primers used for the generation of Met148Ala and Tyr192Ala mutations in the apoA-I gene have been previously described in the "Materials and Methods" section.

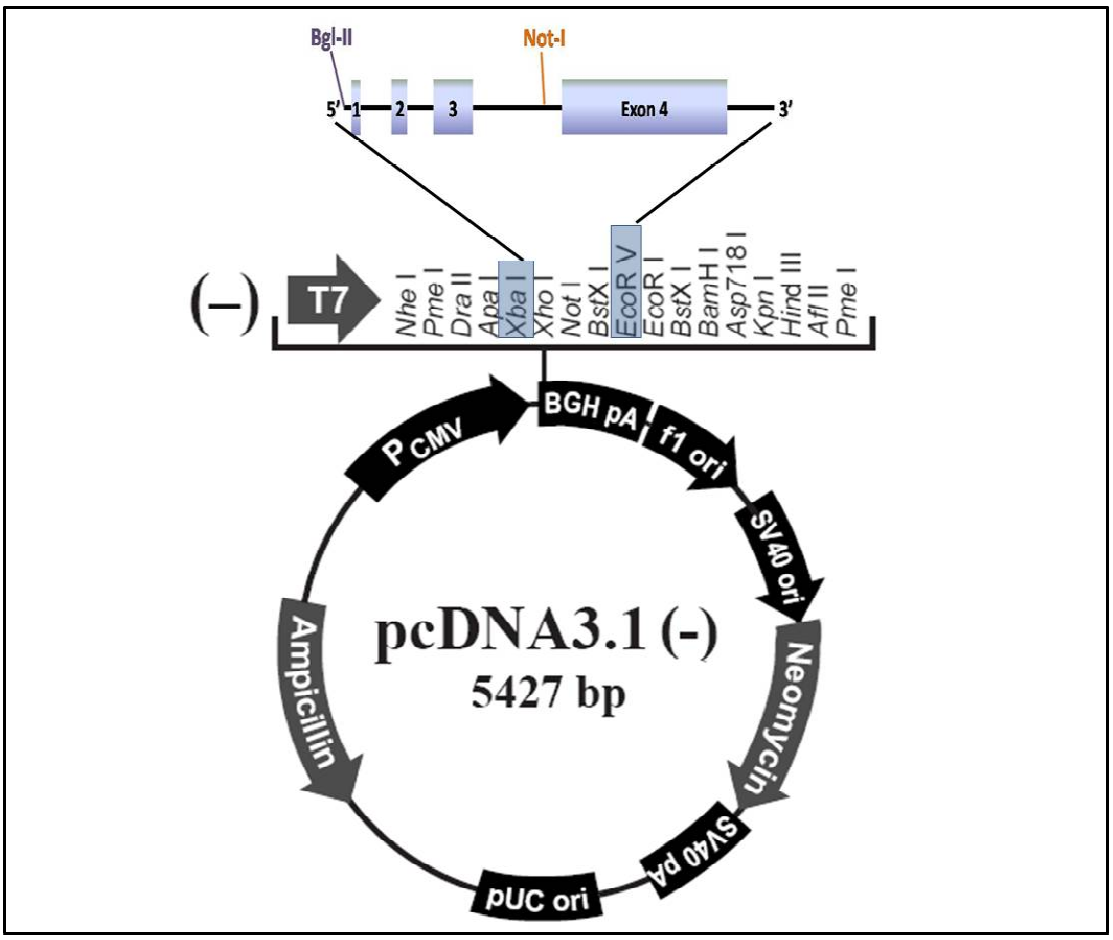

Figure 3.1 The pCDNA3.1-apoAIg(ΔBglII) plasmid.

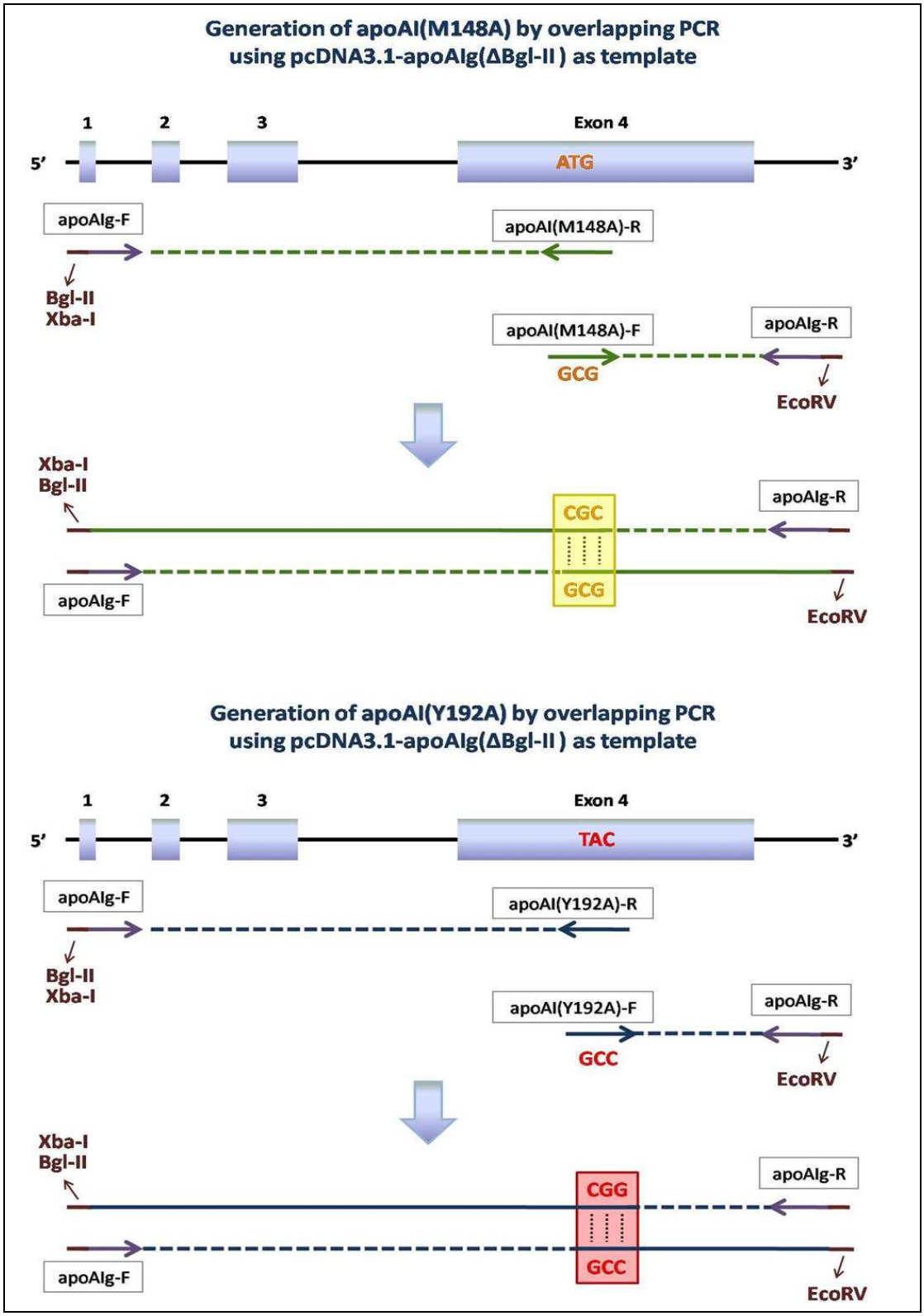

Figure 3.2 Schematic representation of the overlapping PCR technique for the generation of apoA-I(M148A) and apoA-I(Y192A). The nucleotide substitutions created in each case are shown. The flanking primers were designed in a way that the final mutated PCR products would carry the XbaI (5'-TCTAGA-3') and BglII (5'-AGATCT-3') recognition sites at the 5'- terminus, and the EcoRV (5'-GATATC-3') recognition site at the 3'- terminus.

Following synthesis, all PCR products were purified as described and visualized in 1% agarose gels (Figure 3.3).

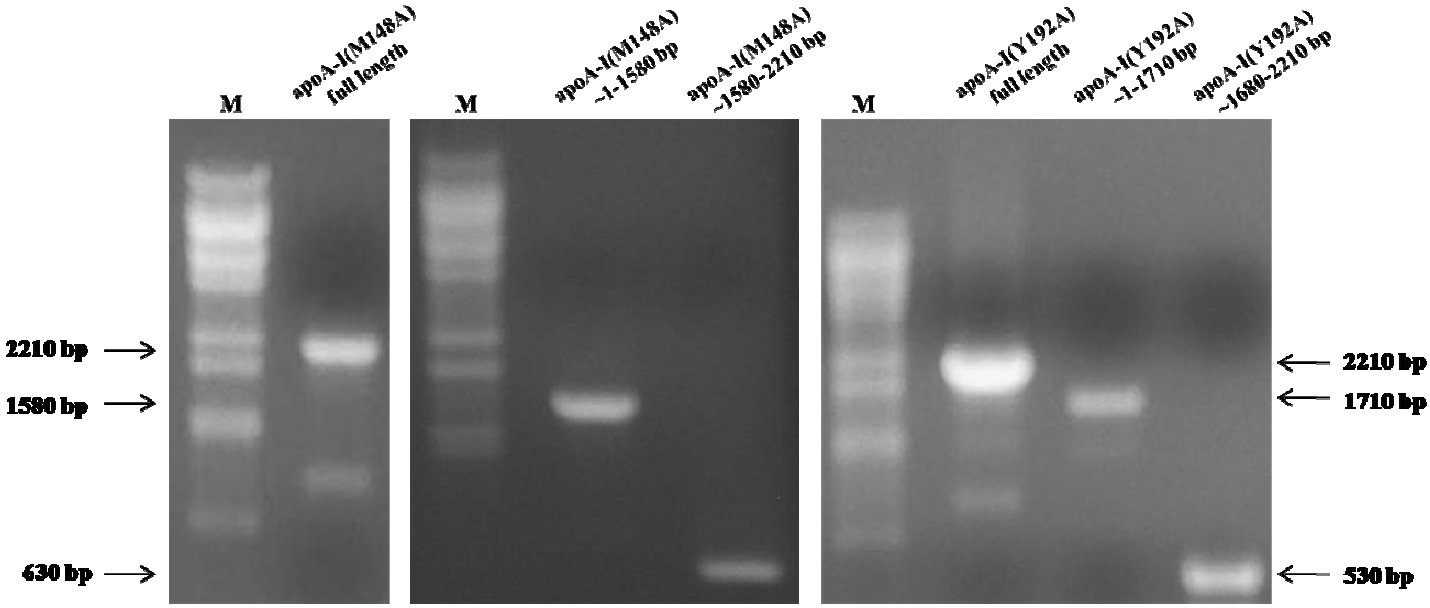

Figure 3.3 In overlapping PCR, the initial reactions generate two DNA fragments having overlapping ends. These fragments are combined in a subsequent 'fusion' reaction and the resulting product is amplified further by PCR. Above are shown the purified products as visualized after agarose gel electrophoresis. M: λ/BstEII DNA ladder

❖ *Cloning of apoA-I(Met148Ala) and apoA-I(Tyr192Ala) into the pAdTrack-CMV shuttle vector.*

As depicted in Figure 3.3, the final mutated PCR products carried the BglII and the EcoRV recognition sites at 5'- and 3'- terminus, respectively. These sites were used for the subsequent cloning of each of the apoA-I mutants in the pAdTrack-CMV shuttle vector (Figure 3.4). In more detail, both mutant sequences as well as the vector were digested with BglII/EcoRV, and purified. The ligation reactions of each one of the bioengineered apoA-I mutants with pAdTrack-CMV were used to transform DH10β competent cells. Single colonies were picked and used to inoculate 2mL LB/kanamycin cultures. After performing mini preps, the clones carrying the insert were chosen for amplification (Figure 3.5). The positive clones of each construct were used to inoculate 200mL LB/kanamycin cultures. Finally, maxi preparation was performed in order to obtain large amounts of each plasmid.

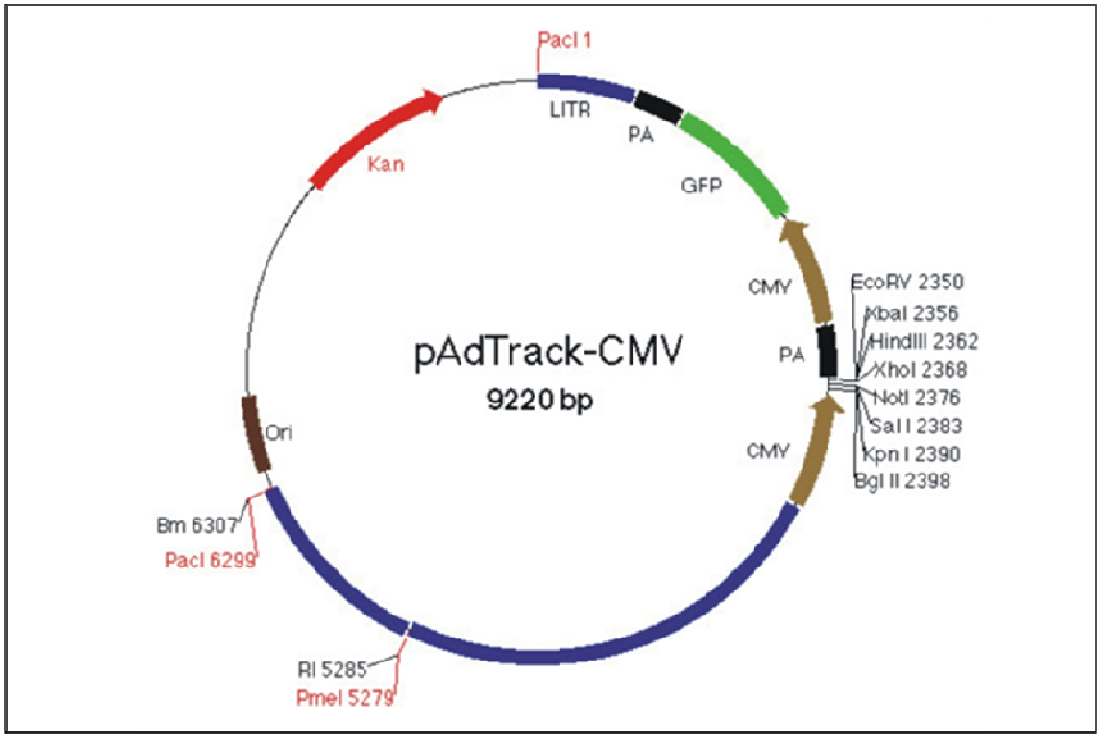

Figure 3.4 The pAdTrack-CMV shuttle vector.

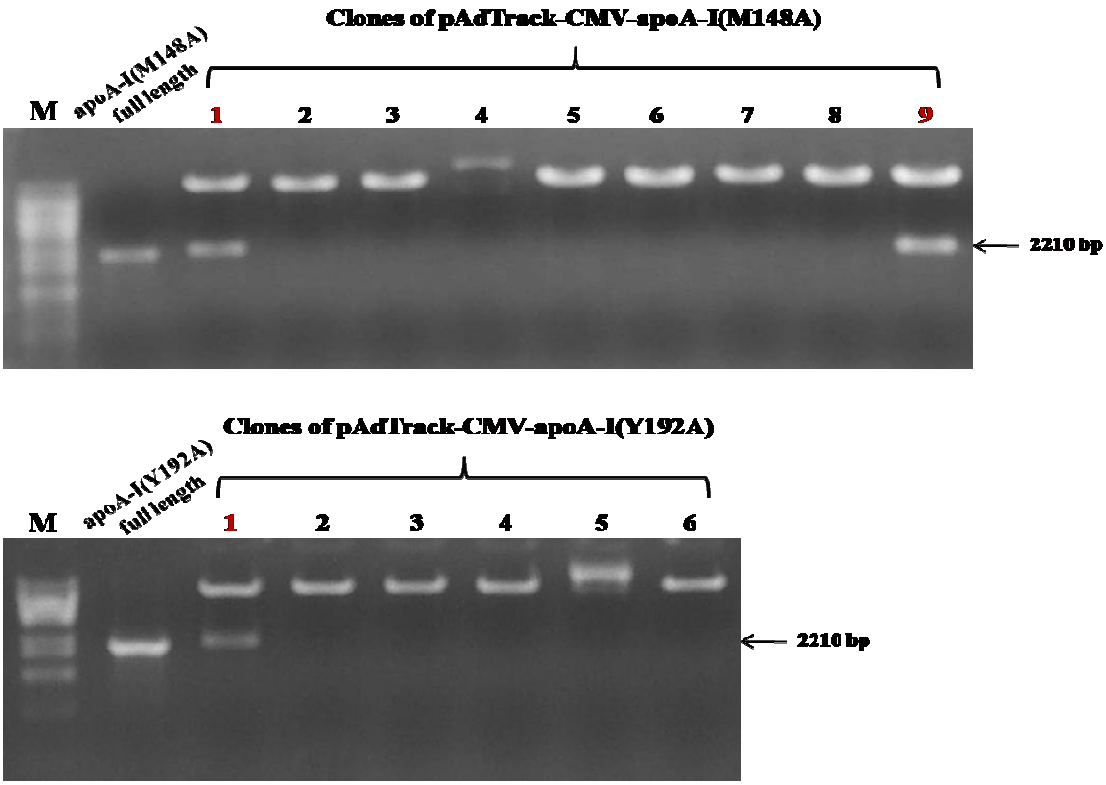

Figure 3.5 The pAdTrack-CMV-apoA-I clones of both mutants were digested with BglII and EcoRV in order to confirm the successful introduction of the apoA-I insert into the vector. The correct clones were chosen and further amplified. M: λ/BstEII DNA ladder

In order to verify that the correct construct has been amplified, restriction analysis was performed in all three pAdTrack-CMV-apoA-I clones (Figure 3.6). Figure 3.7 shows a map of the pAdTrackCMV-apoA-I(M148A) plasmid. The constructs were then sequenced to confirm that the desired mutation was created in each case.

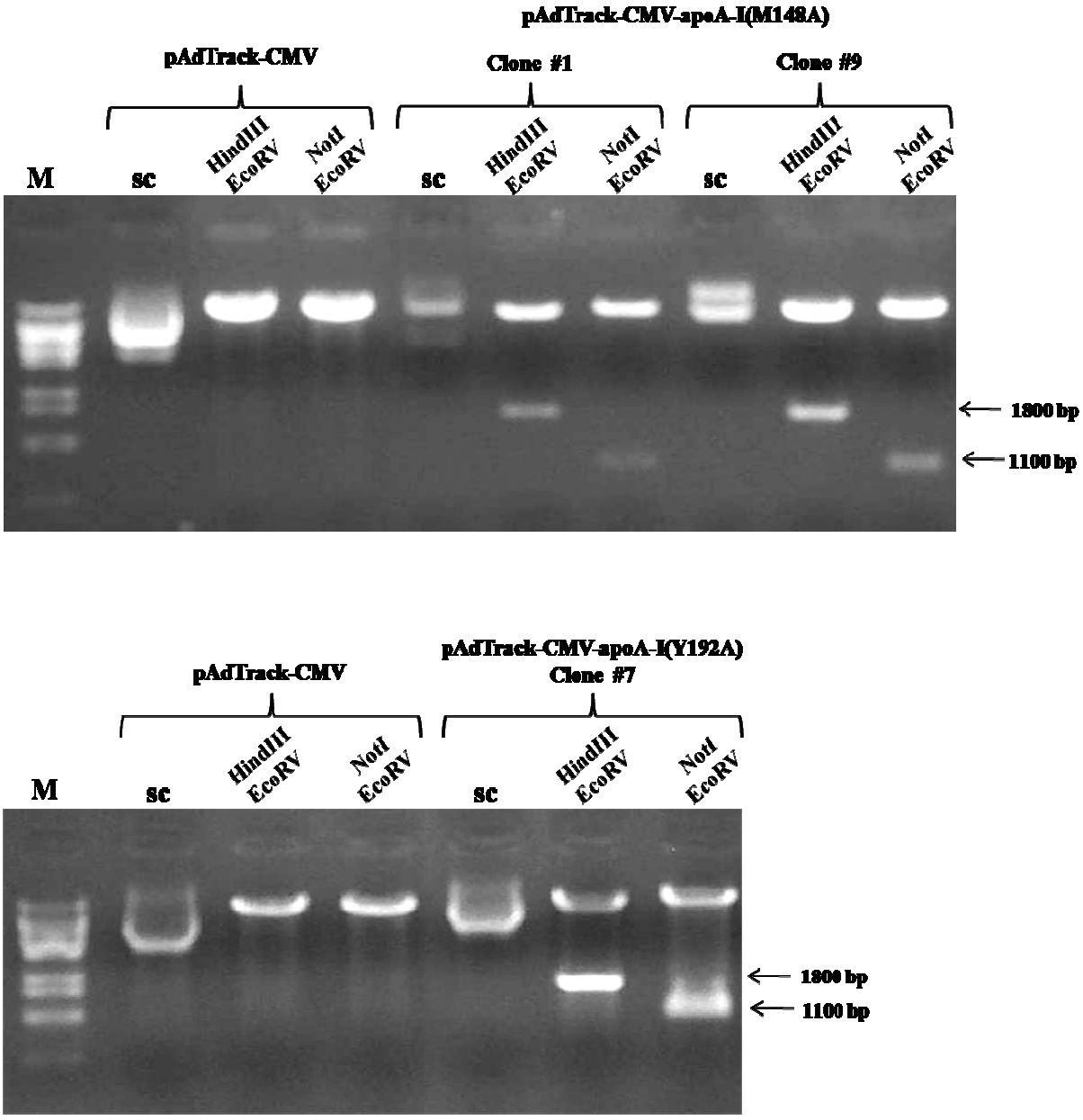

Figure 3.6 Restriction analysis of the mutant pAdTrack-CMV-apoA-I clones. M: λ/BstEII DNA ladder, sc: supercoiled.

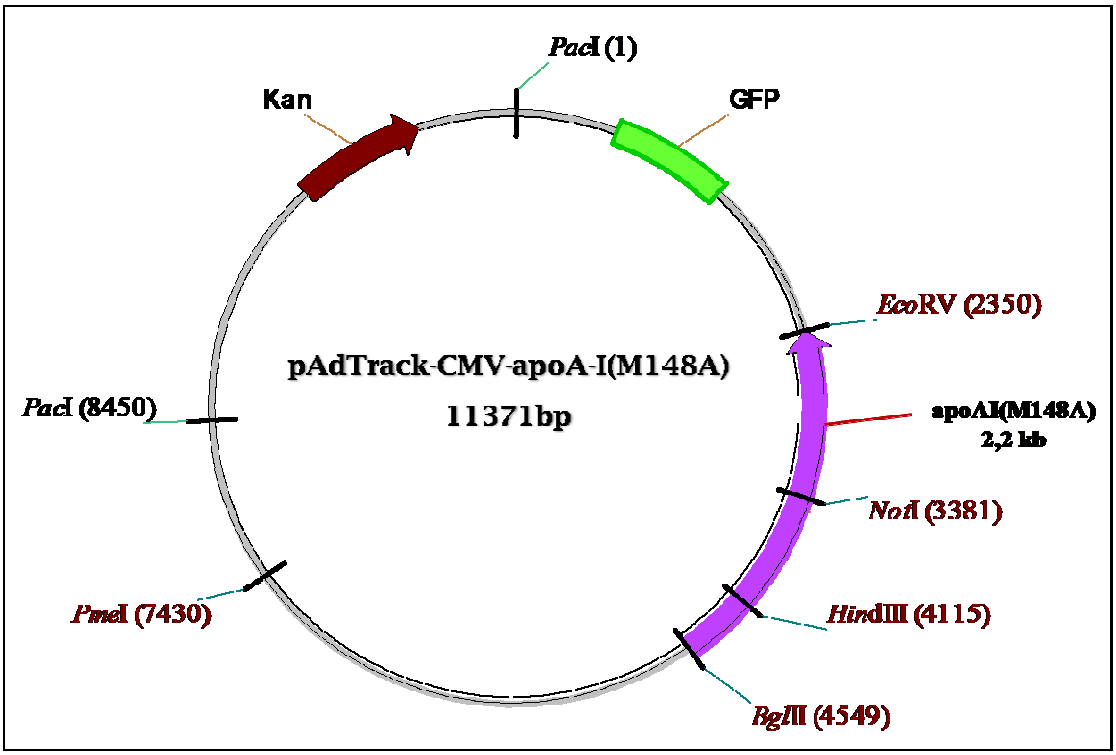

Figure 3.7 The pAdTrack-CMV-apoA-I mutant constructs.

Finally, the transgene (apoA-I mutants) expression in the pAdTrack-CMV shuttle vector was confirmed by transient transfection assay in HEK293T cells. The results demonstrated that all three clones were capable of expressing the apoA-I protein (Figure 3.8).

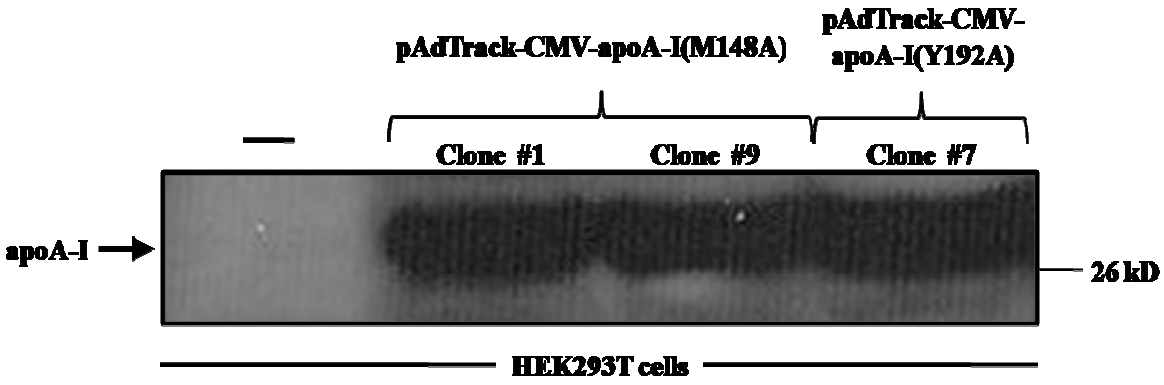

Figure 3.8 Transfection of HEK293T cells with the indicated pAdTrack-CMV-apoA-I constructs carrying the M148A and Y192A mutations and immunoblotting of the protein extracts established the successful expression of the apoA-I protein by all clones tested.

❖ *Generation of Ad-apoA-I(Met148Ala) and Ad-apoA-I(Tyr192Ala) using the AdEasy system.*

The generation of recombinant adenoviruses expressing the above mutated forms of apoA-I was achieved using the AdEasy system, as described in the "Materials and Methods" section (Figure 3.9). According to this, competent BJ5183-AD1 bacteria were transformed with the PmeI-linearized pAdTrack-CMV-apoA-I plasmids. These competent bacteria carry the appropriate enzymes that facilitate the homologous recombination between DNA molecules. The recombinants are then

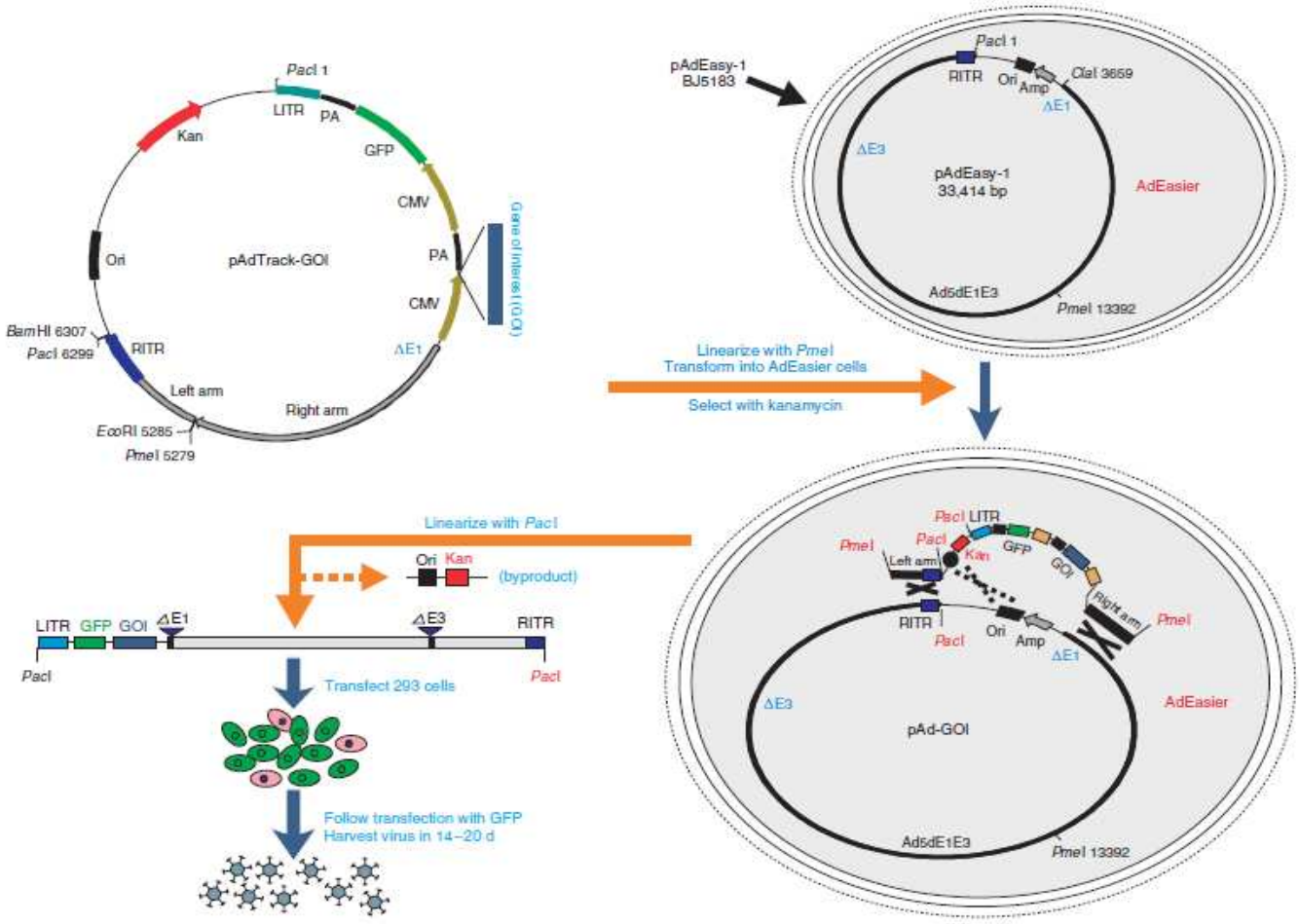

Figure 3.9 Schematic representation of the AdEasy technology [169]. The gene of interest (GOI) is first cloned into a shuttle vector (pAdTrack-CMV). The resultant plasmid is linearized by digesting with restriction endonuclease PmeI and subsequently transformed into competent BJ5183 cells that contain the adenoviral backbone plasmid pAdEasy-1. The confirmed recombinant adenovirus plasmids are digested with PacI to liberate both inverted terminal repeats (ITRs) and transfected into 911 cells. The "left arm" and "right arm" represent the regions mediating homologous recombination between the shuttle vector and the adenoviral backbone vector. Alternative homologous recombination between two Ori sites is shown with dotted lines. PA: polyadenylation site, LITR: left-hand ITR and packaging signal, RITR: right-hand ITR.

selected for kanamycin resistance. The small colonies are more likely to contain the recombinants since the ones carrying the large-sized backbone vector, pAdEasy-1 (~33 kb), grow slower than the ones carrying the pAdTrack-CMV-apoA-I plasmid (~11 kb) alone. The selected colonies were subjected to restriction analysis. PacI digestion of the candidate recombinants releases either a 4.5-kb or a 3-kb fragment, both of which validate the successful recombination between the two vectors (Figure 3.10). The recombinant adenoviruses were generated by transfection of 911 packaging cells with 15μg of each of the PacI-linearized pAd-GFP-apoA-I mutants. Further amplification of the adenoviruses was performed as described in the "Materials and Methods" section.

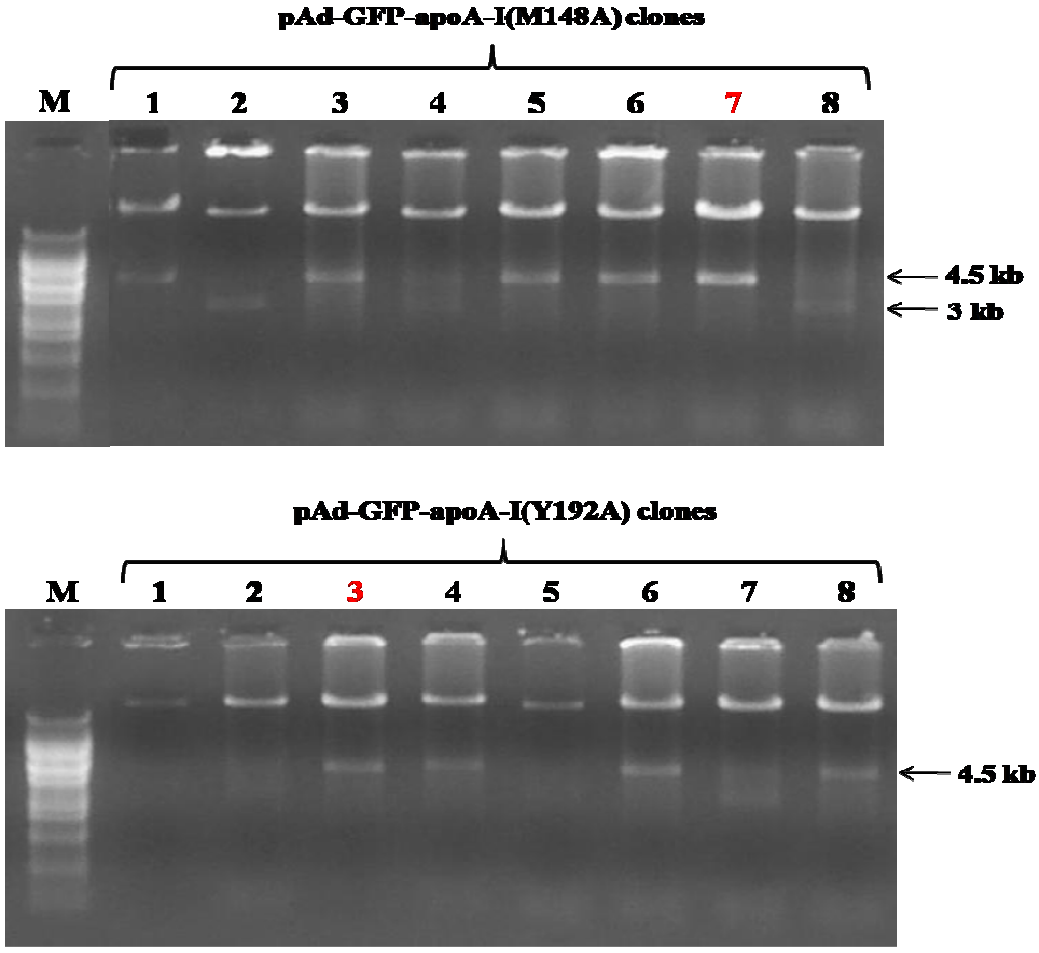

Figure 3.10 Selection and characterization of potential adenovirus recombinants after homologous recombination in BJ5183 cells. Screening of 8 randomly picked clones for each of the two apoA-I mutants. In the case of pAd-GFP-apoA-I(M148A) all but one clone (No 4) were validated by the restriction analysis, while in the case of pAd-GFP-apoA-I(Y12A) half of the tested clones released a 4.5-kb fragment that confirmed the efficient recombination between the two vectors. The numbers in red represent the clones that were chosen for the generation and amplification of adenoviruses expressing the apoA-I mutants. M: λ/BstEII DNA ladder.

Finally, the Fluorescence Forming Assay (FFA) was performed in order to measure the titer of each adenovirus. According to this assay, 911 cells are infected with various dilutions of viral supernatant (10^5, 10^6, 10^7) and 48 h later the number of GFP-positive cells is determined (Figure 3.11). The infectivity titer of pAd-GFP-apoA-I(M148A) was measured to be 8.64 x 10^8 fluorescence forming units (ffu) per milliliter (mL) of lysate, while the viral titer of pAd-GFP-apoA-I(Y192A) reached 16.7 x 10^8 ffu/mL.

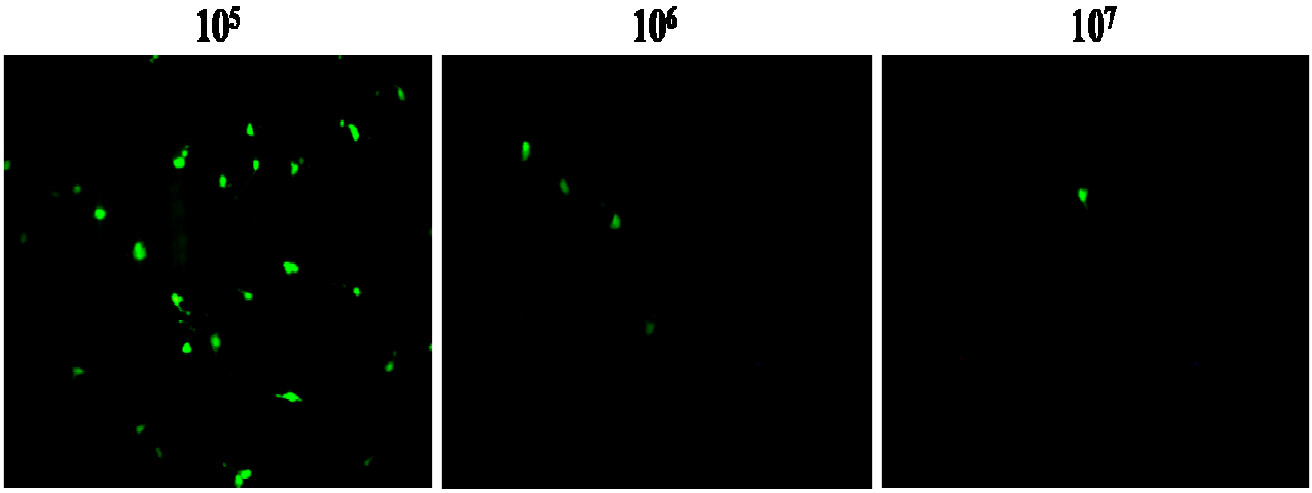

Figure 3.11 Adenoviral titer monitored by GFP expression. Linearized pAdEasy-GFP-apoA-I(M148A) was transfected into 911 cells and the cells were harvested 14 days after transfection. One percent of the freeze/thaw lysate of these cells was used to prepare the appropriate dilutions. 10^5, 10^6 and 10^7 dilutions of the viral supernatant was used to infect 911 cells, and GFP expression of the infected cells was visualized by fluorescence microscopy 48 hrs after infection.

❖ *Future directions*

It is currently well-established that normal high density lipoprotein (HDL) functions in a cardioprotective manner through the action of several mechanisms. In fact, a strong relationship between low levels of HDL and the risk for coronary artery disease has been ascertained. One important pathway of HDL-mediated atheroprotection includes the membrane-associated ABCA1 transporter that removes cholesterol from macrophage foam cells. A number of anti-inflammatory and anti-oxidant properties have also been considered to contribute to this apolipoprotein's ability to inhibit atherosclerosis. However, although normal HDL is anti-inflammatory, HDL isolated from hypercholesterolemic animals and humans has been

shown to promote inflammation. The mechanisms responsible for bringing anti-inflammatory HDL into a pro-inflammatory state remain in most part unknown, but studies suggest that reactive intermediates generated by myeloperoxidase can convert HDL into a dysfunctional form in humans.

Myeloperoxidase (MPO) is known to target HDL for oxidation, thus raising the possibility that this enzyme might provide a specific mechanism for generating dysfunctional HDL in humans. It has been already demonstrated that myeloperoxidase-dependent oxidation of apoA-I blocks HDL's ability to remove excess cholesterol from cells through the ABCA1 pathway. Specific tyrosine and methionine residues, including Met148 and Tyr192, have been implicated in MPO-dependent oxidation of apoA-I leading to the impairment of this protein's ABCA1 transport activity. Such oxidative damage has been speculated to disrupt negatively charged regions on the protein's surface or alter its remodeling, resulting in conformations that fail to interact with ABCA1.

The present study has provided the tools for further investigation of the above mechanisms resulting in MPO-mediated impediment of normal apoA-I function. Apart from Ad-GFP-apoA-I(M148A) and Ad-GFP-apoA-I(Y192A), Ad-GFP-MPO will also be generated, and the three adenoviruses will be further amplified in large-scale. The properties of each of the Ad-GFP-apoA-I mutants will be studied both *in vitro* and *in vivo* through adenovirus-mediated gene transfer in apoA-I knockout mice. *In vitro*, the purified apoA-I mutant proteins will be studied for their ability to activate LCAT and promote ABCA1-dependent cholesterol efflux. *In vivo*, following adenovirus infection, the plasma lipid, apoA-I and hepatic apoA-I mRNA levels will be evaluated. Finally, co-infection of the mice with adenoviruses expressing either of the two mutants and human myeloperoxidase will offer valuable information on the *in vivo* effect of the MPO on plasma lipids, distribution of HDL in different densities, the size and shape of HDL. Mutating the above specific oxidation sites of apoA-I is expected to prevent the protein from being modified by MPO, this way preserving its function and ability to interact with the other key-proteins of the RCT.

In conclusion, since oxidation of HDL by myeloperoxidase may represent a specific molecular mechanism for converting this cardioprotective lipoprotein into a dysfunctional form, this research will assist in gaining great insight on the biogenesis of atherogenic HDL, and lead to potential therapeutic approaches for preventing vascular disease in humans.

PART II: Generation of Wild-Type hApoA-I, hApoA-I(Leu141Arg) and hApoA-(Leu159Arg) transgenic mice

❖ *Subcloning of the wt hapoA-I, hapoA-I(Leu141Arg) and hapoA-I(Leu159Arg) into the pBluescript-TTR1 vector.*

The first step of this project was the construction of three plasmids carrying wild-type and mutated forms of human apoA-I under the control of the mouse transthyretin promoter in a pBluescript backbone. The pBluescript-TTR1 plasmid (Figure 3.13) was linearized by digestion with StuI, dephosphorylated with Shrimp Alkaline Phosphatase and purified as described in the "Materials and Methods" section. Both of the human apoA-I mutants were isolated from the pAdTrack-CMV-apoA-I(L141R) and pAdTrack-CMV-apoA-I(L159R) plasmids, respectively, as BglII/EcoRV fragments (Figure 3.12) and purified. The wild-type human apoA-I gene was isolated from the pCDNA3.1-apoAIg(ΔBglII) plasmid as a BglII/EcoRV fragment as well (Figure 3.1). All fragments were treated with DNA Polymerase I Large (Klenow) Fragment in order to create blunt ends and then purified (Figure 3.14).

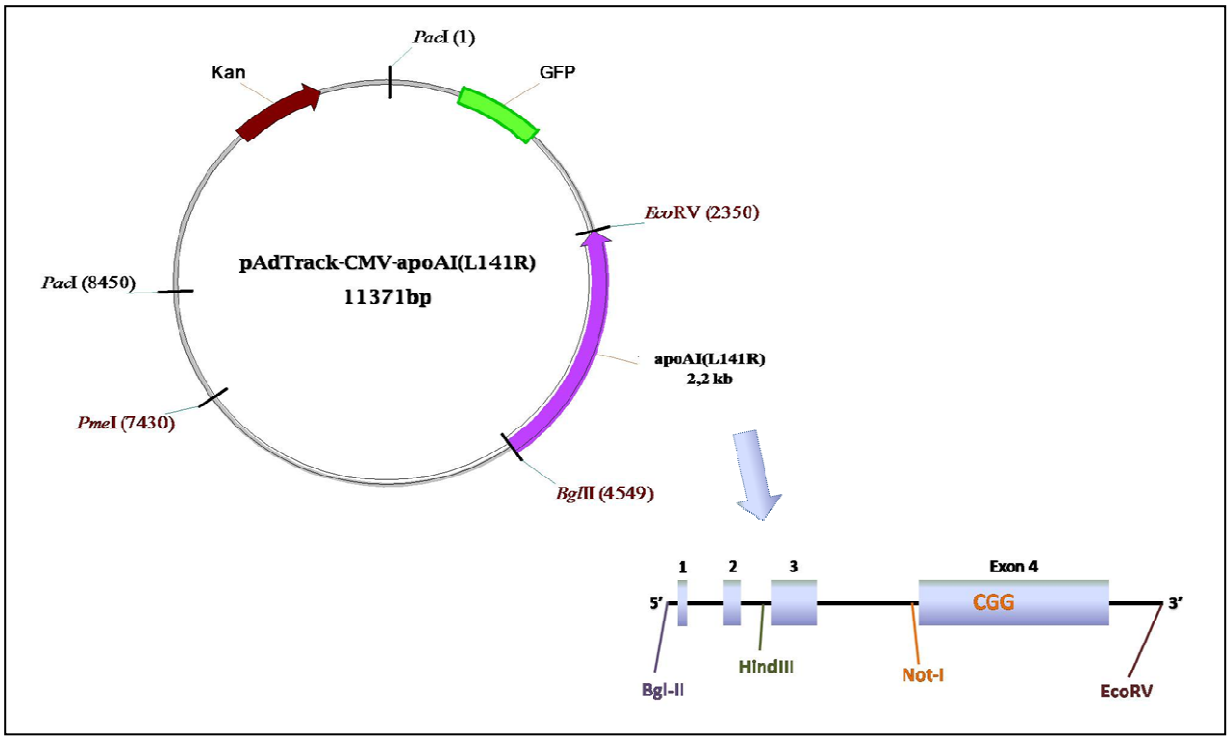

Figure 3.12 ApoA-I(L141R) insert was isolated from the pAdTrack-CMV-apoA-I(L141R) plasmid as a BglII/EcoRV fragment. The same procedure was followed for the isolation of apoA-I(L159R) insert.

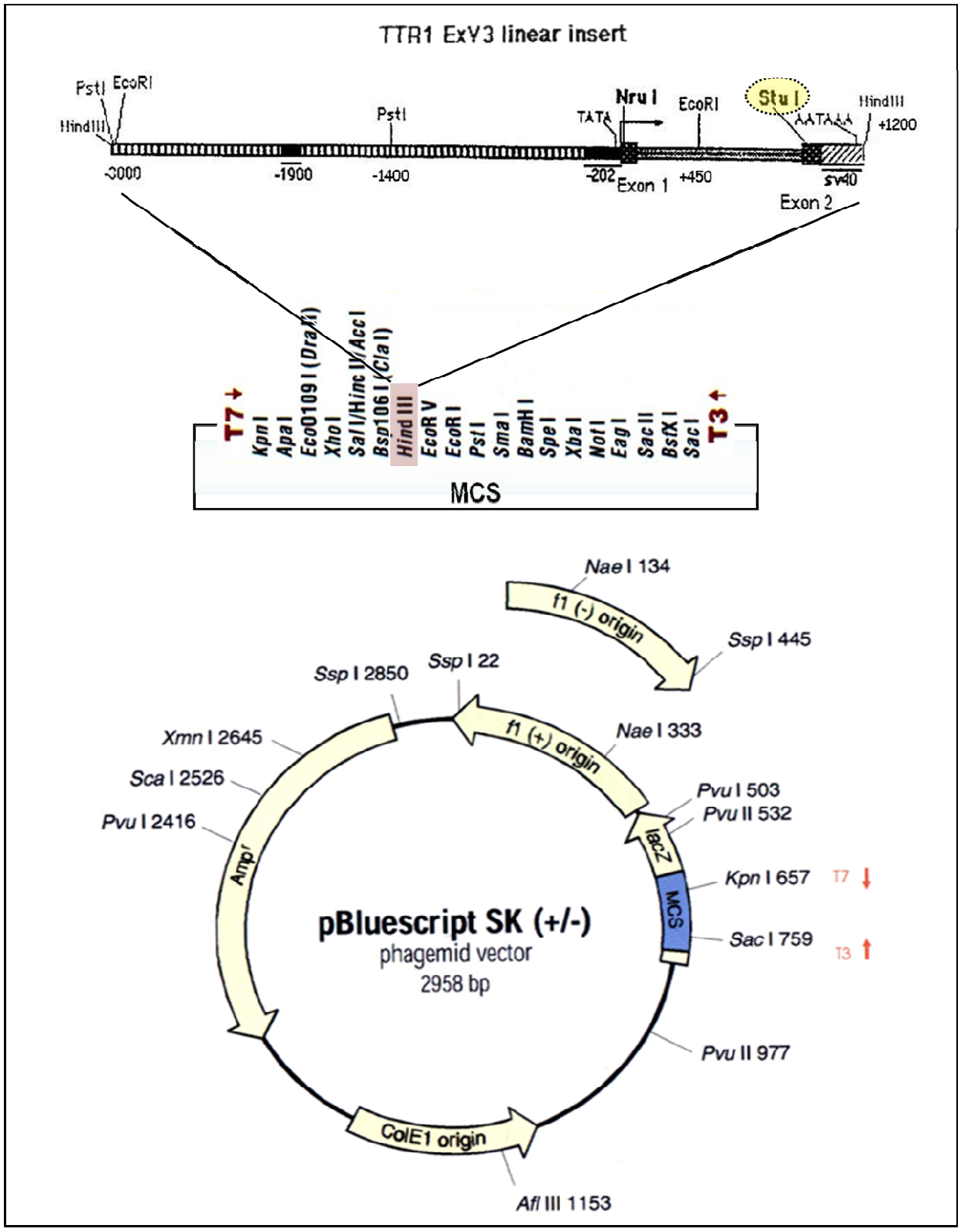

Figure 3.13 The pBluescript-TTR1 plasmid. The TTR1 ExV3 linear insert has been introduced into the pBluescript SK backbone in the HindIII restriction site. Linearization of the vector was achieved by digestion with StuI. The purified apoA-I fragments were introduced downstream of the TTR1 promoter at the StuI site indicated in the figure.

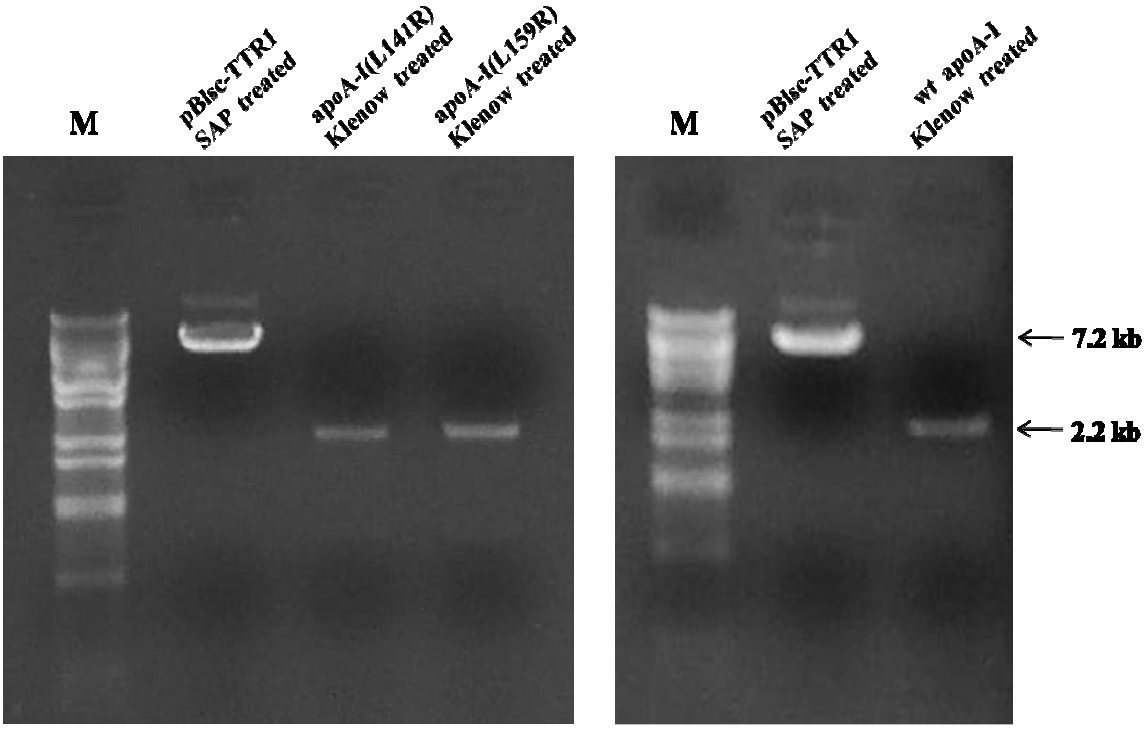

Figure 3.14 The pBluescript-TTR1 vector was linearized by StuI digestion and treated with SAP, while the BglII/EcoRV apoA-I fragments were blunt-ended with Klenow. Above are shown the purified products as visualized after agarose gel electrophoresis. M: λ/BstEII DNA ladder.

The resulting inserts were introduced downstream of the TTR1 promoter at the StuI site (Figure 3.13) and the ligation reactions were used to transform DH10β competent cells. Single colonies were picked and used to inoculate 2mL LB/ampicillin cultures. After performing mini preps, the clones carrying the insert in the correct orientation were chosen based on their HindIII and SmaI restriction pattern (Figure 3.15 and 3.16). One positive clone of each construct was selected and used to inoculate 200mL LB/ampicillin cultures. Maxi preparation was performed for each construct in order to obtain large amounts of endotoxin-free plasmids.

Finally, in order to test the transgenic constructs for expression *in vitro*, all five pBluescript-TTR1-apoAI plasmids were used to transfect HEK293T cells. Protein extracts from the transfected cells were collected at 48h and analyzed by Western Blot using a polyclonal anti-human apoA-I antibody. Results from protein analysis revealed that all constructs expressed apoA-I (Figure 3.17).

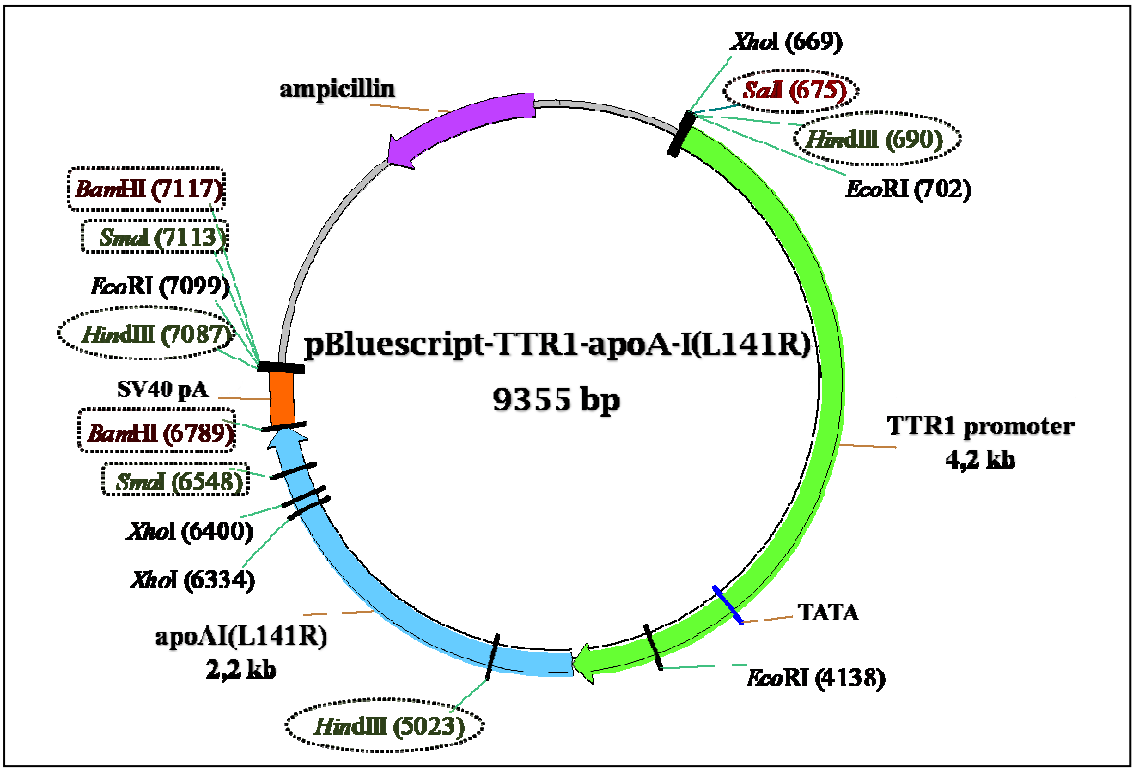

Figure 3.15 The apoA-I fragments were introduced into the StuI site of the pBluescript-TTR1 plasmid. The correct orientation of the insert was tested by HindIII and SmaI restriction analysis. The TTR1-apoA-I injection fragments were isolated by BamHI/SalI double digestion.

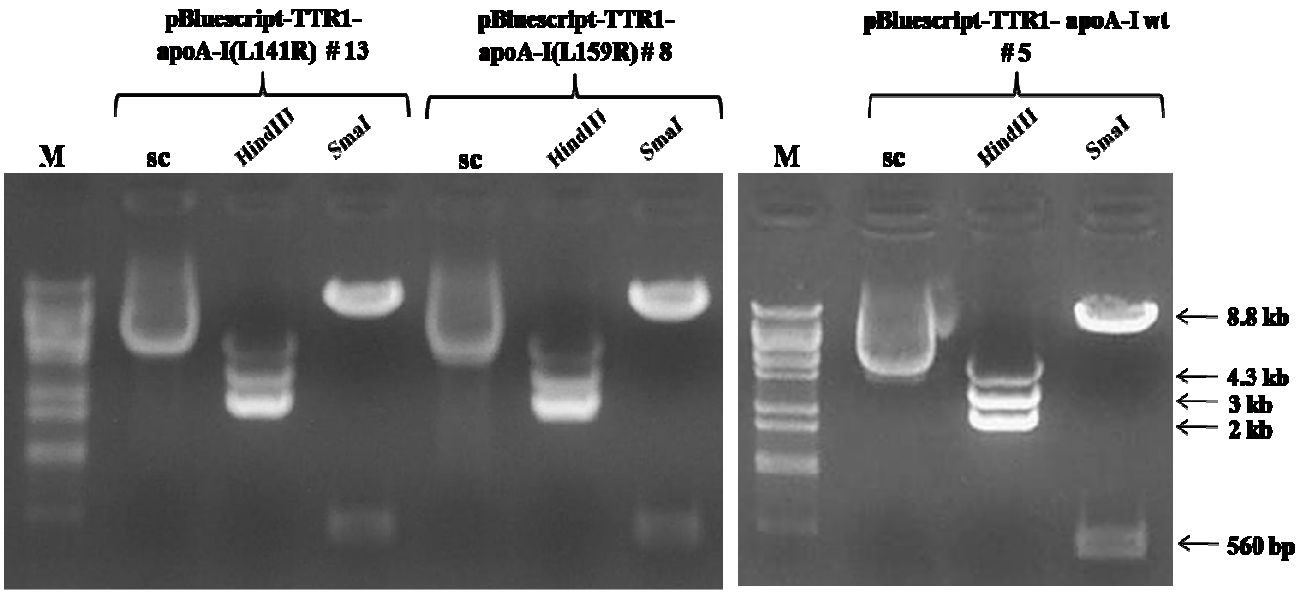

Figure 3.16 Restriction analysis of the three pBlsc-TTR1-apoA-I constructs. The pBlsc-TTR1-apoA-I clones of the wt and mutant apoA-I were digested with HindIII and SmaI in order to confirm the successful introduction of the apoA-I insert into the vector, as well as to verify its orientation. One correct clone from each construct was chosen and further amplified. M: λ/BstEII DNA ladder, sc: supercoiled.

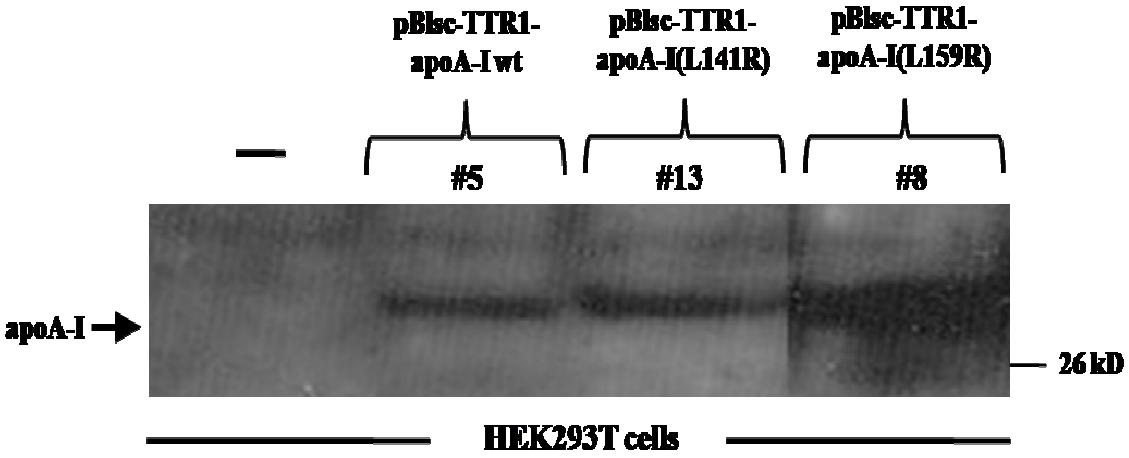

Figure 3.17 Western blot analysis of the protein extracts obtained from HEK293T cells transfected with each of the three pBluescript-TTR1-apoAI constructs confirmed that all three clones express apoA-I (28kD).

❖ *Preparation of the TTR1-hApoA-I Injection Fragments.*

The second step of this project was the isolation and purification of the TTR1-apoA-I wt, TTR1-apoA-I(L141R) and TTR1-apoA-I(L159R) transgenes from the pBluescript backbone. These DNA fragments were subsequently microinjected into the male pronucleus of fertilized mouse eggs for the generation of transgenic mice that would specifically express the wild-type and mutant human apoA-I in the liver.

The TTR1-apoA-I fragments were isolated from the pBluescript-TTR1-apoA-I constructs by BamHI/SalI digestion and purified (Figure 3.18 and 3.19) according to the procedures described in the "Materials and Methods" section. The concentration of the purified injection fragments was determined both by gel quantitation and by using the Quant-iT™ dsDNA BR Assay Kit, as previously indicated, and then diluted in EmbryoMAX injection buffer to a final concentration of 3 ng/μL. These dilutions were subsequently used for the microinjections performed in C57BL/6 fertilized mouse eggs. 24 hrs after the injections the 2-cell stage eggs that had survived the procedure, were transferred into the oviducts of pseudopregnant C57BL/6 female mice. Genotyping of the litters was performed both by Southern Blot and PCR.

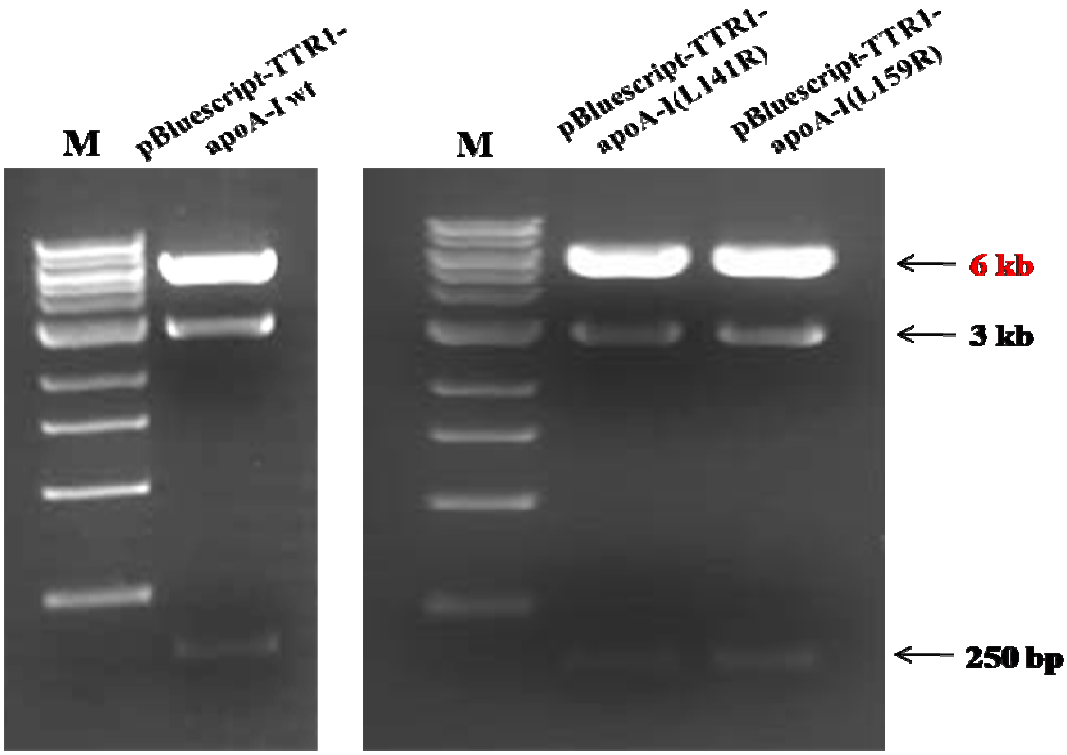

Figure 3.18 The three pBluescript-TTR1-apoA-I plasmids were digested with BamHI and SalI. The 6 kb-molecule corresponds to the TTR1-apoA-I fragment, while the 3 kb- and 250 bp- molecules correspond to the pBluescript backbone and the SV40 pA, respectively (see figure 3.15). M: λ/BstEII DNA ladder.

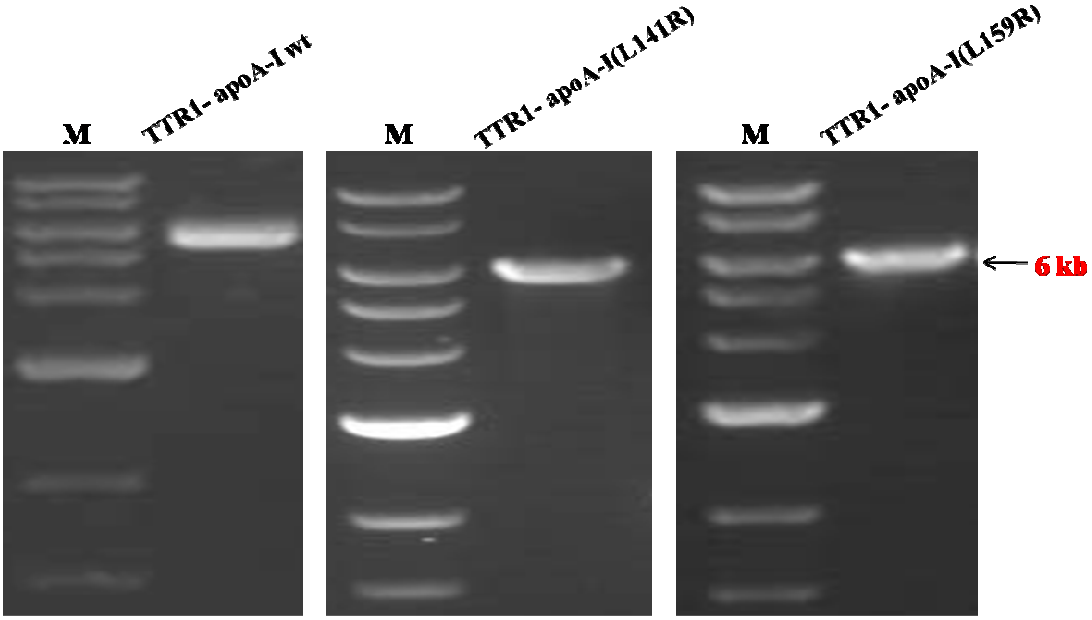

Figure 3.19 The concentrations of the purified TTR1-apoA-I fragments were determined by gel quantitation (~140 ng/μL). This estimation was taken into account along with the results from the Quant-iT™ dsDNA BR Assay Kit measurements. M: 1 kb DNA ladder, NEBs.

❖ *Genotyping of the Founders by Southern Blot and PCR.*

Following the purification of the transgene constructs, pronuclear DNA microinjection was performed for the generation of hapoA-I wt and hapoA-I(L159R) transgenic mice. The generation of hapoA-I(L141R) transgenic mice was deferred in order to avoid congestion of the animals. For this purpose, fertilized oocytes were removed from the oviduct of a mouse and the male pronucleus was microinjected with the appropriate dilution for each of the constructs prepared. The injected eggs were cultured *ex vivo* until the pronuclei had fused and the zygote had developed into a 2-cell embryo. The embryos were then transplanted into a surrogate mother and litters were born ~3 weeks later. The litters were subsequently screened to identify the founder animals for each transgene. DNA for screening was isolated from tail biopsies of the litters 6 weeks after microinjections. The extracted DNA was tested for the presence of the transgene by PCR and Southern blot analysis (Figure 3.20 and 3.21) according to the procedures described in the "Materials and Methods" section.

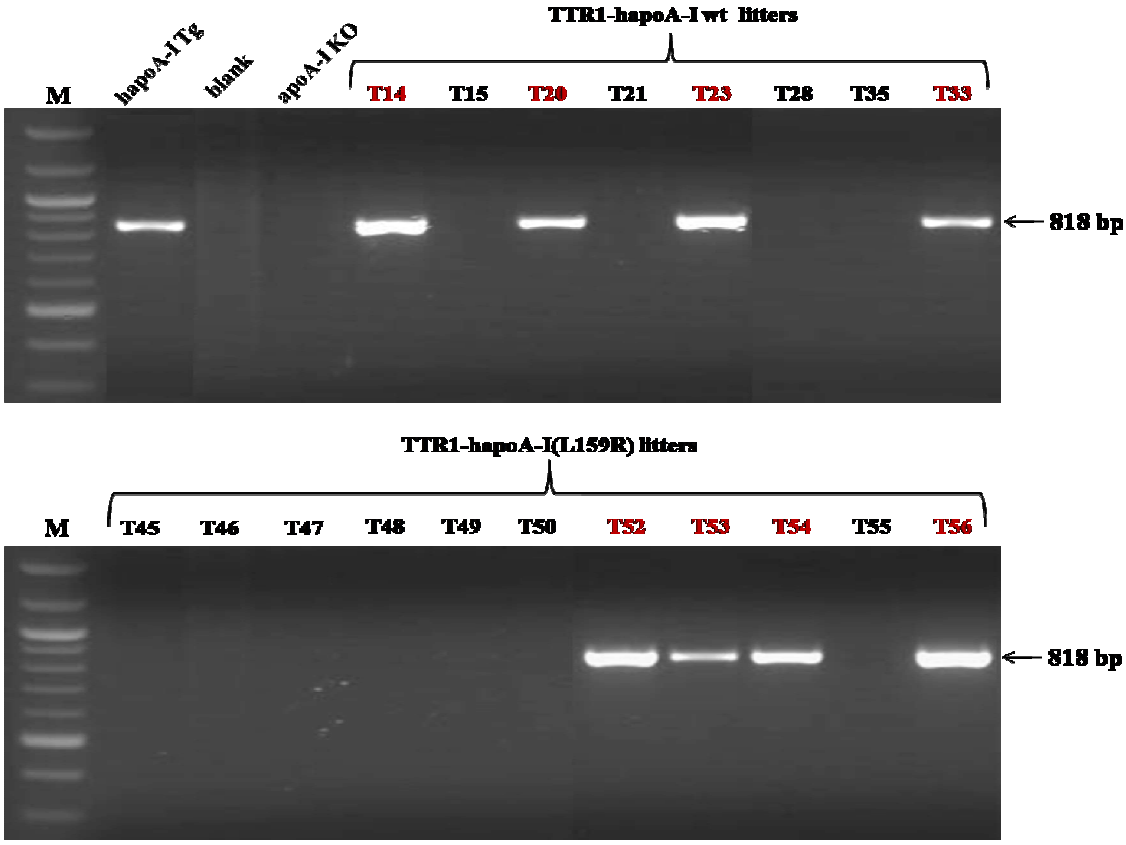

Figure 3.20 Screening of the hapoA-I wt and hapoA-I(L159R) litters by PCR analysis. For each of the two transgenes, four founders were detected. DNA extracted from hapoA-I Tg and apoA-I KO mice were used as positive and negative control, respectively. M: 100 bp DNA ladder, NEBs.

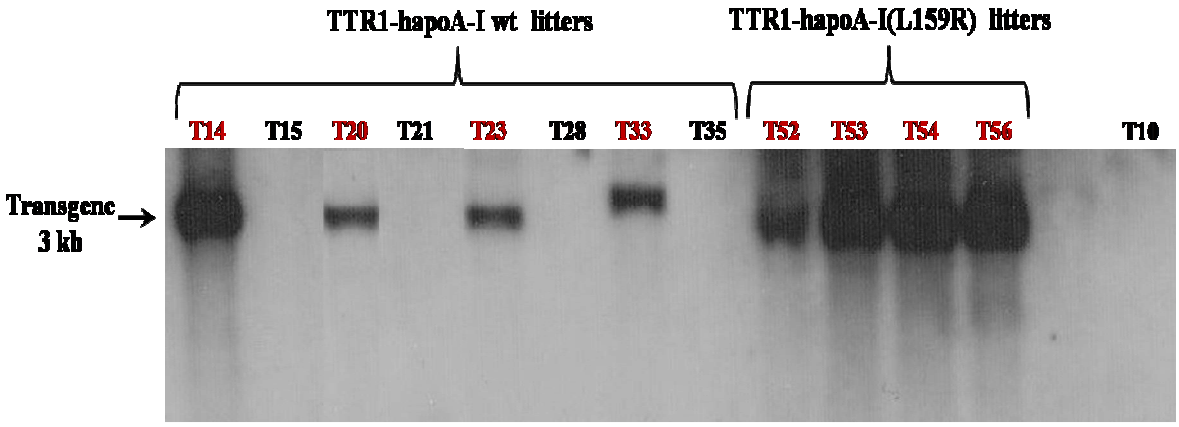

Figure 3.21 Screening of the hapoA-I wt and hapoA-I(L159R) litters by Southern Blot analysis. The same eight mice as in PCR analysis, were identified as transgenic founders. The transgenes in founders T14, and T53, T54, T56 were identified as high-copy, while the rest as low-copy. T10: non-transgenic litter used as negative control.

The radioactive labeled probe that was used for hybridization with the transgenes during Southern Blot analysis was isolated from the pBluescript-TTR1-apoA-I wt plasmid as a HindIII/XhoI fragment (Figure 3.15 and 3.22), that consisted of a part of the wild-type apoA-I sequence, and further processed as previously described. The results obtained from both screening processes confirmed the detection of eight founders.

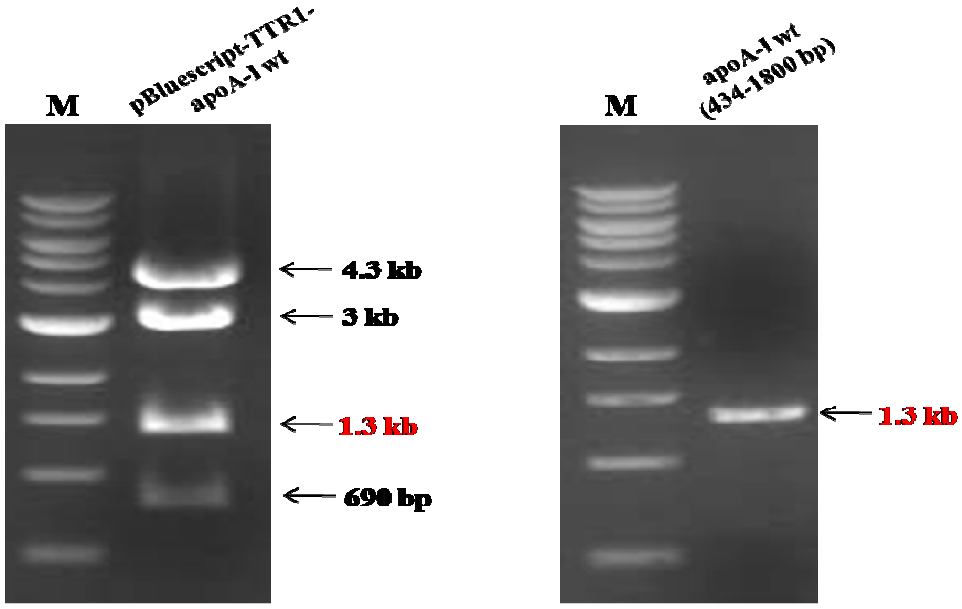

Figure 3.22 Isolation and purification of the probe that was used the identification of transgenic founders by Southern Blot. The sequence of the probe corresponded with the 1.3 kb-fragment released after HindIII/XhoI digestion of the pBluescript-TTR1-apoA-I wt plasmid. M: 1 kb DNA ladder, NEBs.

Finally, the identified founders were analyzed by Western Blot in order to study the transgene expression at the protein level. For this purpose a small quantity of whole blood was obtained from the eight founder mice by tail bleeding. The blood was processed as indicated in the "Materials and Methods" section in order to collect the serum of each mouse. Western blood was then performed to confirm the expression of apoA-I and to assess the levels of protein expression for each founder (Figure 3.23). Founder T33 of the hapoA-I(L159R) transgene was excluded, since it did not express hapoA-I protein.

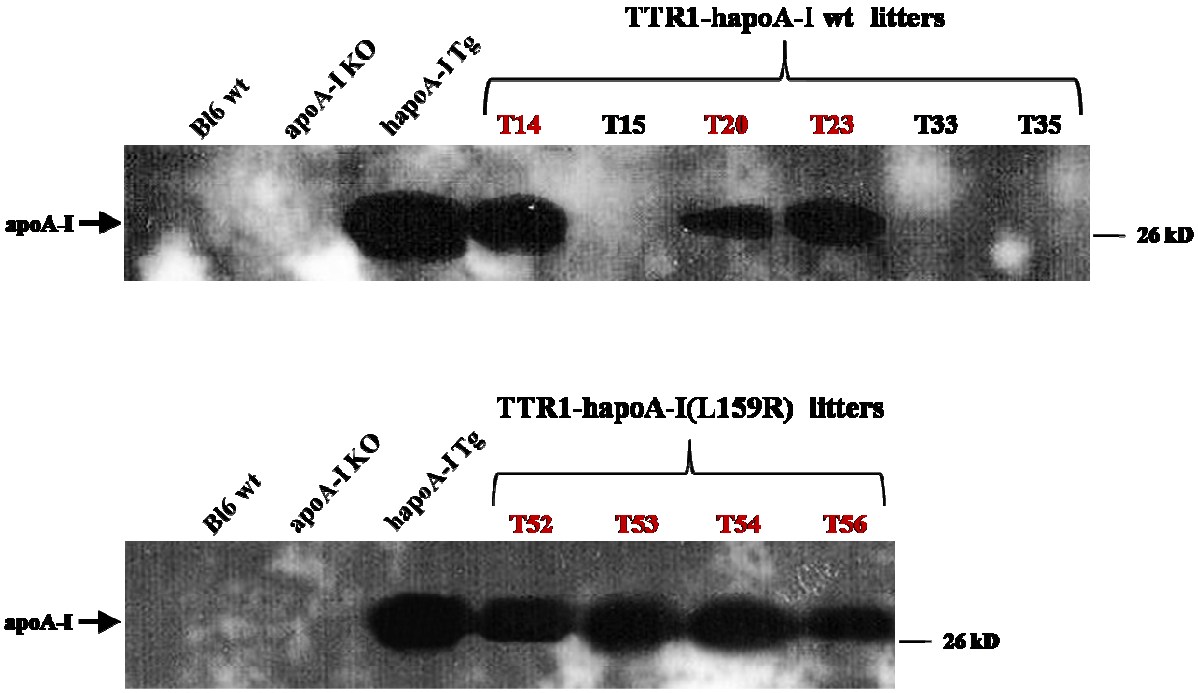

Figure 3.23 Transgene expression was analyzed by Western Blot. Founder T33 did not express the hapoA-I protein, thus it was excluded. Serum isolated from wt Bl6 mouse was used to eliminate the possibility of the antibody's cross-reactivity with mouse apoA-I. Serum isolated from apoA-I KO and hapoA-I Tg mice were used as negative and positive control, respectively.

❖ *Future directions*

Various naturally occurring mutations of apoA-I have been described in humans, half of which are associated with low plasma HDL levels. Mutations associated with low concentrations of HDL are divided into two main groups; those which exhibit reduced capacity to activate LCAT and those associated with amyloidosis. The present study addressed the generation of transgenic mice carrying two mutated forms of human apoA-I, apoA-I(Leu141Arg)$_{Pisa}$ and apoA-I(Leu159Arg)$_{Finland}$. Both mutants belong to the apolipoprotein A-I variants whose reduced capacity of LCAT activation accounts for the low HDL levels observed in carriers of either mutation. Hemizygotes for apoA-I(L141R) are presented with complete HDL deficiency, while heterozygotes develop hypoalphalipoproteinemia with half-normal levels of HDL-cholesterol. ApoA-I(L159R) is associated with dominantly inherited hypoalphalipoproteinemia. Heterozygotes for this mutation exhibit several lipoprotein composition rearrangements and increased catabolism of apoA-I. Both apoA-I variants demonstrate inefficient esterification of the cholesterol of preβ-HDL particles due to reduced LCAT activity. According to a recent study, treatment with LCAT can restore the aberrant HDL phenotype present in both cases. This finding could provide the basis for potential therapeutic approaches of the above defects.

Generating transgenic mice carrying either of the two apoA-I mutants provides long-term animal models that will allow in-depth investigation of their abnormal phenotype and possibly offer a new perspective in diagnosis, prognosis or even therapy. Studying the properties of these structural mutations in apoA-I *in vivo* can significantly contribute to the understanding of the molecular mechanisms affecting HDL biogenesis and lipoprotein homeostasis in the plasma. Finally, further research into the effect of these mutations on the interactions between apoA-I and proteins involved in key-steps of HDL metabolism, will uncover the etiology of genetically determined low levels of HDL.

REFERENCES

[1] Rendell, M. (2004). Advances in diabetes for the millennium: diabetes and cholesterol. MedGenMed 6, 5.

[2] Saini, H.K., Arneja, A.S. and Dhalla, N.S. (2004). Role of cholesterol in cardiovascular dysfunction. Can J Cardiol 20, 333-46.

[3] Shobab, L.A., Hsiung, G.Y. and Feldman, H.H. (2005). Cholesterol in Alzheimer's disease. Lancet Neurol 4, 841-52.

[4] Brown, A.J. (2007). Cholesterol, statins and cancer. Clin Exp Pharmacol Physiol 34, 135-41.

[5] Gotto, A.M., Jr., Pownall, H.J. and Havel, R.J. (1986). Introduction to the plasma lipoproteins. Methods Enzymol 128, 3-41.

[6] Loscalzo, J. (2005) Molecular Mechanisms of Atherosclerosis, Taylor & Francis Group

[7] Zannis, V.I., Chroni, A. and Krieger, M. (2006). Role of apoA-I, ABCA1, LCAT, and SR-BI in the biogenesis of HDL. J Mol Med 84, 276-94.

[8] Shelness, G.S. and Sellers, J.A. (2001). Very-low-density lipoprotein assembly and secretion. Curr Opin Lipidol 12, 151-7.

[9] Willnow, T.E. (1997). Mechanisms of hepatic chylomicron remnant clearance. Diabet Med 14 Suppl 3, S75-80.

[10] Hussain, M.M., Kancha, R.K., Zhou, Z., Luchoomun, J., Zu, H. and Bakillah, A. (1996). Chylomicron assembly and catabolism: role of apolipoproteins and receptors. Biochim Biophys Acta 1300, 151-70.

[11] Rader, D.J. and Daugherty, A. (2008). Translating molecular discoveries into new therapies for atherosclerosis. Nature 451, 904-13.

[12] Rye, K.A., Clay, M.A. and Barter, P.J. (1999). Remodelling of high density lipoproteins by plasma factors. Atherosclerosis 145, 227-38.

[13] Warden, C.H., Hedrick, C.C., Qiao, J.H., Castellani, L.W. and Lusis, A.J. (1993). Atherosclerosis in transgenic mice overexpressing apolipoprotein A-II. Science 261, 469-72.

[14] Amouyel, P., Isorez, D., Bard, J.M., Goldman, M., Lebel, P., Zylberberg, G. and Fruchart, J.C. (1993). Parental history of early myocardial infarction is associated with decreased levels of lipoparticle AI in adolescents. Arterioscler Thromb 13, 1640-4.

[15] Tailleux, A. et al. (2000). Decreased susceptibility to diet-induced atherosclerosis in human apolipoprotein A-II transgenic mice. Arterioscler Thromb Vasc Biol 20, 2453-8.

[16] Asztalos, B.F., Sloop, C.H., Wong, L. and Roheim, P.S. (1993). Two-dimensional electrophoresis of plasma lipoproteins: recognition of new apo A-I-containing subpopulations. Biochim Biophys Acta 1169, 291-300.

[17] Miller, N.E. (1987). Associations of high-density lipoprotein subclasses and apolipoproteins with ischemic heart disease and coronary atherosclerosis. Am Heart J 113, 589-97.

[18] Asztalos, B.F., de la Llera-Moya, M., Dallal, G.E., Horvath, K.V., Schaefer, E.J. and Rothblat, G.H. (2005). Differential effects of HDL subpopulations on cellular ABCA1- and SR-BI-mediated cholesterol efflux. J Lipid Res 46, 2246-53.

[19] Fielding, C.J. and Fielding, P.E. (2001). Cellular cholesterol efflux. Biochim Biophys Acta 1533, 175-89.

[20] Fielding, C.J. (2007) High-Density Lipoproteins. From Basic Biology to Clinical Aspects., WILEY-VCH Verlag GmbH & Co. KGaA

[21] Asztalos, B.F., Roheim, P.S., Milani, R.L., Lefevre, M., McNamara, J.R., Horvath, K.V. and Schaefer, E.J. (2000). Distribution of ApoA-I-containing HDL subpopulations in patients with coronary heart disease. Arterioscler Thromb Vasc Biol 20, 2670-6.

[22] Asztalos, B.F. and Schaefer, E.J. (2003). High-density lipoprotein subpopulations in pathologic conditions. Am J Cardiol 91, 12E-17E.

[23] Asztalos, B.F., Collins, D., Cupples, L.A., Demissie, S., Horvath, K.V., Bloomfield, H.E., Robins, S.J. and Schaefer, E.J. (2005). Value of high-density lipoprotein (HDL) subpopulations in predicting recurrent cardiovascular events in the Veterans Affairs HDL Intervention Trial. Arterioscler Thromb Vasc Biol 25, 2185-91.

[24] Ohashi, R., Mu, H., Wang, X., Yao, Q. and Chen, C. (2005). Reverse cholesterol transport and cholesterol efflux in atherosclerosis. QJM 98, 845-56.

[25] Johnson, W.J., Phillips, M.C. and Rothblat, G.H. (1997). Lipoproteins and cellular cholesterol homeostasis. Subcell Biochem 28, 235-76.

[26] Fielding, C.J., Shore, V.G. and Fielding, P.E. (1972). A protein cofactor of lecithin:cholesterol acyltransferase. Biochem Biophys Res Commun 46, 1493-8.

[27] Zannis, V.I., Chroni, A., Kypreos, K.E., Kan, H.Y., Cesar, T.B., Zanni, E.E. and Kardassis, D. (2004). Probing the pathways of chylomicron and HDL metabolism using adenovirus-mediated gene transfer. Curr Opin Lipidol 15, 151-66.

[28] Soutar, A.K., Garner, C.W., Baker, H.N., Sparrow, J.T., Jackson, R.L., Gotto, A.M. and Smith, L.C. (1975). Effect of the human plasma apolipoproteins and phosphatidylcholine acyl donor on the activity of lecithin: cholesterol acyltransferase. Biochemistry 14, 3057-64.

[29] Schaefer, E.J., Heaton, W.H., Wetzel, M.G. and Brewer, H.B., Jr. (1982). Plasma apolipoprotein A-1 absence associated with a marked reduction of high density lipoproteins and premature coronary artery disease. Arteriosclerosis 2, 16-26.

[30] Breslow, J.L., Ross, D., McPherson, J., Williams, H., Kurnit, D., Nussbaum, A.L., Karathanasis, S.K. and Zannis, V.I. (1982). Isolation and characterization of cDNA clones for human apolipoprotein A-I. Proc Natl Acad Sci U S A 79, 6861-5.

[31] Karathanasis, S.K., Zannis, V.I. and Breslow, J.L. (1983). Isolation and characterization of the human apolipoprotein A-I gene. Proc Natl Acad Sci U S A 80, 6147-51.

[32] Bruns, G.A., Karathanasis, S.K. and Breslow, J.L. (1984). Human apolipoprotein A-I--C-III gene complex is located on chromosome 11. Arteriosclerosis 4, 97-102.

[33] Cheung, P., Kao, F.T., Law, M.L., Jones, C., Puck, T.T. and Chan, L. (1984). Localization of the structural gene for human apolipoprotein A-I on the long arm of human chromosome 11. Proc Natl Acad Sci U S A 81, 508-11.

[34] Karathanasis, S.K. (1985). Apolipoprotein multigene family: tandem organization of human apolipoprotein AI, CIII, and AIV genes. Proc Natl Acad Sci U S A 82, 6374-8.

[35] Karathanasis, S.K., McPherson, J., Zannis, V.I. and Breslow, J.L. (1983). Linkage of human apolipoproteins A-I and C-III genes. Nature 304, 371-3.

[36] Zannis, V.I., Kan, H.Y., Kritis, A., Zanni, E.E. and Kardassis, D. (2001). Transcriptional regulatory mechanisms of the human apolipoprotein genes in vitro and in vivo. Curr Opin Lipidol 12, 181-207.

[37] Papazafiri, P., Ogami, K., Ramji, D.P., Nicosia, A., Monaci, P., Cladaras, C. and Zannis, V.I. (1991). Promoter elements and factors involved in hepatic transcription of

the human ApoA-I gene positive and negative regulators bind to overlapping sites. J Biol Chem 266, 5790-7.

[38] Widom, R.L., Ladias, J.A., Kouidou, S. and Karathanasis, S.K. (1991). Synergistic interactions between transcription factors control expression of the apolipoprotein AI gene in liver cells. Mol Cell Biol 11, 677-87.

[39] Ge, R., Rhee, M., Malik, S. and Karathanasis, S.K. (1994). Transcriptional repression of apolipoprotein AI gene expression by orphan receptor ARP-1. J Biol Chem 269, 13185-92.

[40] Ladias, J.A., Hadzopoulou-Cladaras, M., Kardassis, D., Cardot, P., Cheng, J., Zannis, V. and Cladaras, C. (1992). Transcriptional regulation of human apolipoprotein genes ApoB, ApoCIII, and ApoAII by members of the steroid hormone receptor superfamily HNF-4, ARP-1, EAR-2, and EAR-3. J Biol Chem 267, 15849-60.

[41] Rottman, J.N., Widom, R.L., Nadal-Ginard, B., Mahdavi, V. and Karathanasis, S.K. (1991). A retinoic acid-responsive element in the apolipoprotein AI gene distinguishes between two different retinoic acid response pathways. Mol Cell Biol 11, 3814-20.

[42] Tzameli, I. and Zannis, V.I. (1996). Binding specificity and modulation of the ApoA-I promoter activity by homo- and heterodimers of nuclear receptors. J Biol Chem 271, 8402-15.

[43] Vu-Dac, N., Schoonjans, K., Laine, B., Fruchart, J.C., Auwerx, J. and Staels, B. (1994). Negative regulation of the human apolipoprotein A-I promoter by fibrates can be attenuated by the interaction of the peroxisome proliferator-activated receptor with its response element. J Biol Chem 269, 31012-8.

[44] Widom, R.L., Rhee, M. and Karathanasis, S.K. (1992). Repression by ARP-1 sensitizes apolipoprotein AI gene responsiveness to RXR alpha and retinoic acid. Mol Cell Biol 12, 3380-9.

[45] Huuskonen, J., Vishnu, M., Chau, P., Fielding, P.E. and Fielding, C.J. (2006). Liver X receptor inhibits the synthesis and secretion of apolipoprotein A1 by human liver-derived cells. Biochemistry 45, 15068-74.

[46] Delerive, P., Galardi, C.M., Bisi, J.E., Nicodeme, E. and Goodwin, B. (2004). Identification of liver receptor homolog-1 as a novel regulator of apolipoprotein AI gene transcription. Mol Endocrinol 18, 2378-87.

[47] Beers, A., Haas, M.J., Wong, N.C. and Mooradian, A.D. (2006). Inhibition of apolipoprotein AI gene expression by tumor necrosis factor alpha: roles for MEK/ERK and JNK signaling. Biochemistry 45, 2408-13.

[48] Novak, E.M. and Bydlowski, S.P. (1997). NFY transcription factor binds to regulatory element AIC and transactivates the human apolipoprotein A-I promoter in HEPG2 cells. Biochem Biophys Res Commun 231, 140-3.

[49] Harnish, D.C., Malik, S. and Karathanasis, S.K. (1994). Activation of apolipoprotein AI gene transcription by the liver-enriched factor HNF-3. J Biol Chem 269, 28220-6.

[50] Kardassis, D., Tzameli, I., Hadzopoulou-Cladaras, M., Talianidis, I. and Zannis, V. (1997). Distal apolipoprotein C-III regulatory elements F to J act as a general modular enhancer for proximal promoters that contain hormone response elements. Synergism between hepatic nuclear factor-4 molecules bound to the proximal promoter and distal enhancer sites. Arterioscler Thromb Vasc Biol 17, 222-32.

[51] Kan, H.Y., Georgopoulos, S. and Zannis, V. (2000). A hormone response element in the human apolipoprotein CIII (ApoCIII) enhancer is essential for intestinal expression of the ApoA-I and ApoCIII genes and contributes to the hepatic expression of the two linked genes in transgenic mice. J Biol Chem 275, 30423-31.

[52] Kan, H.Y., Georgopoulos, S., Zanni, M., Shkodrani, A., Tzatsos, A., Xie, H.X. and Zannis, V.I. (2004). Contribution of the hormone-response elements of the proximal ApoA-I promoter, ApoCIII enhancer, and C/EBP binding site of the proximal ApoA-I promoter to the hepatic and intestinal expression of the ApoA-I and ApoCIII genes in transgenic mice. Biochemistry 43, 5084-93.

[53] Zannis, V.I., Cole, F.S., Jackson, C.L., Kurnit, D.M. and Karathanasis, S.K. (1985). Distribution of apolipoprotein A-I, C-II, C-III, and E mRNA in fetal human tissues. Time-dependent induction of apolipoprotein E mRNA by cultures of human monocyte-macrophages. Biochemistry 24, 4450-5.

[54] Glickman, R.M. and Green, P.H. (1977). The intestine as a source of apolipoprotein A1. Proc Natl Acad Sci U S A 74, 2569-73.

[55] Zannis, V.I., Kurnit, D.M. and Breslow, J.L. (1982). Hepatic apo-A-I and apo-E and intestinal apo-A-I are synthesized in precursor isoprotein forms by organ cultures of human fetal tissues. J Biol Chem 257, 536-44.

[56] Zannis, V.I., Karathanasis, S.K., Keutmann, H.T., Goldberger, G. and Breslow, J.L. (1983). Intracellular and extracellular processing of human apolipoprotein A-I: secreted apolipoprotein A-I isoprotein 2 is a propeptide. Proc Natl Acad Sci U S A 80, 2574-8.

[57] Chau, P., Fielding, P.E. and Fielding, C.J. (2007). Bone morphogenetic protein-1 (BMP-1) cleaves human proapolipoprotein A1 and regulates its activation for lipid binding. Biochemistry 46, 8445-50.

[58] Law, S.W. and Brewer, H.B., Jr. (1984). Nucleotide sequence and the encoded amino acids of human apolipoprotein A-I mRNA. Proc Natl Acad Sci U S A 81, 66-70.

[59] Vaisar, T. et al. (2007). Shotgun proteomics implicates protease inhibition and complement activation in the antiinflammatory properties of HDL. J Clin Invest 117, 746-56.

[60] Chroni, A., Liu, T., Gorshkova, I., Kan, H.Y., Uehara, Y., Von Eckardstein, A. and Zannis, V.I. (2003). The central helices of ApoA-I can promote ATP-binding cassette transporter A1 (ABCA1)-mediated lipid efflux. Amino acid residues 220-231 of the wild-type ApoA-I are required for lipid efflux in vitro and high density lipoprotein formation in vivo. J Biol Chem 278, 6719-30.

[61] Chroni, A., Liu, T., Fitzgerald, M.L., Freeman, M.W. and Zannis, V.I. (2004). Cross-linking and lipid efflux properties of apoA-I mutants suggest direct association between apoA-I helices and ABCA1. Biochemistry 43, 2126-39.

[62] Wang, N., Chen, W., Linsel-Nitschke, P., Martinez, L.O., Agerholm-Larsen, B., Silver, D.L. and Tall, A.R. (2003). A PEST sequence in ABCA1 regulates degradation by calpain protease and stabilization of ABCA1 by apoA-I. J Clin Invest 111, 99-107.

[63] Vaughan, A.M. and Oram, J.F. (2005). ABCG1 redistributes cell cholesterol to domains removable by high density lipoprotein but not by lipid-depleted apolipoproteins. J Biol Chem 280, 30150-7.

[64] Wang, N., Lan, D., Chen, W., Matsuura, F. and Tall, A.R. (2004). ATP-binding cassette transporters G1 and G4 mediate cellular cholesterol efflux to high-density lipoproteins. Proc Natl Acad Sci U S A 101, 9774-9.

[65] Wang, N., Ranalletta, M., Matsuura, F., Peng, F. and Tall, A.R. (2006). LXR-induced redistribution of ABCG1 to plasma membrane in macrophages enhances cholesterol mass efflux to HDL. Arterioscler Thromb Vasc Biol 26, 1310-6.

[66] Acton, S., Rigotti, A., Landschulz, K.T., Xu, S., Hobbs, H.H. and Krieger, M. (1996). Identification of scavenger receptor SR-BI as a high density lipoprotein receptor. Science 271, 518-20.

[67] Liadaki, K.N. et al. (2000). Binding of high density lipoprotein (HDL) and discoidal reconstituted HDL to the HDL receptor scavenger receptor class B type I. Effect of lipid association and APOA-I mutations on receptor binding. J Biol Chem 275, 21262-71.

[68] Stangl, H., Hyatt, M. and Hobbs, H.H. (1999). Transport of lipids from high and low density lipoproteins via scavenger receptor-BI. J Biol Chem 274, 32692-8.

[69] Nolte, R.T. and Atkinson, D. (1992). Conformational analysis of apolipoprotein A-I and E-3 based on primary sequence and circular dichroism. Biophys J 63, 1221-39.

[70] Brouillette, C.G. and Anantharamaiah, G.M. (1995). Structural models of human apolipoprotein A-I. Biochim Biophys Acta 1256, 103-29.

[71] Palgunachari, M.N., Mishra, V.K., Lund-Katz, S., Phillips, M.C., Adeyeye, S.O., Alluri, S., Anantharamaiah, G.M. and Segrest, J.P. (1996). Only the two end helixes of eight tandem amphipathic helical domains of human apo A-I have significant lipid affinity. Implications for HDL assembly. Arterioscler Thromb Vasc Biol 16, 328-38.

[72] Tanaka, M., Dhanasekaran, P., Nguyen, D., Ohta, S., Lund-Katz, S., Phillips, M.C. and Saito, H. (2006). Contributions of the N- and C-terminal helical segments to the lipid-free structure and lipid interaction of apolipoprotein A-I. Biochemistry 45, 10351-8.

[73] Tanaka, M., Tanaka, T., Ohta, S., Kawakami, T., Konno, H., Akaji, K., Aimoto, S. and Saito, H. (2009). Evaluation of lipid-binding properties of the N-terminal helical segments in human apolipoprotein A-I using fragment peptides. J Pept Sci 15, 36-42.

[74] Ajees, A.A., Anantharamaiah, G.M., Mishra, V.K., Hussain, M.M. and Murthy, H.M. (2006). Crystal structure of human apolipoprotein A-I: insights into its protective effect against cardiovascular diseases. Proc Natl Acad Sci U S A 103, 2126-31.

[75] Beckstead, J.A., Block, B.L., Bielicki, J.K., Kay, C.M., Oda, M.N. and Ryan, R.O. (2005). Combined N- and C-terminal truncation of human apolipoprotein A-I yields a folded, functional central domain. Biochemistry 44, 4591-9.

[76] Silva, R.A., Hilliard, G.M., Fang, J., Macha, S. and Davidson, W.S. (2005). A three-dimensional molecular model of lipid-free apolipoprotein A-I determined by cross-linking/mass spectrometry and sequence threading. Biochemistry 44, 2759-69.

[77] Tanaka, M., Koyama, M., Dhanasekaran, P., Nguyen, D., Nickel, M., Lund-Katz, S., Saito, H. and Phillips, M.C. (2008). Influence of tertiary structure domain properties on the functionality of apolipoprotein A-I. Biochemistry 47, 2172-80.

[78] Davidson, W.S. and Silva, R.A. (2005). Apolipoprotein structural organization in high density lipoproteins: belts, bundles, hinges and hairpins. Curr Opin Lipidol 16, 295-300.

[79] Thomas, M.J., Bhat, S. and Sorci-Thomas, M.G. (2006). The use of chemical cross-linking and mass spectrometry to elucidate the tertiary conformation of lipid-bound apolipoprotein A-I. Curr Opin Lipidol 17, 214-20.

[80] Marcel, Y.L. and Kiss, R.S. (2003). Structure-function relationships of apolipoprotein A-I: a flexible protein with dynamic lipid associations. Curr Opin Lipidol 14, 151-7.

[81] Tricerri, M.A., Behling Agree, A.K., Sanchez, S.A., Bronski, J. and Jonas, A. (2001). Arrangement of apolipoprotein A-I in reconstituted high-density lipoprotein disks: an alternative model based on fluorescence resonance energy transfer experiments. Biochemistry 40, 5065-74.

[82] Borhani, D.W., Rogers, D.P., Engler, J.A. and Brouillette, C.G. (1997). Crystal structure of truncated human apolipoprotein A-I suggests a lipid-bound conformation. Proc Natl Acad Sci U S A 94, 12291-6.

[83] Panagotopulos, S.E., Horace, E.M., Maiorano, J.N. and Davidson, W.S. (2001). Apolipoprotein A-I adopts a belt-like orientation in reconstituted high density lipoproteins. J Biol Chem 276, 42965-70.

[84] Koppaka, V., Silvestro, L., Engler, J.A., Brouillette, C.G. and Axelsen, P.H. (1999). The structure of human lipoprotein A-I. Evidence for the "belt" model. J Biol Chem 274, 14541-4.

[85] Segrest, J.P., Jones, M.K., Klon, A.E., Sheldahl, C.J., Hellinger, M., De Loof, H. and Harvey, S.C. (1999). A detailed molecular belt model for apolipoprotein A-I in discoidal high density lipoprotein. J Biol Chem 274, 31755-8.

[86] Klon, A.E., Segrest, J.P. and Harvey, S.C. (2002). Comparative models for human apolipoprotein A-I bound to lipid in discoidal high-density lipoprotein particles. Biochemistry 41, 10895-905.

[87] Gorshkova, I.N., Liu, T., Kan, H.Y., Chroni, A., Zannis, V.I. and Atkinson, D. (2006). Structure and stability of apolipoprotein a-I in solution and in discoidal high-density lipoprotein probed by double charge ablation and deletion mutation. Biochemistry 45, 1242-54.

[88] Jonas, A., Wald, J.H., Toohill, K.L., Krul, E.S. and Kezdy, K.E. (1990). Apolipoprotein A-I structure and lipid properties in homogeneous, reconstituted spherical and discoidal high density lipoproteins. J Biol Chem 265, 22123-9.

[89] Segrest, J.P., Garber, D.W., Brouillette, C.G., Harvey, S.C. and Anantharamaiah, G.M. (1994). The amphipathic alpha helix: a multifunctional structural motif in plasma apolipoproteins. Adv Protein Chem 45, 303-69.

[90] Li, H.H., Lyles, D.S., Pan, W., Alexander, E., Thomas, M.J. and Sorci-Thomas, M.G. (2002). ApoA-I structure on discs and spheres. Variable helix registry and conformational states. J Biol Chem 277, 39093-101.

[91] Curtiss, L.K., Bonnet, D.J. and Rye, K.A. (2000). The conformation of apolipoprotein A-I in high-density lipoproteins is influenced by core lipid composition and particle size: a surface plasmon resonance study. Biochemistry 39, 5712-21.

[92] Kono, M., Okumura, Y., Tanaka, M., Nguyen, D., Dhanasekaran, P., Lund-Katz, S., Phillips, M.C. and Saito, H. (2008). Conformational flexibility of the N-terminal domain of apolipoprotein a-I bound to spherical lipid particles. Biochemistry 47, 11340-7.

[93] Singaraja, R.R. et al. (2006). Both hepatic and extrahepatic ABCA1 have discrete and essential functions in the maintenance of plasma high-density lipoprotein cholesterol levels in vivo. Circulation 114, 1301-9.

[94] Timmins, J.M. et al. (2005). Targeted inactivation of hepatic Abca1 causes profound hypoalphalipoproteinemia and kidney hypercatabolism of apoA-I. J Clin Invest 115, 1333-42.

[95] Takahashi, K., Kimura, Y., Nagata, K., Yamamoto, A., Matsuo, M. and Ueda, K. (2005). ABC proteins: key molecules for lipid homeostasis. Med Mol Morphol 38, 2-12.

[96] Chroni, A., Koukos, G., Duka, A. and Zannis, V.I. (2007). The carboxy-terminal region of apoA-I is required for the ABCA1-dependent formation of alpha-HDL but not prebeta-HDL particles in vivo. Biochemistry 46, 5697-708.

[97] Fitzgerald, M.L., Morris, A.L., Chroni, A., Mendez, A.J., Zannis, V.I. and Freeman, M.W. (2004). ABCA1 and amphipathic apolipoproteins form high-affinity molecular complexes required for cholesterol efflux. J Lipid Res 45, 287-94.

[98] Jonas, A., Zorich, N.L., Kezdy, K.E. and Trick, W.E. (1987). Reaction of discoidal complexes of apolipoprotein A-I and various phosphatidylcholines with lecithin cholesterol acyltransferase. Interfacial effects. J Biol Chem 262, 3969-74.

[99] Bolin, D.J. and Jonas, A. (1994). Binding of lecithin:cholesterol acyltransferase to reconstituted high density lipoproteins is affected by their lipid but not apolipoprotein composition. J Biol Chem 269, 7429-34.

[100] McManus, D.C., Scott, B.R., Frank, P.G., Franklin, V., Schultz, J.R. and Marcel, Y.L. (2000). Distinct central amphipathic alpha-helices in apolipoprotein A-I contribute to the in vivo maturation of high density lipoprotein by either activating lecithin-cholesterol acyltransferase or binding lipids. J Biol Chem 275, 5043-51.

[101] Sorci-Thomas, M.G., Curtiss, L., Parks, J.S., Thomas, M.J., Kearns, M.W. and Landrum, M. (1998). The hydrophobic face orientation of apolipoprotein A-I amphipathic helix domain 143-164 regulates lecithin:cholesterol acyltransferase activation. J Biol Chem 273, 11776-82.

[102] Reardon, C.A. et al. (2001). In vivo studies of HDL assembly and metabolism using adenovirus-mediated transfer of ApoA-I mutants in ApoA-I-deficient mice. Biochemistry 40, 13670-80.

[103] Scott, B.R., McManus, D.C., Franklin, V., McKenzie, A.G., Neville, T., Sparks, D.L. and Marcel, Y.L. (2001). The N-terminal globular domain and the first class A amphipathic helix of apolipoprotein A-I are important for lecithin:cholesterol acyltransferase activation and the maturation of high density lipoprotein in vivo. J Biol Chem 276, 48716-24.

[104] Thuahnai, S.T., Lund-Katz, S., Williams, D.L. and Phillips, M.C. (2001). Scavenger receptor class B, type I-mediated uptake of various lipids into cells. Influence of the nature of the donor particle interaction with the receptor. J Biol Chem 276, 43801-8.

[105] Ji, Y. et al. (1997). Scavenger receptor BI promotes high density lipoprotein-mediated cellular cholesterol efflux. J Biol Chem 272, 20982-5.

[106] Ueda, Y., Royer, L., Gong, E., Zhang, J., Cooper, P.N., Francone, O. and Rubin, E.M. (1999). Lower plasma levels and accelerated clearance of high density lipoprotein (HDL) and non-HDL cholesterol in scavenger receptor class B type I transgenic mice. J Biol Chem 274, 7165-71.

[107] Krieger, M. (2001). Scavenger receptor class B type I is a multiligand HDL receptor that influences diverse physiologic systems. J Clin Invest 108, 793-7.

[108] Liu, T., Krieger, M., Kan, H.Y. and Zannis, V.I. (2002). The effects of mutations in helices 4 and 6 of ApoA-I on scavenger receptor class B type I (SR-BI)-mediated cholesterol efflux suggest that formation of a productive complex between reconstituted high density lipoprotein and SR-BI is required for efficient lipid transport. J Biol Chem 277, 21576-84.

[109] Gotto, A.M., Jr. and Brinton, E.A. (2004). Assessing low levels of high-density lipoprotein cholesterol as a risk factor in coronary heart disease: a working group report and update. J Am Coll Cardiol 43, 717-24.

[110] Barter, P.J., Nicholls, S., Rye, K.A., Anantharamaiah, G.M., Navab, M. and Fogelman, A.M. (2004). Antiinflammatory properties of HDL. Circ Res 95, 764-72.

[111] Mackness, M.I., Durrington, P.N. and Mackness, B. (2004). The role of paraoxonase 1 activity in cardiovascular disease: potential for therapeutic intervention. Am J Cardiovasc Drugs 4, 211-7.

[112] Mineo, C., Deguchi, H., Griffin, J.H. and Shaul, P.W. (2006). Endothelial and antithrombotic actions of HDL. Circ Res 98, 1352-64.

[113] Yuhanna, I.S. et al. (2001). High-density lipoprotein binding to scavenger receptor-BI activates endothelial nitric oxide synthase. Nat Med 7, 853-7.
[114] Mineo, C., Yuhanna, I.S., Quon, M.J. and Shaul, P.W. (2003). High density lipoprotein-induced endothelial nitric-oxide synthase activation is mediated by Akt and MAP kinases. J Biol Chem 278, 9142-9.
[115] Kontush, A. and Chapman, M.J. (2006). Antiatherogenic small, dense HDL--guardian angel of the arterial wall? Nat Clin Pract Cardiovasc Med 3, 144-53.
[116] Barter, P., Kastelein, J., Nunn, A. and Hobbs, R. (2003). High density lipoproteins (HDLs) and atherosclerosis; the unanswered questions. Atherosclerosis 168, 195-211.
[117] Asztalos, B.F., Cupples, L.A., Demissie, S., Horvath, K.V., Cox, C.E., Batista, M.C. and Schaefer, E.J. (2004). High-density lipoprotein subpopulation profile and coronary heart disease prevalence in male participants of the Framingham Offspring Study. Arterioscler Thromb Vasc Biol 24, 2181-7.
[118] Libby, P. and Ridker, P.M. (2004). Inflammation and atherosclerosis: role of C-reactive protein in risk assessment. Am J Med 116 Suppl 6A, 9S-16S.
[119] Blankenberg, S., Barbaux, S. and Tiret, L. (2003). Adhesion molecules and atherosclerosis. Atherosclerosis 170, 191-203.
[120] Robbesyn, F., Salvayre, R. and Negre-Salvayre, A. (2004). Dual role of oxidized LDL on the NF-kappaB signaling pathway. Free Radic Res 38, 541-51.
[121] Cockerill, G.W., Rye, K.A., Gamble, J.R., Vadas, M.A. and Barter, P.J. (1995). High-density lipoproteins inhibit cytokine-induced expression of endothelial cell adhesion molecules. Arterioscler Thromb Vasc Biol 15, 1987-94.
[122] Baker, P.W., Rye, K.A., Gamble, J.R., Vadas, M.A. and Barter, P.J. (1999). Ability of reconstituted high density lipoproteins to inhibit cytokine-induced expression of vascular cell adhesion molecule-1 in human umbilical vein endothelial cells. J Lipid Res 40, 345-53.
[123] Robbesyn, F., Garcia, V., Auge, N., Vieira, O., Frisach, M.F., Salvayre, R. and Negre-Salvayre, A. (2003). HDL counterbalance the proinflammatory effect of oxidized LDL by inhibiting intracellular reactive oxygen species rise, proteasome activation, and subsequent NF-kappaB activation in smooth muscle cells. FASEB J 17, 743-5.
[124] Mackness, B., Hine, D., Liu, Y., Mastorikou, M. and Mackness, M. (2004). Paraoxonase-1 inhibits oxidised LDL-induced MCP-1 production by endothelial cells. Biochem Biophys Res Commun 318, 680-3.
[125] Sugatani, J., Miwa, M., Komiyama, Y. and Ito, S. (1996). High-density lipoprotein inhibits the synthesis of platelet-activating factor in human vascular endothelial cells. J Lipid Mediat Cell Signal 13, 73-88.
[126] Navab, M. et al. (2004). The oxidation hypothesis of atherogenesis: the role of oxidized phospholipids and HDL. J Lipid Res 45, 993-1007.
[127] Navab, M. et al. (2000). Normal high density lipoprotein inhibits three steps in the formation of mildly oxidized low density lipoprotein: step 1. J Lipid Res 41, 1481-94.
[128] Navab, M. et al. (2000). Normal high density lipoprotein inhibits three steps in the formation of mildly oxidized low density lipoprotein: steps 2 and 3. J Lipid Res 41, 1495-508.
[129] Forte, T.M. et al. (2002). Altered activities of anti-atherogenic enzymes LCAT, paraoxonase, and platelet-activating factor acetylhydrolase in atherosclerosis-susceptible mice. J Lipid Res 43, 477-85.
[130] Sattler, W., Maiorino, M. and Stocker, R. (1994). Reduction of HDL- and LDL-associated cholesterylester and phospholipid hydroperoxides by phospholipid

hydroperoxide glutathione peroxidase and Ebselen (PZ 51). Arch Biochem Biophys 309, 214-21.

[131] Tselepis, A.D. and John Chapman, M. (2002). Inflammation, bioactive lipids and atherosclerosis: potential roles of a lipoprotein-associated phospholipase A2, platelet activating factor-acetylhydrolase. Atheroscler Suppl 3, 57-68.

[132] Navab, M. et al. (2001). HDL and the inflammatory response induced by LDL-derived oxidized phospholipids. Arterioscler Thromb Vasc Biol 21, 481-8.

[133] Rosenblat, M., Vaya, J., Shih, D. and Aviram, M. (2005). Paraoxonase 1 (PON1) enhances HDL-mediated macrophage cholesterol efflux via the ABCA1 transporter in association with increased HDL binding to the cells: a possible role for lysophosphatidylcholine. Atherosclerosis 179, 69-77.

[134] Galle, J., Ochslen, M., Schollmeyer, P. and Wanner, C. (1994). Oxidized lipoproteins inhibit endothelium-dependent vasodilation. Effects of pressure and high-density lipoprotein. Hypertension 23, 556-64.

[135] Navab, M., Anantharamaiah, G.M., Reddy, S.T., Van Lenten, B.J., Ansell, B.J. and Fogelman, A.M. (2006). Mechanisms of disease: proatherogenic HDL--an evolving field. Nat Clin Pract Endocrinol Metab 2, 504-11.

[136] Daugherty, A., Dunn, J.L., Rateri, D.L. and Heinecke, J.W. (1994). Myeloperoxidase, a catalyst for lipoprotein oxidation, is expressed in human atherosclerotic lesions. J Clin Invest 94, 437-44.

[137] Shao, B., Bergt, C., Fu, X., Green, P., Voss, J.C., Oda, M.N., Oram, J.F. and Heinecke, J.W. (2005). Tyrosine 192 in apolipoprotein A-I is the major site of nitration and chlorination by myeloperoxidase, but only chlorination markedly impairs ABCA1-dependent cholesterol transport. J Biol Chem 280, 5983-93.

[138] Zheng, L. et al. (2004). Apolipoprotein A-I is a selective target for myeloperoxidase-catalyzed oxidation and functional impairment in subjects with cardiovascular disease. J Clin Invest 114, 529-41.

[139] Zheng, L., Settle, M., Brubaker, G., Schmitt, D., Hazen, S.L., Smith, J.D. and Kinter, M. (2005). Localization of nitration and chlorination sites on apolipoprotein A-I catalyzed by myeloperoxidase in human atheroma and associated oxidative impairment in ABCA1-dependent cholesterol efflux from macrophages. J Biol Chem 280, 38-47.

[140] Bergt, C., Fu, X., Huq, N.P., Kao, J. and Heinecke, J.W. (2004). Lysine residues direct the chlorination of tyrosines in YXXK motifs of apolipoprotein A-I when hypochlorous acid oxidizes high density lipoprotein. J Biol Chem 279, 7856-66.

[141] Hawkins, C.L., Pattison, D.I. and Davies, M.J. (2003). Hypochlorite-induced oxidation of amino acids, peptides and proteins. Amino Acids 25, 259-74.

[142] Levine, R.L., Mosoni, L., Berlett, B.S. and Stadtman, E.R. (1996). Methionine residues as endogenous antioxidants in proteins. Proc Natl Acad Sci U S A 93, 15036-40.

[143] Shao, B., Oda, M.N., Oram, J.F. and Heinecke, J.W. (2006). Myeloperoxidase: an inflammatory enzyme for generating dysfunctional high density lipoprotein. Curr Opin Cardiol 21, 322-8.

[144] Shao, B., Cavigiolio, G., Brot, N., Oda, M.N. and Heinecke, J.W. (2008). Methionine oxidation impairs reverse cholesterol transport by apolipoprotein A-I. Proc Natl Acad Sci U S A 105, 12224-9.

[145] Sorci-Thomas, M.G. and Thomas, M.J. (2002). The effects of altered apolipoprotein A-I structure on plasma HDL concentration. Trends Cardiovasc Med 12, 121-8.

[146] Zannis, V.I., Kardassis, D. and Zanni, E.E. (1993). Genetic mutations affecting human lipoproteins, their receptors, and their enzymes. Adv Hum Genet 21, 145-319.

[147] Gorshkova, I.N., Liu, T., Zannis, V.I. and Atkinson, D. (2002). Lipid-free structure and stability of apolipoprotein A-I: probing the central region by mutation. Biochemistry 41, 10529-39.

[148] Miccoli, R. et al. (1996). Compound heterozygosity for a structural apolipoprotein A-I variant, apo A-I(L141R)Pisa, and an apolipoprotein A-I null allele in patients with absence of HDL cholesterol, corneal opacifications, and coronary heart disease. Circulation 94, 1622-8.

[149] Miccoli, R., Zhu, Y., Daum, U., Wessling, J., Huang, Y., Navalesi, R., Assmann, G. and von Eckardstein, A. (1997). A natural apolipoprotein A-I variant, apoA-I (L141R)Pisa, interferes with the formation of alpha-high density lipoproteins (HDL) but not with the formation of pre beta 1-HDL and influences efflux of cholesterol into plasma. J Lipid Res 38, 1242-53.

[150] Koukos, G., Chroni, A., Duka, A., Kardassis, D. and Zannis, V.I. (2007). LCAT can rescue the abnormal phenotype produced by the natural ApoA-I mutations (Leu141Arg)Pisa and (Leu159Arg)FIN. Biochemistry 46, 10713-21.

[151] Miettinen, H.E., Gylling, H., Miettinen, T.A., Viikari, J., Paulin, L. and Kontula, K. (1997). Apolipoprotein A-IFin. Dominantly inherited hypoalphalipoproteinemia due to a single base substitution in the apolipoprotein A-I gene. Arterioscler Thromb Vasc Biol 17, 83-90.

[152] Miettinen, H.E., Jauhiainen, M., Gylling, H., Ehnholm, S., Palomaki, A., Miettinen, T.A. and Kontula, K. (1997). Apolipoprotein A-IFIN (Leu159-->Arg) mutation affects lecithin cholesterol acyltransferase activation and subclass distribution of HDL but not cholesterol efflux from fibroblasts. Arterioscler Thromb Vasc Biol 17, 3021-32.

[153] McManus, D.C., Scott, B.R., Franklin, V., Sparks, D.L. and Marcel, Y.L. (2001). Proteolytic degradation and impaired secretion of an apolipoprotein A-I mutant associated with dominantly inherited hypoalphalipoproteinemia. J Biol Chem 276, 21292-302.

[154] Eriksson, M., Carlson, L.A., Miettinen, T.A. and Angelin, B. (1999). Stimulation of fecal steroid excretion after infusion of recombinant proapolipoprotein A-I. Potential reverse cholesterol transport in humans. Circulation 100, 594-8.

[155] Chiesa, G. et al. (2002). Recombinant apolipoprotein A-I(Milano) infusion into rabbit carotid artery rapidly removes lipid from fatty streaks. Circ Res 90, 974-80.

[156] Nissen, S.E. et al. (2003). Effect of recombinant ApoA-I Milano on coronary atherosclerosis in patients with acute coronary syndromes: a randomized controlled trial. JAMA 290, 2292-300.

[157] Shah, P.K. (2007). Emerging HDL-based Therapies for Atherothrombotic Vascular Disease. Curr Treat Options Cardiovasc Med 9, 60-70.

[158] Garber, D.W. et al. (2001). A new synthetic class A amphipathic peptide analogue protects mice from diet-induced atherosclerosis. J Lipid Res 42, 545-52.

[159] Navab, M., Anantharamaiah, G.M., Hama, S., Garber, D.W., Chaddha, M., Hough, G., Lallone, R. and Fogelman, A.M. (2002). Oral administration of an Apo A-I mimetic Peptide synthesized from D-amino acids dramatically reduces atherosclerosis in mice independent of plasma cholesterol. Circulation 105, 290-2.

[160] Navab, M. et al. (2004). Oral D-4F causes formation of pre-beta high-density lipoprotein and improves high-density lipoprotein-mediated cholesterol efflux and reverse cholesterol transport from macrophages in apolipoprotein E-null mice. Circulation 109, 3215-20.

[161] Jin, W., Millar, J.S., Broedl, U., Glick, J.M. and Rader, D.J. (2003). Inhibition of endothelial lipase causes increased HDL cholesterol levels in vivo. J Clin Invest 111, 357-62.

[162] Badellino, K.O., Wolfe, M.L., Reilly, M.P. and Rader, D.J. (2006). Endothelial lipase concentrations are increased in metabolic syndrome and associated with coronary atherosclerosis. PLoS Med 3, e22.

[163] Barter, P.J. et al. (2007). Effects of torcetrapib in patients at high risk for coronary events. N Engl J Med 357, 2109-22.

[164] Nissen, S.E. et al. (2007). Effect of torcetrapib on the progression of coronary atherosclerosis. N Engl J Med 356, 1304-16.

[165] Nicholls, S.J., Tuzcu, E.M., Brennan, D.M., Tardif, J.C. and Nissen, S.E. (2008). Cholesteryl ester transfer protein inhibition, high-density lipoprotein raising, and progression of coronary atherosclerosis: insights from ILLUSTRATE (Investigation of Lipid Level Management Using Coronary Ultrasound to Assess Reduction of Atherosclerosis by CETP Inhibition and HDL Elevation). Circulation 118, 2506-14.

[166] Kastelein, J.J. et al. (2007). Effect of torcetrapib on carotid atherosclerosis in familial hypercholesterolemia. N Engl J Med 356, 1620-30.

[167] Bots, M.L. et al. (2007). Torcetrapib and carotid intima-media thickness in mixed dyslipidaemia (RADIANCE 2 study): a randomised, double-blind trial. Lancet 370, 153-60.

[168] Vergeer, M. et al. (2008). Cholesteryl ester transfer protein inhibitor torcetrapib and off-target toxicity: a pooled analysis of the rating atherosclerotic disease change by imaging with a new CETP inhibitor (RADIANCE) trials. Circulation 118, 2515-22.

[169] Luo, J. et al. (2007). A protocol for rapid generation of recombinant adenoviruses using the AdEasy system. Nat Protoc 2, 1236-47.